Elżbieta Walerian

DESCRIPTION OF NOISE PROPAGATION IN A BUILT-UP AREA

29/1995

WARSZAWA 1995

ISSN 0208-5658

Praca wpłynęła do Redakcji dnia 12 października 1995 r.

Praca habilitacyjna

recenzent – Prof. dr hab. Członek Rzecz. PAN – Ignacy Malecki

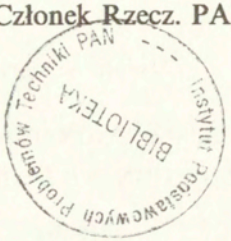

Instytut Podstawowych Problemów Techniki PAN
Nakład 100 egz. Ark. wyd. 8,5 Ark. druk. 11,0
Oddano do drukarni w październiku 1995 r.

Wydawnictwo Spółdzielcze sp. z o.o.
Warszawa, ul. Jasna 1

Elżbieta Walerian

Polish Academy of Sciences,
Institute of Fundamental Technological Research,
ul.Świętokrzyska 21, 00-049 Warszawa, Poland

DESCRIPTION OF NOISE PROPAGATION IN A BUILT-UP AREA

SUMMARY

The noise propagation model has been prepared to be applied in the environmental noise model as a computer aid in town planning.

The noise propagation model contains the simple-harmonic point source. By such sources any noise source can be modeled. As elementary events are taken: transmission through space and semi-transparent obstacles, reflection from obstacles, and diffraction at obstacles wedges (edges).

The sound equivalent level in front of the obstacles can be calculated. It is obtained from the sum of the acoustical pressure of the waves coming to the observation point by different paths, after chains of all the possible interactions up to K-order.

From the data of acoustical pressure other quantities needed for noise characteristics can be obtained. These data can also be used in the sound auralization for subjective noise rating.

Generally, the propagation model can be used for all systems for which the high frequency approximation is an appropriate one, and where transmissions, reflections from panels, and diffraction at wedges (edges) are predominant processes.

CONTENTS

SYMBOLS

A_n - the point of reflection at the n-panel (Eq.2.15), (Eq.3.4),

$A(i)_p$ - the point of reflection at the p-panel, on the i-path (Eq.2.8),

C_n - the point of transmission at the n-panel (Eq.2.15), (Eq.3.2),

$C(i)_s$ - the point of transmission at the s-panel, on the i-path (Eq.2.8),

$D(S,E,P)$ - the operator describing diffraction (Eq.2.13),

$D(\nu;S,P)$ - the diffraction coefficient (Eq.2.13), (Eq.3.30),

$D^s(R,\rho_{om},\rho_m)$ - the deformation factor for the spherical wave, (Eq.3.35),

$D^c(R,\rho_m)$ - the deformation factor for the cylindrical wave, (Eq.3.36),

E_m - the active point at the m-wedge (edge) (Eq.3.29),

$E_m^{(r)}$ - the active point the $m^{(r)}$-wedge (edge), being the mirror image of the m-wedge (edge) with respect to the r-panel (Eq.4.25),

$I(N,k)$ - the number of i-paths at which k interaction of transmission and reflection occur in the system of N panels (Eq.4.4),

$E_m(l)$ - the active point at mirror of the m-wedge (edge) created after reflections on the l- path (Eq.4.56),

i - the image unit,

K - the highest order of interactions,

k - the number of interaction (Eq.4.4),

k_t - the number of transmissions in the sequence of k interactions (Eq.4.9),

k_r - number of reflections in the sequence of k interactions (Eq.4.9),

k_d - number of diffractions in the sequence of k interactions (Eq.4.48),

k - the wave number $k=2\pi/\lambda$,

L_{eq}[dB(A)] - the sound equivalent level (Eq.2.2),

M - the number of wedges (edges) in the set {m} containing all the wedges (edges),

N - the number of panels in the system,

p(P) - the total acoustical pressure at the observation point P (Eq.2.16),

$p^g(P)$ - the geometrical part acoustical field (Eq.2.16), (Eq.4.2), (Eqs.4.12, 4.11),

$p^d(P)$ - the diffraction part acoustical field (Eq.2.16), (Eq.4.3), (Eq.4.30), (Eqs.4.45-4.47), (Eqs. 4.53-4.55), (Eqs.4.56-59),

$P(\rho,\varphi,z)$ - the observation point position in the coordinates system with z-axis identical with the wedge (edge),

$P(\rho_m,\varphi_m,z_m)$ = P(m) - the observation point position in the coordinates system with z-axis identical with the m-wedge (edge) (Eq.3.30),

$P^{(r)}$ - the image observation points resulting from the wave history after diffraction at the m(n)-wedge (Eq.2.15),

$P^{(n,r)}$ - the mirror image of the observation point $P^{(r)}$ with respect to the n-panel (Eq.2.15),

$P^{(\ldots,p,\ldots,s,\ldots)}$ = P(i) - the image observation point resulting from all the possible reflection on the i-path (Eq.4.13),

P(l,j) - the image observation point resulting from all the possible reflection on the i-path and l-path (Eq.4.50), (Eq.4.56),

$P(\nu;\varphi_m,\varphi_{mO})$ - the directional factor (Eq.3.34),

Q(...) - the source model (Eq.2.1),

Q(S) - the unit simple-harmonic point source model (Eq.2.7),

$Q[E_m(S)]$ - the source of diffraction wave, created at the m-wedge (edge) by the source S (Eq.3.40),

$Q[E_m[S(i)]]$ - the source of diffraction waves, created at the m-wedge (edge) by the source S(i) resulting from the reflections on the i-path (Eq.4.29),

$Q[E_m[S(i)]](l)$ - the image of the source $Q[E_m[S(i)]]$ resulting

from reflections on the 1-path (Eq.4.53),

$Q\left[E_{m+1}[E_m(S)]\right]$ - the source of diffraction waves, created at the (m+1)-wedge (edge) by the source $Q[E_m(S)]$ (Eq.4.32),

$Q\left[E_{m+1}[E_m[S(i)]](l)\right]$ - the source of diffraction waves, created at the (m+1)-wedge (edge) by the source $Q[E_m[S(i)]](l)$ (Eq.4.53),

$R(S,A,P)$ - the operator describing reflection (Eqs.2.11,2.12),

$R(A)$ - the reflection coefficient at the point A (Eqs.2.11,2.12),

$S(\rho_0,\varphi_0,z_0)$ - the source position in the coordinates system with z-axis identical with the wedge (edge).

$S(\rho_{0m},\varphi_{0m},z_{0m}) = S(m)$ - the source position in the coordinates system with z-axis identical with the m-wedge (edge) (Eq.3.30),

$S^{(p)}$ - the position of image source resulting from the wave history before the interaction with the m(n)-wedge (Eq.2.15),

$S^{(p,n)}$ - the mirror image of the source at $S^{(p)}$ with respect to the n-panel (Eq.2.15),

$S^{(\ldots,s,\ldots,p,\ldots,n)} = S(i)$ - the position of image source resulting from k_r reflections on the i-path (Eq.4.10),

$T(S,P)$ - the operator describing transmission (Eqs.2.9, 2.10),

$T(C)$ - the transmission coefficient at the point C (Eq.2.10),

$V^c(R,R_{em},\rho_m)$ - the cylindrical wave created at the m-wedge (edge) (Eq.3.37),

$\alpha(m)$ - the parameter describing reflection properties of m-wedge (edge) (Eq.3.32),

$\beta(m)$ - the parameter describing reflection properties of m-wedge (edge) (Eq.3.33),

$\eta(\ldots)$ - the step function,

$\nu\pi$ - the outer space around the wedge ($\nu=3/2$ for the right angle wedge, $\nu=2$ for the edge of half-plane) (Eq.2.13),

$\hat{\Pi}(\ldots)$ - the operator describing wave propagation (Eq.2.1), (Eq.2.3),

$\hat{\Pi}(n)$ - the operator describing interactions with the n-panel

(Eq.2.15),

$\hat{\Pi}(\mu)$ - the operator describing interactions with the μ-object (Eq.4.1),

$[\hat{\Pi}^i_k(n),\ldots,\hat{\Pi}^i_1(n)]$ - the i-sequence of operators, being an ordered combination of 3N elements of the set of transmission, reflection and diffraction operators $\{\hat{\Pi}(n)\}$, taken k at a time (2.14),

$[\hat{\Pi}^i_k(n),\ldots,\hat{\Pi}^i_1(n)]$ - the i-sequence of operators, being an ordered combination of 2N elements of the subset of transmission and reflection operators $\{\hat{\Pi}(n)\}$, taken k at a time (4.7),

$[\hat{\Pi}^i_k(\mu),\ldots,\hat{\Pi}^i_1(\mu)]$ - the i-sequence of operators, being an ordered combination of 2N+M elements of the set of operators $\{\hat{\Pi}(\mu)\}$, taken k at a time (Eq.4.3),

$\hat{\Pi}_o(\ldots)$ - the operator describing human perception (Eqs.2.1,2.2),

$\hat{\Pi}_a(R,\kappa,\omega)$ - the operator describing attenuation in the air (Eq.2.3),

$\hat{\Pi}_s(\{\underline{R}\},\eta,R_w,\omega)$ - the operator describing interaction with obstacles (Eq.2.3),

$\hat{\Pi}_w(\{\underline{R}_f\},R_{wf},\omega)$ - the operator describing penetration through a building facade (Eq.2.3),

1. INTRODUCTION

The development of the modern civilization brings into human life, as a by-product, still growing noise. The problem is especially urgent in transportation. The growing number of cars causes environmental pollution where noise is one of factors. On the other hand, development in sciences offers the acoustical field description of better accuracy. New techniques in metrology allow monitoring of environmental noise. A Combination of these abilities with the up-date technical measures against noise gives the ground for efficient policy in noise abatement [1-8].

An action against noise can be undertaken at its source, on its propagation path to an observation point, or at the observation point. The subject of this work is outdoor noise propagation in an urban area. Generally, the most efficiently noise abatement problem can be solved at the stage of planning. To this end, a tool for noise prediction is needed. The general procedure of noise prediction in urban area (environmental noise model) has to contain a source model, a propagation model and an observer perception characteristics. Three kinds of treatment are involved:

- development of empirical formulae,
- scale modeling of a site,
- construction of analytical model.

For construction of the source model [9-15] the way of the simplified analytical models is used. The models describing a source radiation in the half-space contain the averaged values of the parameters established by field measurements.

For construction of the propagation model all three kinds of the treatments are applied. The empirical model, founded on a large number of measurements, can offer a general description of noise propagation in a built-up area. The generality of the description is achieved at the expense of accuracy, as it is in the case when the urban system is described only by a single

parameter: the ratio of the ground area of buildings to the site area [16].

The scale modeling with, for example, the scale factor 1:30 raises a lot of problems of the site modeling with proper frequency dependence [17,18]. The investigation with such a scale factor requires the special instrumentation and is not easily adjustable to a change of the sites. More advisable is the application of scale models for a small segment of a built-up area [18-21] or investigation of some special effects such as, for example, transmission between rooms through windows, in a built-up area [22]. For such cases the scale factor $(1/d) > 0.1$ does not create so many problems in modeling.

The most flexible and widely applicable are the analytical models. They may be applied at various stages of an urban area designing. They are cheaper than individual data collecting for the empirical formulae, more useful than scale-modeling and more universal than both of them. The principal problem is how to describe the acoustical field in a space with reflecting obstacles. This is the common case for noise propagation in industrial halls, offices, concert halls, and from highways into the urban area. One of the possibilities is a determined simulation of the wave paths. Another possibility is offered by the statistical description of acoustical energy distribution.

By use of the statistical description, the part of acoustical field caused by an enclosure existence (difference between the total field and the free field) can simply be the reverberant field [23-26]. The description is valid under special conditions concerning an enclosure size and its walls features [27-29].

In the case of large industrial halls and offices the acoustical field is mostly governed by processes of collisions with fitting. By modeling the acoustic energy distribution as phonon random walk in a fitted space, the statistical description is applied [30-33]. As the fitting, generally, is irregular in shape and position, the diffusion equation is applied to the

spreading of acoustical energy [34]. For this kind of rooms also the special models, being combinations of the geometrical acoustics and the diffusion process, are developed [35-38]. The mutual comparison of the models [39] give the ground for an estimation of their application ranges.

The same statistical description, as that used for industrial halls, can be applied for a built-up area [40-43]. For a built-up area with loosely scattered, independent houses, the diffusion model is advised. Then, the probability of sound energy scattering depends on the obstacles space density. In the extreme, this description leads to application of the diffusion equation [44-46]. For the case of a heavy built-up area, the determined model is more advisable. There, the sound pressure is watched how it changes, after all possible interactions with obstacles, on the path from a source to an observation point.

The general procedure of finding the sound field in a limited space requires solution of the wave equation for the appropriate boundary conditions what results in the sum of normal modes of an enclosure. The limitation is constituted by the shape of the boundary which has to allow a separation of variables [47-49]. For complicated cases, the equation can be solved by the finite-difference method [50-52]. This allows to describe the field in complex acoustical systems (limited space with obstacles). Obstacles can be of any shape with acoustical properties given by the surface normal impedance.

In practice, the geometrical acoustics is more frequently applied to enclosures than the wave theory. It is used in a form of the ray-tracing procedure [53-55] and the image method [56-58]. For a built-up area, the propagation model of the image-sources is preferred. In the cases of noise propagation between buildings it is used to represent the specular reflections from buildings walls [59-65].

In the model which simulates waves propagation in the space with obstacles, as the elementary phenomena are treated:

- spreading of the acoustical wave in the space,
- interaction of the acoustical wave with obstacles.

By assumption that the spreading occurs in an ideal medium at rest, the medium inhomogeneity and weather conditions are left apart, and the main attention is paid to the multiple interactions with obstacles.

In the noise abatement, the obstacles are treated as objects providing the acoustical shadow. The diffraction accounts for the field in shadow regions. The simplest obstacle, purposely applied on the wave path as a measure against noise, is a plane acoustical screen. For such a screen - regarded as an ideal half-plane of zero acoustical velocity or pressure on its surface - exists the exact solution by MacDonald [66] describing the field around the obstacle due to the point source. Also, the exact solution exists for the half-plane of one side ideally soft and other ideally hard [67,68], and for the half-plane defined by the finite surface normal impedance [69,70].

The Kirchhoff diffraction theory, assuming nonreflective opaque screen, combined by Maekawa with experimental data, results in the expression [71] which is widely used in acoustical practice. Rubinowicz, developing the Kirchhoff theory, provides the procedure which allows to take into account reflections from an obstacle surface and the effects caused by its edges (wedges) separately. The effects connected with edges, described as diffraction, are presented in a form of the linear integral along edges [72]. The both methods of diffraction calculation are widely applied to screen-type obstacles. For barriers being screens of limited length and, also, for screens with edges of more complicated shape, the theories are applied independently to their straight segments into which edges can be divided [71-76]. The diffraction theories of Kirchhoff and Rubinowicz find its justification in the far field approximation of the exact solution and their accuracy can be assessed [77,78].

Generally, broad obstacles can be treated as

three-dimensional objects with wedges. The interaction with the obstacle as a whole can be obtained by the combinations of the solutions describing the wave interaction with a wedge created by obstacle walls [66, 79-82]. In noise abatement problems, some practical approximations are used [83-87]. The expressions contain reflections from the obstacles impedance walls and diffraction at wedges. As in the case of multi-wedges obstacle the interactions between wedges are possible, the double and higher order diffraction occur. This effect can be described by use of the Keller geometrical theory of diffraction [88,89].

Generally, when the efficiency of an obstacle playing a role of acoustical screen is deal with, the description of its interaction with environment is needed. It is important as this interaction causes the degradation of the screen efficiency [90]. The simplest example is the screen on the ground. In the case of impedance ground the applied description has been founded on the known canonical solution of diffraction at edges and reflection from an impedance plane [91-93]. The same way of description has been used for the two parallel screens along highway [94-96]. The screen efficiency in a shallow room has been described by use of the mirror image method with application of the Maekawa expression [97,98]. For more complex acoustical systems as it is in concert halls, where several reflections and diffractions are considered, the Rubinowicz theory has been applied [99-102]. For an urban system the description including multiple reflections and the single diffraction at screens edges has been applied [103,104]. The description containing multiple reflections and multiple diffractions has also been prepared [13], where for multiple diffraction the Keller geometrical theory of diffraction has been used in the form developed for a building wedges [105]. The three methods [13,103,104] result in the computer simulation programs which can be used in the acoustical climate forecasting.

The aim of this work is to construction the environmental noise model offering a general procedure, describing an arbitrary

sequence of wave interactions with obstacles, which has to be suitable for computer simulation. In the general environmental noise model the attention is focused on the detailed description of noise propagation in a built-up area (Chap.2) where the elements of the waves theory are included. It means that multiple reflections and multiple diffractions are considered. Since any source can be modeled by point sources of a given power spectrum, the propagation model is prepared for the unit simple-harmonic point source. As such, the propagation model can simply be identified with the transfer function of the urban system.

The wave interaction with obstacles, composed of limited panels, is divided into:

- transmission through panels,
- reflections from panels,
- diffraction at wedges (edges).

For urban area, where dimensions of buildings are large enough in relation to the wavelength predominant in traffic noise, the high frequency approximation are justified. The used description of diffraction is in a form of a product of the undisturbed wave and the diffraction coefficient. Of the same form are descriptions of transmission and reflection, taking into account that for reflection, the undisturbed wave is emitted by the image source. Thus, all the three kinds of interactions, as having the uniform description, can be used to build up a chain of interactions to which the wave subjected to on its path from the source to the observation point. The chain can contain an arbitrary number of interactions in an arbitrary sequence.

The description of diffraction used here differs from the Keller geometrical theory in this that it is related to the undisturbed wave at the observation point while in the Keller theory it is related to the incident wave at the wedge. As the Keller diffraction theory is an extension of the ray tracing theory, the presented description can be treated as an extension of the image method. The presented propagation model can be used

for all the systems for which the high frequency approximation (far field conditions) is an appropriate one, and where transmissions, reflections from panels and diffraction at their wedges are the predominant processes.

The most important components in the acoustical energy calculation are a few first reflections. The diffraction is introduced into the propagation model to make the total field smooth at the boundaries of shadow and reflection waves and to eliminate the regions where the sound level tends to minus infinity. It is possible that a smooth field can be obtained after summation of a large number of reflections, but preparing a simulation program computation time strongly increases. The addition of diffraction smooths the field offering a more precise physical description and saves the computation time.

The patterns of propagation model have been proved during scale indoor experiments. The interactions in a system which comprises the ground, a plane screen and a building facade have been investigated. The screen and facade were parallel, thus, depending on the order of interactions, all possible sequences of interactions were present. The first series of experiments [19] has been performed in the frequency domain, with use of diffraction description coming from the asymptotic expression of MacDonald solution [66]. The second series [20] has been carried on in the time domain, with the expression for diffraction given according to the Rubinowicz theory [72]. Both diffraction theories applied in theoretical description, for far field conditions, reduce to the action of secondary source at a wedge.

As the obstacles are assumed to be constructed of panels, the elements with which a wave interacts, are wedges of a given inner angle, among which a plane screen is the special case. The interaction with these basic elements are presented in Chap.3.

The total acoustical field at the observation point is the sum of terms resulted from the different paths by which the wave can reach the observation point. The multiple interactions with

obstacles on the wave path, forming the terms of the total acoustical field, are described in Chap.4 where the total acoustical field is divided into geometrical and diffraction parts. The processes containing only transmission and reflections compose the geometrical part of the field. When diffraction appears between transmission and reflections, the process is ascribed to the diffraction part of the field. Making use of the vast literature on multiple reflections [57, 58, 106-109], the efficient procedure describing multiple interactions has been prepared [110-112] where the diffraction part contains single and double diffraction. Now, the diffraction terms are presented in a general form describing an arbitrary chain of the three kinds of interactions: transmission, reflection, diffraction.

In Chap.5 the applicability of the environment noise model are analyzed where it shown how the developed model, with use of state-of-the-art in computers application, can be used as an efficient tool in the computer system for soundscape designing.

In Appendix are presented the results of the early prepared PROP3 computer program. The PROP3 computer program has been prepared for the two options. The first option as the source model contains point sources emitting the signal of a given spectrum. These sources can be used for a complex source model construction. The second option contains the highway model [14] as highways are the predominant noise sources in urban area. The PROP3 has been adjusted to obstacles (buildings) whose shape can be approximated by the shoe-box. The plane acoustical screens have been also included. The double diffraction at the parallel building wedges and at the edges of two parallel screens have been taken into account. As examples the shielding efficiency of the single building and of the system of buildings in an urban area have been calculated [110,111,113].

2. NOISE MODEL CONSTRUCTION

2.1. Noise propagation through an urban area

In order to solve the noise abatement problem in urban area the model of environmental noise, offering the procedure of the sound equivalent level calculation, is needed. Formally, it can be presented in the form:

$$L_{eq}[dB(A)] = \hat{\Pi}_o(...)\ \hat{\Pi}(...)\ Q(...), \qquad (2.1)$$

where the source model is represented by $Q(...)$, the operator $\hat{\Pi}(...)$ describes wave propagation, the operator $\hat{\Pi}_o(...)$ - the human perception.

It is widely discussed how to determine the noise annoyance objectively [114-120]. Despite of all doubts, following the ISO recommendation, the sound equivalent level is used for rating the annoyance in legislation. Thus, the operator $\hat{\Pi}_o(...)$, acting on the acoustical pressure coming from the action of the propagation operator on the the source (Eq.2.1), should give the sound equivalent level. In the time domain the sound equivalent level is defined by the time average

$$L_{eq}[dB(A)] = 10 \log \left\{ \frac{1}{T} \int_{-T/2}^{T/2} \left[p_A^2(t)/p_o^2 \right] dt \right\}, \qquad (2.2)$$

$$p_o = 2\ 10^{-5}\ N/m^2$$

where $p_A(t)$ is the A-weighted sound pressure observed at the observation point during the time interval T. In the frequency domain it means calculation of the A-weighted mean sound energy level (Chap.5).

The operator $\hat{\Pi}(...)$ can be taken as describing the probability of interactions [40-46] or in the deterministic form [13,103,104,111,113].

Herein, the determined model is proposed where the propagation operator $\hat{\Pi}(...)$ can incorporate three groups of events: attenuation in a propagation medium, interaction with obstacles, penetration into buildings

$$\hat{\Pi}(...) = \hat{\Pi}_w(\underline{R}_f, R_{wf}, \omega)\ \hat{\Pi}_s(\underline{R}, \eta, R_w, \omega)\ \hat{\Pi}_a(R, \kappa, \omega). \qquad (2.3)$$

The operator $\hat{\Pi}_a(R,\kappa,\omega)$, describing attenuation in the air, depends on:

- R - distance travelled in the air,
- κ - set of parameters describing the air as a propagation medium (density, temperature, wind velocity...),
- ω - angular frequency.

The air in the vicinity of highway has not composition of the standard air under the normal conditions. It is caused by pollution generated by vehicles [121]. Depending on the shaping of the surrounding terrain and meteorological conditions, the pollution distribution changes with distance and height. Thus, pollution causes not only the changes of air composition but also inhomogeneity of the propagation medium, and, as a result, the refraction in addition to this caused by temperature gradient [7]. The meteorological conditions, especially wind velocities, are the parameters whose influence is hard to be precisely described. In spite of these difficulties it should be borne in mind that the predominant wind can affect the L_{eq} in noticeable extend [122-131]. In practice, the attenuation in the air as a statistical process, can be expressed in the form of exponential decay with a travelled distance R:

$$p(P) = p_{id}(P)\exp(-\gamma R), \qquad (2.4)$$

where $p_{id}(P)$ is the acoustical pressure at the point P in an ideal medium, and the attenuation coefficient

$$\gamma = \gamma(\omega,T,H,CO_2,\ldots), \qquad (2.5)$$

is a function of an angular frequency ω, temperature T, humidity H, pollution concentration (e.g. CO_2), and other air parameters. When only the simple relation to the travelled distance is observed, with the attenuation coefficient dependence on the first three parameters (Eq.2.5), the attenuation in the air can be easily introduced into the propagation model [132]. However, in the presented model it is temporally disregarded.

The operator $\hat{\Pi}_s(\{\underline{R}\},\{Z\},\{R_w\},\omega)$, describing interaction with obstacles, depends on:

$\{\underline{R}\}$ - set of vectors describing obstacle geometry,

$\{Z(\omega)\}$ - set of normal surface impedances of obstacles,

$\{R_w(\omega)\}$ - set of insulations of obstacles.

Generally, the explicit form of the operator $\hat{\Pi}_s(\{\underline{R}\},Z,R_w,\omega)$ depends on that how the obstacles are described and what kinds of interactions are taken into account. It is the subject of this work to find the operator $\hat{\Pi}_s(\{\underline{R}\},Z,R_w,\omega)$.

The operator $\hat{\Pi}_w(\{\underline{R}_f\},\{R_{wf}\},\omega)$, describing penetration through a building facade into the rooms, depends on:

$\{\underline{R}_f\}$ - set of vectors describing facade geometry,

$\{R_{wf}(\omega)\}$ - set of insulations of facades.

In spite of attempts to describe the penetration of sound through such structures as building windows [59,133-135] there is lacking the efficient theoretical description of sound penetration through the facade of reach shape (balconies, decoration elements,...) and inhomogeneous insulation (windows). These problems are left apart in the presented environmental noise model and the sound level is estimated in front of a building facade.

In the operator $\hat{\Pi}_s(\ldots)$ two types of interactions can be separated:

$$\hat{\Pi}_s(\ldots) = \hat{\Pi}_{SB}(\ldots)\ \hat{\Pi}_{SD}(\ldots). \qquad (2.6)$$

The operator $\hat{\Pi}_{SB}(\ldots)$ contains description of interactions at a small distance comparing with wavelength ($kR<<1$), the operator $\hat{\Pi}_{SD}(\ldots)$ - interactions at a large distance ($kR>>1$). The division is made as a consequence of using two different asymptotic expressions of interactions for the two extreme regions where the behavior of waves shows substantial differences.

The operator $\hat{\Pi}_{SB}(\ldots)$ is needed when interactions at elements of a building facade such as balconies, architectural details surrounding windows, and the like, are considered. These effects are left apart in the presented model as obstacles are assumed to be modeled by panels whose dimensions are larger than the length of the wave under consideration. Thus, the large-distance approximation seems to be an appropriate one for noise propagation in urban area when the A-weighting of sound energy is borne in mind.

The other substantial problem of the environmental noise model in urban area (Eq.1.1) is the source model $Q(\ldots)$. It is possible to find the determined model for some stationary sources present in a built-up area. However, the most frequent noise sources in an urban area are transportation routes, especially, highways. Thus, the appropriate determined stationary model, equivalent to the real noise generation by a highway, is searched for.

A highway as a noise source consists of moving, individual vehicles. First, the individual vehicle model as a noise source has to be established. The predominant noise sources in a vehicle are: an engine, an exhaust, tires, and a case. The emitted noise depends on the vehicle brand, type, maintenance, operating parameters (e.g. gear used), moving speed and the kind of road surface [136-143].

Observing all these changeable parameters, vehicles have been divided into classes and for each of them the equivalent point source is introduced. The equivalent source is characterized by the acoustical power level [144-150] and the height above the ground [151]. This model of a vehicle as a noise source is valid in the far field conditions.

A lot of attention is paid to the statistics of the vehicle flow [152-160]. The investigations give the ground for the highway noise fluctuation analyses and prediction of such noise indices as L_1, L_{10}, L_{50}, L_{90}. Though, for calculation of the sound equivalent level L_{eq} in a given period of time, it is enough to know the mean flow rate of vehicles of the i-class, on the j-lane of highway [132,152,161].

The highway model, introduced into the environmental noise model in urban area (Eq.2.1), which comprise point sources of given power spectra, allows to prepare the noise propagation model for the unit simple-harmonic point source Q(S).

2.2. Propagation model construction

The wave from the unit simple-harmonic point source Q(S), after propagation through a built-up area, produces at the observation point the acoustical pressure

$$p(P) = \hat{\Pi}\,(\ldots)\,Q(S). \tag{2.7}$$

The above relation represents the transfer function of an urban system which is searched for.

The appropriate explicit form of the operator $\hat{\Pi}(\ldots)$ which describes propagation in an urban area has to be found. As it was mentioned above, the problem is limited to establishing the operators describing the interactions with obstacles. It means that propagation is assumed in an ideal medium with disregarding

the air attenuation, and that the acoustical pressure is given in front of a building facade, with omitting transmission through a building facade into the room.

The urban system under consideration is represented by the semi-space with obstacles. The obstacles are modeled by panels. The plane acoustical screen is represented by a single panel. The buildings are approximated by the shoe-boxes.

Since obstacles dimensions and their distances are large in relation to the wavelength predominant in the A-weighted traffic spectrum, the large-distance approximation ($kR >> 1$) is justified.

The large-distance interaction with obstacle constructed of panels can be divided into reflection and transmission through a panel, treated as unlimited one, and diffraction at the wedges (edges). Thus, the operator $\hat{\Pi}(...)$ (Eq.2.7) contains the sum of the parallel chains of the elementary interactions of transmission, reflection and diffraction at wedges (edges):

$$\hat{\Pi}(...) = \sum_{i} T[...,C(i)_s,...] * ...* R[...,A(i)_p,...] * ...*$$

$$* D[...,E(i)_m,...] * ... \qquad (2.8)$$

Each i-chain describes the different wave path to the observation point (Fig.2.1). The operators T(...), R(...), D(...) give the kind of interaction while $C(i)_s$, $A(i)_p$, $E(i)_m$ are the points at the s-panel, p-panel and m-wedge (edge), respectively, where the interactions occur during travelling over the i-path.

The operator T(S,P) describes spreading in the empty space. When it acts on the simple-harmonic source Q(S) of the unit strength, at point S:

$$T(S,P)\ Q(S) = \frac{\exp[ikR(S,P)]}{R(S,P)}, \qquad (2.9)$$

then it gives the undisturbed spherical wave at the observation

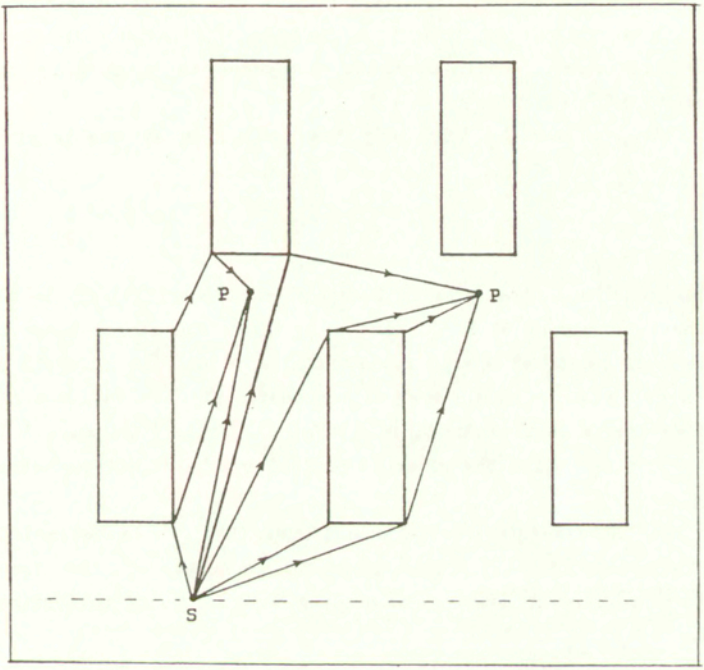

Fig.2.1. The different wave paths to the observation point.

point P.

Transmission through the semi-transparent plane of the transmission coefficient T also results in the empty space transmission:

$$T(S,C,P)\ Q(S) = T(C)\ T(S,P)\ Q(S). \qquad (2.10)$$

Now, the source strength equals that of the source at S times, the transmission coefficient of the panel $T(C)$. The point C is the transmission point at which the panel is punched by the direct path from S to P.

The operator R(S,A,P) describes reflection at the point A from the plane of the reflection coefficient R:

$$R(S,A,P)\ Q(S) = R(A)\ T(S',P)\ Q(S). \qquad (2.11)$$

This results in transmission from the point source at S' to the observation point at P. The source at S' is the mirror image of the real source at S with respect to the plane. The strength of the source at S' equals that of the source at S it is image of, times the reflection coefficient $R(A)$. The reflection point A is the point at which the panel is punched by the direct path from S' to P.

As the transmission operator T(S,P) (Eq.2.9) is defined in relation to the (S,P)-distance, the concept of the image observation point can also be used in description of reflection. Then

$$R(S,A,P)\ Q(S) = R(A)\ T(S,P')\ Q(S), \qquad (2.12)$$

where P' is the mirror image of the real observation point at P with respect to the plane.

The operator describing diffraction at a wedge (edge):

$$D(S,E,P)\ Q(S) = D(\nu;S,P)\ T(S,P)\ Q(S), \qquad (2.13)$$

is proportional to the undisturbed wave (Eq.2.9) by the coefficient $D(\nu;S,P)$. The point E is the active point at the wedge (edge), e. g. the point through which passes the shortest path from the source at S to the observation point at P (Fermat principle). The coefficient $D(\nu;S,P)$ is the function of the wedge kind, described by the parameter ν, and the source $S(\rho_0,\varphi_0,z_0)$ and the observation point $P(\rho,\varphi,z)$ positions which are given in the coordinates system with z-axis identical with the wedge (edge). The angle $\nu\pi=2\pi-2\Omega$ presents the outer space of the wedge of the inner angle 2Ω.

To describe the diffraction coefficient the approximate solution for the ideally hard wedge is used [66]. Basing on these solutions it is possible to divide the field into connected pair of the geometrical wave and diffracted one, related to the same primary source [162]. The geometrical wave make the jump at its boundary of existence, the diffracted wave is to smooth this jump. The same what is true for the pair when the reflection coefficient is equal to one, is true for other values of reflection coefficient. Thus, the shape of a wedge decides the form of diffracted wave. The reflection feature of wedge surfaces, defined by reflection coefficients, result in multiplication of reflection wave by an appropriate reflection coefficient. Therefore, the same has to be done with the connected diffracted wave which has to smooth field at geometrical boundaries. This concept has its confirmation in the solution where the Keller geometrical theory of diffraction has been applied [163]. The procedure is also used in acoustical practice when impedance wedges are dealt with [83-87].

Here, the diffraction coefficient is adopted in the form which is valid far from geometrical boundary. Near boundary it is approximated by its maximum value which is reached at the boundary [111,112].

An extension in obstacle shapes is possible. For obstacles whose shape can be approximate by other shapes than wedges, the

diffraction coefficient can be found from the canonical solutions [66].

According to the assumption of the large-distance interactions, transmission and reflection are treated as the interaction with an unlimited plane, being extension of an limited panel up to infinity. The interaction with the wedges is regarded as an independent process (Chap.3).

The reflection process is described by reflection coefficient known from the solution of a spherical wave propagation over an impedance ground [7,85,164-171]. It has the form which depends on the source and observation positions. For the large-distance interaction which is dealt with, the spherical wave reflection coefficient can be approximated by the plane wave reflection coefficient which depends only on the incident wave angle [7,168]. In presented model the average value coming from the reverberation absorption coefficient is assumed to make the propagation model presentation more clear. However, the spherical reflection coefficient can be introduced into interaction chains in the same way as the diffraction coefficient.

Transmission of sound is only important for a thin obstacle like a plane acoustical screen because a building as a whole is an opaque obstacle. The transmission process depends on the insulation property of the panel and can be presented in the form of the insulation coefficient [172].

The transmission and reflection coefficients, which both can be a function of frequency, constitute the acoustical parameters of panels, obtained experimentally. The recent sound intensity technique starts to provide the data of reflection and insulation coefficients measured in situ [174-179].

The above description of interactions with obstacles is referred to the point at which the interaction takes place. Thus, the reflection and transmission coefficients depend on the place of interactions. This gives the opportunity to deal with obstacles of inhomogeneous surfaces. For example windows at a

building facade, as having the different refection coefficient than the surrounding facade, can be taken under consideration. In this case the jump of the reflection coefficient causes diffraction at boundaries where the jump appears, it means, at a window framing.

In the presented model, all the three kinds of interactions are linear in relation to the undisturbed wave due to the appropriate source. The proportional coefficients are transmission, reflection and diffraction coefficients (Eqs.2.9-13). The transmission and reflection coefficients are regarded as the panel acoustical parameters. The reflection process specifics requires determination of the image-source position S'. The specifics of diffraction requires calculation of diffraction coefficient, defined by the source and the observation point position in relation to the wedge.

Since the acoustical wave can reach the observation point by different chains of the three kinds of interactions with panels composing obstacles, for the system containing N panels, and interactions up to the K-order, the acoustical pressure at the observation point is:

$$p(P) = \sum_{k=1}^{K} \sum_{i=1}^{I(N,k)} \hat{\Pi}^{i}_{k'}(n) * \ldots * \hat{\Pi}^{i}_{1}(n)\, Q(S) =$$

$$= \sum_{k=1}^{K} \sum_{i=1}^{I(N,k)} \prod_{k'=1}^{k} \hat{\Pi}^{i}_{k'}(n)\, Q(S). \qquad (2.14)$$

The i-sequence of the set of operators $[\hat{\Pi}^{i}_{k}(n),\ldots,\hat{\Pi}^{i}_{1}(n)]$, describing the i-path, is one of the possible combinations of 3N elements of the set of transmission, reflection and diffraction operators $\{\hat{\Pi}(n)\}$, taken k at a time.

The interaction with the n-panel is given by:

$$\hat{\Pi}(n) = \begin{cases} T\left(S^{(p)},C_n,P^{(r)}\right) = T(C_n)\ T\left(S^{(p)},P^{(r)}\right), \\ R\left(S^{(p)},A_n,P^{(r)}\right) = R(A_n)\ T\left(S^{(p,n)},P^{(r)}\right) = \\ \qquad = R(A_n)\ T\left(S^{(p)},P^{(n,r)}\right), \\ D\left(S^{(p)},E_{m(n)},P^{(r)}\right) = \\ \qquad = D\left(\nu;S^{(p)}[m(n)],P^{(r)}[m(n)]\right)\ T\left(S^{(p)},P^{(r)}\right) \end{cases} \tag{2.15}$$

where the source at $S^{(p)}$ and the point $P^{(r)}$ describe the wave history before and after interaction with the n-panel, respectively. The source at $S^{(p,n)}$ is the mirror image of the source at $S^{(p)}$ with respect to the n-panel. The point $P^{(n,r)}$ is the mirror image of the source $P^{(r)}$ with respect to the n-panel. For each diffraction process, occurring at the m(n)-wedge of the n-panel, the source at $S^{(p)}$ and observation point $P^{(r)}$ positions are given in the different local coordinates system with z-axis identical with the m(n)-wedge.

As transmission does not change the radiating source position, only appearance of reflection in the chain of interaction influences the diffraction coefficient. When reflection occurs before diffraction then, in the diffraction coefficient, appears the image source of appropriate order, describing the wave history before diffraction. Reflection after diffraction results in appearance of the appropriate image observation point, describing the wave history after diffraction.

The total acoustical field p(P), for large-distance interactions, is the sum of the geometrical part $p^g(P)$ and the diffraction part $p^d(P)$:

$$p(P) = p^g(P) + p^d(P). \tag{2.16}$$

The geometrical part $p^g(P)$ contains the terms being chains of transmissions and reflections. The terms are represented by waves

emitted by the set of point sources. These sources are: the real source and the image sources of appropriate order, representing all the possible reflections. Since the point source is assumed, it is completely defined by its position and strength which, in the cases of transmission and reflections, is proportional to the transmission and reflection coefficients, respectively.

The chains of interactions containing, at least, one diffraction process are terms of the diffraction part of the field $p^d(P)$. The diffraction is assumed to be one of the elementary processes on the wave path. Diffraction of the wave from the real source, as an independent process, means a creation of the secondary source of diffraction waves at the wedge. The wave before reaching the wedge can be transmitted through and reflected from panels. This results in creation of a set of image sources. Next, these sources create the secondary sources at the wedge. Transmissions and reflections on the wave paths after diffraction can be represented by a set of image secondary sources of diffraction waves created at the wedge or a set of image observation points. Here, the both concepts are applied.

The explicit forms of the terms of acoustical field in its geometrical $p^g(P)$ and diffraction $p^d(P)$ parts are presented in Chap.4.

3. INTERACTION WITH PANELS

3.1. Interaction with a wedge

Let us analyze the wave interaction with the wedge formed by the two panels of reflection coefficients $R(n)$, $R(n+1)$, respectively (Fig.3.1). The wedge as a whole is assumed to be opaque. The geometrical part of the field around it is

$$p^{g}_{n,n+1}(P) =$$

$$= \eta(C_n)\, T(S,P)\, Q(S) + \eta(C_{n+1})\, T(S,P)\, Q(S) + \qquad (3.1)$$

$$+ \eta(A_n)\, T(S^{(n)},P)\, Q(S) + \eta(A_{n+1})\, T(S^{(n+1)},P)\, Q(S).$$

The first two terms in Eq.3.1 describe the direct wave. The factors $\eta(C_n)$ $\eta(C_{n+1})$ give the regions where the direct wave exists:

$$\eta(C_n) = \begin{cases} 0, & C_n \in (n)\text{-panel}, \\ 1, & C_n \notin (n)\text{-panel}, \end{cases} \qquad (3.2)$$

$$\eta(C_{n+1}) = \begin{cases} 0, & C_{n+1} \in (n+1)\text{-panel}, \\ 1, & C_{n+1} \notin (n+1)\text{-panel}, \end{cases} \qquad (3.3)$$

where C_n ,C_{n+1} are the transmission points at the plane of the n-panel and (n+1)-panel, respectively.

The third term in Eq.3.1 describes the wave reflected from the n-panel of reflection coefficient $R(n)$, represented by the source at $S^{(n)}$. The factor $\eta(A_n)$ gives the regions where the reflected wave exists:

$$\eta(A_n) = \begin{cases} R(n), & A_n \in (n)\text{-panel}, \\ 0, & A_n \notin (n)\text{-panel}, \end{cases} \qquad (3.4)$$

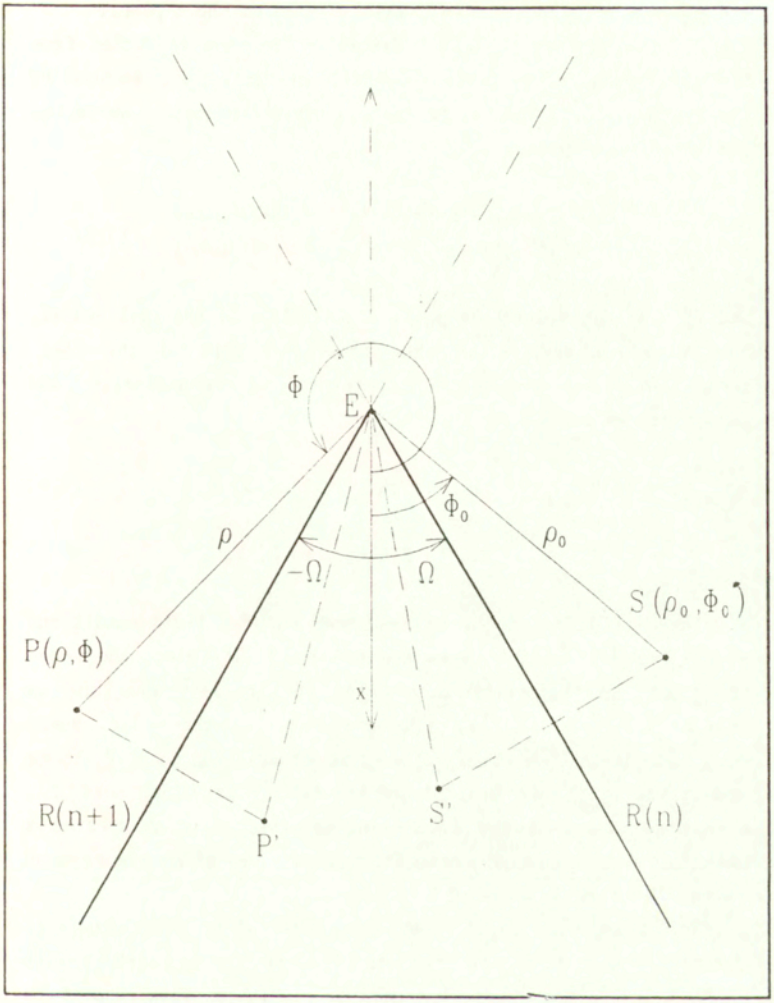

Fig.3.1. The layout for the case of the wave interaction with the wedge.

and A_n is the reflection point at the plane of the n-panel.

The fourth term in Eq.3.1 describes the wave reflected from the (n+1)-panel of reflection coefficient $R(n+1)$, represented by the source $S^{(n+1)}$. The factor $\eta(A_{n+1})$ gives the regions where the reflected wave exists:

$$\eta(A_{n+1}) = \begin{cases} R(n+1), & A_{n+1} \in (n+1)\text{-panel}, \\ 0, & A_{n+1} \notin (n+1)\text{-panel}. \end{cases} \qquad (3.5)$$

and A_{n+1} is the reflection point at the plane of the (n+1)-panel.

The above results in the geometrical part of the field containing the appropriate operators of transmission and reflection as below:

$$p^{g}_{n,n+1}(P) = T(S,C_n,P)\ Q(S) + T(S,C_{n+1},P)\ Q(S) + \qquad (3.6)$$

$$+ R(S,A_n,P)\ Q(S) + R(S,A_{n+1},P)\ Q(S).$$

The diffraction field is described for far field conditions where four diffraction waves are present [162]. Since the wedge walls act as reflection panels for the incident wave and as baffles for the secondary sources created at the wedge, apart from the real source at S and the real observation point P, there appear the image source at S' and the image observation point P'. Each combination of the source and observation point creates a pair representing one of the diffraction waves which are present in the whole outer space of the wedge.

The source $S(\rho_0,\varphi_0,z_0)$ and the observation point $P(\rho,\varphi,z)$ positions are given in the coordinates system with z-axis identical with the wedge. The real source images with respect to the n-panel and (n+1)-panel are:

$$S^{(n)} = S(\rho_0, 2\Omega-\varphi_0, z_0), \qquad (3.7)$$

$$S^{(n+1)} = S[\rho_0, 2(2\pi-\Omega)-\varphi_0, z_0]. \tag{3.8}$$

The same is for the observation points:

$$P^{(n)} = P(\rho, 2\Omega-\varphi, z), \tag{3.9}$$

$$P^{(n+1)} = P[\rho, 2(2\pi-\Omega)-\varphi, z]. \tag{3.10}$$

The diffraction part of the field resulted from interactions with the wedge is

$$p^{d}_{n,n+1}(P) = D(S,E,P)\ Q(S) + D(S,E,P')\ Q(S) + \tag{3.11}$$
$$+ D(S',E,P)\ Q(S) + D(S',E,P')\ Q(S),$$

where

$$D(S,E,P)\ Q(S) = T(E,P)\ D\begin{bmatrix}S\\E\\P\end{bmatrix} T(S,E)\ Q(S) = \tag{3.12}$$
$$= D(\nu;S,P)\ T(S,P)\ Q(S),$$

$$D(S,E,P')\ Q(S) = T(E,P')\ D\begin{bmatrix}S\\E\\P\end{bmatrix} T(S,E)\ Q(S) = \tag{3.13}$$
$$= \begin{cases} R(n)\ D(\nu;S,P^{(n)})T(S,P^{(n)})\ Q(S), \\ R(n+1)\ D(\nu;S,P^{(n+1)})\ T(S,P^{(n+1)})\ Q(S), \end{cases}$$

$$D(S',E,P)\ Q(S) = T(E,P)\ D\begin{bmatrix}S\\E\\P\end{bmatrix} T(S',E)\ Q(S) = \tag{3.14}$$
$$= \begin{cases} R(n)\ D(\nu;S^{(n)},P)\ T(S^{(n)},P)\ Q(S), \\ R(n+1)\ D(\nu;S^{(n+1)},P)\ T(S^{(n+1)},P)\ Q(S), \end{cases}$$

$$D(S',E,P')\ Q(S) = T(E,P')\ D\begin{bmatrix}S\\E\\P\end{bmatrix} T(S',E)\ Q(S) = \tag{3.15}$$

$$= \begin{cases} R(n)\ R(n)\ D(\nu;S^{(n)},P^{(n)})\ T(S^{(n)},P^{(n)})\ Q(S), \\ R(n)\ R(n+1)\ D(\nu;S^{(n)},P^{(n+1)})\ T(S^{(n)},P^{(n+1)})\ Q(S), \\ R(n+1)\ R(n)\ D(\nu;S^{(n+1)},P^{(n)})\ T(S^{(n+1)},P^{(n)})\ Q(S), \\ R(n+1)\ R(n+1)\ D(\nu;S^{(n+1)},P^{(n+1)})\ T(S^{(n+1)},P^{(n+1)})\ Q(S). \end{cases}$$

For each possible source-point pair (S^*,P^*), when their appropriate coordinates (Eqs.3.8-10) are taken, the diffraction coefficient is given by

$$D(\nu;S^*,P^*) = P(\nu;\varphi_o^*,\varphi^*)\ D^s(R^*,\rho_o,\rho)\ V^c(R^*,R_e,\rho), \tag{3.16}$$

$$P(\nu;\varphi^*,\varphi_o^*) = \frac{1}{2\nu}\ \sin(\pi/\nu)\ \frac{1}{\cos\dfrac{\pi}{\nu} - \cos\dfrac{(\varphi^* - \varphi_o^*)}{\nu}}, \tag{3.17}$$

$$D^s(R^*,\rho_o,\rho) = \frac{R^*}{\sqrt{R_e\ \rho_o}}, \tag{3.18}$$

$$V^c(R^*,R_e,\rho) = \frac{\exp\{i[k(R_e-R^*)+\pi/4]\}}{\sqrt{2\pi k\rho}}, \tag{3.19}$$

$$R^* = \sqrt{R_e^2 - 4\rho_o\rho\ \cos^2[(\varphi^*-\varphi_o^*)/2]}, \tag{3.20}$$

$$R_e = \sqrt{(\rho_o+\rho)^2 + (z-z_o)^2}\ . \tag{3.21}$$

After putting into Eqs.3.12-15 expressions Eqs.3.16-21 with appropriate coordinates, the diffraction part of the field (Eq.3.11) can be expressed in relation to the real source $S(\rho_o,\varphi_o,z_o)$ and real observation point $P(\rho,\varphi,z)$ positions.

The terms in Eq.3.11 take on the forms:

$$D(S,E,P)\ Q(S) = \tag{3.22}$$

$$= P_1(\nu;\varphi_o,\varphi)\ D^s(R,\rho_o,\rho)\ V^c(R,R_e,\rho)\ T(S,P)\ Q(S),$$

$$D(S,E,P')\ Q(S) = \tag{3.23}$$

$$= \begin{Bmatrix} R(n) \\ R(n+1) \end{Bmatrix} P_2(\nu;\varphi_o,\varphi)\ D^s(R,\rho_o,\rho)\ V^c(R,R_e,\rho)\ T(S,P)\ Q(S),$$

$$D(S',E,P)\ Q(S) = \tag{3.24}$$

$$= \begin{Bmatrix} R(n) \\ R(n+1) \end{Bmatrix} P_2(\nu;\varphi_o,\varphi)\ D^s(R,\rho_o,\rho)\ V^c(R,R_e,\rho)\ T(S,P)\ Q(S),$$

$$D(S',E,P')\ Q(S) = \tag{3.25}$$

$$= \begin{Bmatrix} R(n)\ R(n) \\ R(n)\ R(n+1) \\ R(n+1)\ R(n) \\ R(n+1)\ R(n+1) \end{Bmatrix} P_1(\nu;\varphi_o,\varphi)\ D^s(R,\rho_o,\rho)\ V^c(R,R_e,\rho)\ T(S,P)\ Q(S),$$

where

$$P_1(\nu;\varphi,\varphi_o) = \frac{1}{2\nu}\sin(\pi/\nu)\ \frac{1}{\cos\dfrac{\pi}{\nu} - \cos\dfrac{(\varphi-\varphi_o)}{\nu}}, \tag{3.26}$$

$$P_2(\nu;\varphi,\varphi_o) = \frac{1}{2\nu}\sin(\pi/\nu)\,\frac{1}{\cos\frac{\pi}{\nu}+\cos\frac{2\pi-(\varphi+\varphi_o)}{\nu}}. \qquad (3.27)$$

Here, the intention is to make the m-wedge the independent linear object where the interaction takes place. It means to present the diffraction coefficient dependence on the panels reflection coefficients $R(n)$, $R(n+1)$ as an average effect. The approximate expression has been found:

$$p_m^d(P) = D(S,E_m,P)\,Q(S) =$$

$$= \eta(S,E_m,P)\,T(S,P)\,Q(S), \qquad (3.28)$$

where

$$\eta(S,E_m,P) = \begin{cases} D[\nu;S(m),P(m)], & E_m \in (m)\text{-edge}, \\ 0, & E_m \notin (m)\text{-edge}, \end{cases} \qquad (3.29)$$

$$D[\nu;S(m),P(m)] = \qquad (3.30)$$

$$= \eta(\varphi_m-\Omega)\,\eta(2\pi-\Omega-\varphi_m)\,P(\nu;\varphi_{om},\varphi_m)\,D^{s(c)}(R,\rho_{om},\rho_m)\,V^c(R,R_{em},\rho_m),$$

The point E_m is the active point at the m-edge. According to the Rubinowicz theory [72] only vicinity of the point E_m effectively participates in radiation of the cylindrical wave emitted by the wedge. Thus, for the wedge of limited length, the relation Eq.3.29 is established.

The factors $\eta(\varphi_m-\Omega)\,\eta(2\pi-\Omega-\varphi_m)$ (Eq.3.30) represent the simple step functions providing that the real observation point cannot lie in the inner space of the wedge (Fig.3.1).

In Eq.3.30 the factor

$$P(\nu;\varphi_{om},\varphi_m) = \alpha(m)\ P_1(\nu;\varphi,\varphi_o) + \beta(m)\ P_2(\nu;\varphi,\varphi_o), \qquad (3.31)$$

combines the secondary source directional factors $P_1(\nu;\varphi,\varphi_o)$, $P_2(\nu;\varphi,\varphi_o)$ (Eqs.3.26,3.27) with the averaged reflection properties of the m-wedge, where

$$\alpha(m) = 1 + (1/4)\ [R(n) + R(n+1)]^2, \qquad (3.32)$$

$$\beta(m) = R(n) + R(n+1). \qquad (3.33)$$

Substitution $R(n)=R(n+1)=1$ results in the well known directional factor $P(\nu;\varphi_{om},\varphi_m)$ for the hard wedge. For $R(n)\neq R(n+1)\neq 1$ the factor

$$P(\nu;\varphi_m,\varphi_{mo}) = \frac{1}{\nu}\ \sin(\pi/\nu) \left\{ \frac{[\alpha(m)/2]}{\cos\frac{\pi}{\nu} - \cos\frac{(\varphi_m-\varphi_{om})}{\nu}} + \right. \qquad (3.34)$$

$$\left. + \frac{[\beta(m)/2]}{\cos\frac{\pi}{\nu} + \cos\frac{2\pi-(\varphi_m+\varphi_{om})}{\nu}} \right\}.$$

represents the directional patterns of the wave emitted by the m-wedge of the given reflection properties (Eqs.3.32,3.33).

When the spherical wave reaches the wedge, as it is in the case of the wave emitted by the real source Q(S), the deformation factor in Eq.3.30 is:

$$D^s(R,\rho_{om},\rho_m) = \frac{R}{\sqrt{R_{em}\ \rho_{om}}}. \qquad (3.35)$$

When the wave reaching the wedge is of the cylindrical type [112], as it is during diffraction of order higher than one, then:

$$D^{c}(R,\rho_m) = \sqrt{\frac{R}{\rho_{om}}}\,. \tag{3.36}$$

In Eq.3.30 the factor

$$V^{c}(R,R_{em},\rho_m) = \frac{\exp\{i[k(R_{em}-R)+\pi/4]\}}{\sqrt{2\pi k\rho_m}}, \tag{3.37}$$

represents the cylindrical wave radiated by the m-wedge where:

$$R = \sqrt{R_{em}^2 - 4\rho_{om}\rho_m\cos^2[(\varphi_m-\varphi_{om})/2]}, \tag{3.38}$$

$$R_{em} = \begin{cases} \sqrt{(\rho_{om}+\rho_m)^2+(z_m-z_{om})^2}, & \text{for spherical incident wave} \\ \rho_{om}+\rho_m, & \text{for cylindrical incident wave.} \end{cases} \tag{3.39}$$

For the observation point in the outer space of the m-wedge, when the point E_m belongs to the m-wedge of limited length then the diffraction can be understood as radiation of the linear source at m-wedge

$$T(E_m,P)\ Q[E_m(S)] = \tag{3.40}$$

$$= P(\nu;\varphi_{om},\varphi_m)\left[D^{s(c)}(R,\rho_{om},\rho_m)\ T(S,P)\ Q(S)\right] V^{c}(R,R_{em},\rho_m),$$

as it represents transmission through the space of the cylindrical wave $V^{c}(R,R_{em},\rho_m)$ (Eq.3.37) borne at the m-wedge. The source at the m-wedge is the secondary source of the complex amplitude given by $[D^{s(c)}(R,\rho_{om},\rho_m)\ T(S,P)\ Q(S)]$ and of the directional patterns given by $P(\nu;\varphi_{om},\varphi_m)$.

According to Eqs.3.6, 3.28-39 the field, resulted from wave interaction with the m-wedge formed by the n-panel and (n+1)-

panel, now is:

$$p_{n,n+1}(P) = p^{g}_{n,n+1}(P) + p^{d}_{m}(P) = \tag{3.41}$$

$$= T(S,C_n,P)\ Q(S) + T(S,C_{n+1},P)\ Q(S) +$$

$$+ R(S,A_n,P)\ Q(S) + R(S,A_{n+1},P)\ Q(S) +$$

$$+ D(S,E_m,P)\ Q(S).$$

As it follows from the above, a building of the shoes-box shape placed on the ground, in interaction with a wave, is represented by five panels: four side-panels and one as a roof, and the three pairs of parallel, right angle wedges of $\nu=3/2$. For the edge of half-plane $\nu=2$. Screens and buildings walls, placed perpendicular to the ground, construct with the ground surface the inner space of right angle wedge for which $\nu=1/2$. In the last case, when the acoustical velocity or pressure equals zero at the wedge walls, then there is no diffraction but geometrical field (Eq.3.34). This is approximately true for near hard walls of a wedge. In urban area, interactions with wedges of other inner angle than the right one are also met. For example, at wedges of a canyon which is passed through by a highway. The procedure of description is the same but the appropriate value of a wedge parameter ν has to be used.

3.2. Interaction with a plane screen

The n-panel, playing the role of an acoustical screen, can be semi-transparent. The wave interactions with it comprise: transmission through the panel, reflection from it and diffractions caused by its M edges. When the panel is placed on the ground, and it is assumed that the right angle wedge formed

by the screen and the ground do not cause diffraction, then M=3. The acoustical field due to the unit simple-harmonic point source at S, created by interactions with the n-panel, can be written in the form containing all possible components of the total field:

$$p_n(P) = \eta^d(C_n)\ T(S,P)\ Q(S) + \eta(A_n)\ T(S^{(n)},P)\ Q(S) + \\ + \sum_{m=1}^{3} \eta(S^{dr},E_m,P)\ T(S,P)\ Q(S) + \\ + \eta^t(C_n)\ T(S,P)\ Q(S) + \sum_{m=1}^{3} \eta(S^t,E_m,P)\ T(S,P)\ Q(S)\ . \qquad (3.42)$$

The first term in Eq.3.42 describes the direct wave. The factor $\eta^d(C_n)$ gives the regions where the direct wave exists:

$$\eta^d(C_n) = \begin{cases} 0, & C_n \in \text{(n)-panel}, \\ 1, & C_n \notin \text{(n)-panel}, \end{cases} \qquad (3.43)$$

where C_n is the transmission point at the plane of the n-panel.

The second term in Eq.3.42 describes the wave reflected from the n-panel of reflection coefficient $R(n)$, represented by the source at $S^{(n)}$. The factor $\eta(A_n)$ gives the regions where the reflected wave exists:

$$\eta(A_n) = \begin{cases} R(n), & A_n \in \text{(n)-panel}, \\ 0, & A_n \notin \text{(n)-panel}, \end{cases} \qquad (3.44)$$

and A_n is the reflection point at the plane of the n-panel.

The third term in Eq.3.42 is the diffraction term which contains the diffraction effect of the direct and reflected waves. The factor $\eta(S^{dr},E_m,P)$ for the m-edge is:

$$\eta(S^{dr},E_m,P) = \begin{cases} D[\nu;S^{dr}(m),P(m)], & E_m \in \text{(m)-edge}, \\ 0, & E_m \notin \text{(m)-edge}, \end{cases} \qquad (3.45)$$

The diffraction coefficient $D[\nu;S^{dr}(m),P(m)]$ is given by Eqs.3.30-39, where $\nu=2$ has to be substituted. This gives:

$$D[\nu;S^{dr}(m),P(m)] = \tag{3.46}$$

$$= P(\nu=2;\varphi_{om},\varphi_m)\ D^{s(c)}(R,\rho_{om},\rho_m)\ V^c(R,R_{em},\rho_m),$$

$$P(\nu=2;\varphi_m,\varphi_{mo}) = -\frac{1}{2}\left\{\frac{[\alpha(m)/2]}{\cos\frac{(\varphi_m-\varphi_{om})}{2}} + \frac{[\beta(m)/2]}{\cos\frac{(\varphi_m+\varphi_{om})}{2}}\right\}. \tag{3.47}$$

Here, the coefficients $\alpha(m)$, $\beta(m)$ provide opportunity for consideration of a screen which has a different reflection coefficients on its opposite sides.

The fourth term in Eq.3.42 describes the wave transmitted through the n-panel of transmission coefficient $T(n)$. The source of transmitted wave is at the same position as the real source but has the strength equal to $T(n)$. The factor $\eta(C_n)$ gives the regions where the transmitted wave exists:

$$\eta^t(C_n) = \begin{cases} T(n), & C_n \in \text{(n)-panel}, \\ 0, & C_n \notin \text{(n)-panel}, \end{cases} \tag{3.48}$$

The fifth term in Eq.3.42 describes the diffraction waves connected with the source of transmitted wave. For these waves the n-panel is an opening in the screen created by the plane complemental to the n-panel. It means that the z-axis along the m^t-edge is of the opposite sign than this one along the m-edge. The screen reflection coefficient $R(1)$, $R(2) = 0$ (Fig.3.2). Thus, the source $S(m^t)$ and observation point $P(m^t)$ positions, in relation, to the m-edge are:

$$S(m^t) = S(\rho_{om},\pi+\varphi_{om},z_{om}), \tag{3.49}$$

$$P(m^t) = P(\rho_m, \varphi - \pi, z). \tag{3.50}$$

Substitution of the coordinates (Eqs.3.49,3.50) into expressions Eqs.3.29-39 results in:

$$\eta(S^t, E_m, P) = \begin{cases} D[\nu; S^t(m), P(m)], & E_m \in (m)\text{-edge}, \\ 0, & E_m \notin (m)\text{-edge}, \end{cases} \tag{3.51}$$

$$D[\nu; S(m^t), P(m^t)] = \tag{3.52}$$

$$= P(\nu=2; \varphi_{om}^t, \varphi_m^t)\ D^{s(c)}(R, \rho_{om}, \rho_m)\ V^c(R, R_{em}, \rho_m),$$

$$P(\nu=2; \varphi_{om}^t, \varphi_m^t) = \frac{1}{2} \frac{[T(n)/2]}{\cos \frac{(\varphi_m - \varphi_{om})}{2}}. \tag{3.53}$$

The diffraction field containing all the waves diffracted at the m-edge is:

$$p^d(S, E_m, P) = \eta(S^{dr}, E_m, P)\ T(S,P)\ Q(S) + \eta(S^t, E_m, P)\ T(S,P)\ Q(S) =$$

$$= \eta(S, E_m, P)\ T(S,P)\ Q(S), \tag{3.54}$$

where

$$\eta(S, E_m, P) = \begin{cases} D[\nu; S(m), P(m)], & E_m \in (m)\text{-edge}, \\ 0, & E_m \notin (m)\text{-edge}, \end{cases} \tag{3.55}$$

$$D[\nu; S(m), P(m)] = \tag{3.56}$$

$$= P(\nu=2; \varphi_{om}, \varphi_m)\ D^{s(c)}(R, \rho_{om}, \rho_m)\ V^c(R, R_{em}, \rho_m),$$

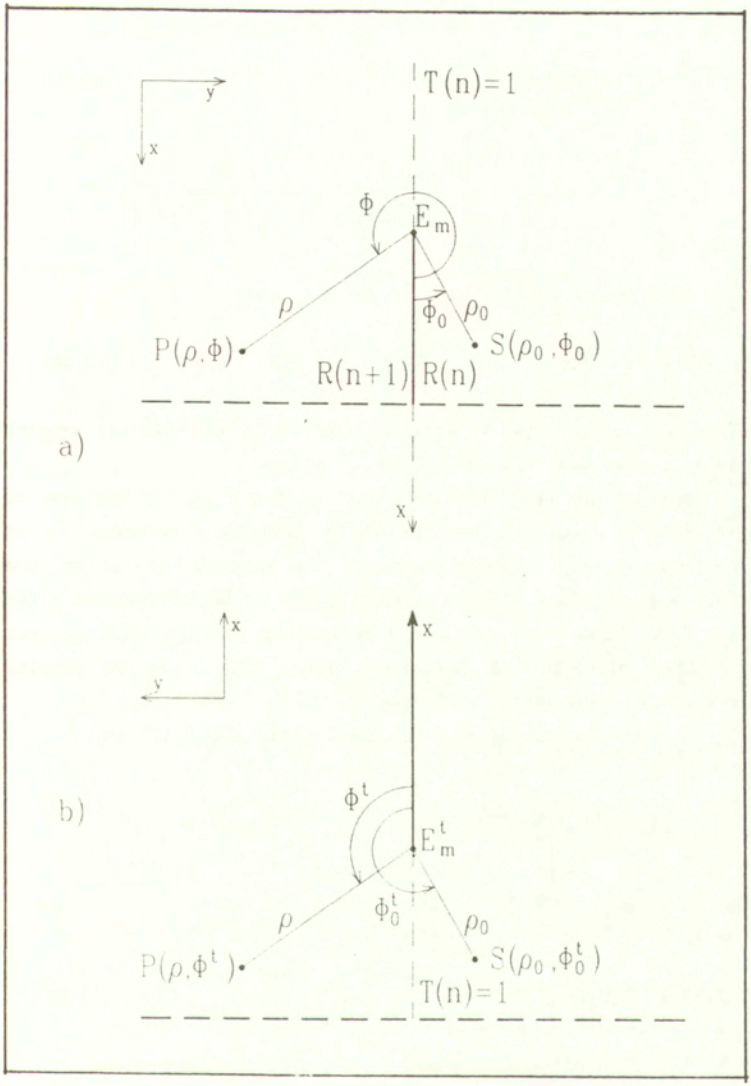

Fig.3.2. The layout for the case of the wave interaction with a semi transparent plane screen: a) action of the real source, b) action of the source of transmitted wave.

$$P(\nu=2;\varphi_m,\varphi_{mo}) = \tag{3.57}$$

$$= -\frac{1}{2}\left\{\frac{[\alpha^t(m)/2]}{\cos\frac{(\varphi_m-\varphi_{om})}{2}} + \frac{[\beta(m)/2]}{\cos\frac{(\varphi+\varphi_o)}{2}}\right\}.$$

The coefficient $\beta(m)$ is given by Eq.3.33 and

$$\alpha^t(m) = [1 - T(n)] + (1/4)\,[R(1) + R(2)]^2. \tag{3.58}$$

The coefficient $\alpha^t(m)$ is equal to $\alpha(m)$ (Eq.3.32) when the n-panel is an opaque one ($T(n)=0$).

Summing up, the diffraction part of the field in the case of interaction with the m-wedge of an arbitrary parameter ν is described by Eqs.3.28-39, where for the special case of an edge $\nu=2$, and, in place of $\alpha(m)$ (3.32), it has to be substituted $\alpha^t(m)$ (Eq.3.58). The transmission and reflection coefficients, present in the definition of parameters $\alpha(m)$, $\beta(m)$, can be complex quantities dependent upon frequency.

The geometrical part of the total field (Eq.3.42) is:

$$p^g(P) = p^t(S,C_n,P) + p^r(S,A_n,P) = \tag{3.59}$$

$$= \eta(C_n)\;T(S,P)\;Q(S) + \eta(A_n)\;T(S^{(n)},P)\;Q(S),$$

where

$$\eta(C_n) = \eta^d(C_n) + \eta^t(C_n) = \begin{cases} T(n), & C_n \in (n)\text{-panel}, \\ 1, & C_n \notin (n)\text{-panel}, \end{cases} \tag{3.60}$$

and

$$\eta(C_n)\;T(S,P)\;Q(S) = T(S,C_n,P)\;Q(S), \tag{3.61}$$

$$\eta(A_n)\ T(S^{(n)},P)\ Q(S) = R(S,A_n,P)\ Q(S). \qquad (3.62)$$

The diffraction part of the total field (Eq.3.42) is:

$$\sum_{m=1}^{3} p^d(S,E_m,P) = \sum_{m=1}^{3} \eta(S,E_m,P)\ T(S,P)\ Q(S), \qquad (3.63)$$

where:

$$\eta(S,E_m,P)\ T(S,P)\ Q(S) = D(S,E_m,P)\ Q(S). \qquad (3.64)$$

According to Eqs.3.59-64 the field resulting from wave interaction with the n-panel playing the role of a plane acoustical screen placed on the ground (Eq.3.42), now, is:

$$p_n(P) = T(S,C_n,P)\ Q(S) + R(S,A_n,P)\ Q(S) + \sum_{m=1}^{3} D(S,E_m,P)\ Q(S). \qquad (3.65)$$

4. ACOUSTICAL FIELD IN AN URBAN SYSTEM

As it has be shown in Chap. 3, from the point of view of a wave interaction, the urban system can be regarded as a composition of N panels and M wedges (some of them can be edges). By panels the wave is transmitted through and reflected from, by wedges it is diffracted, thus:

$$\left.\begin{array}{l} \left.\begin{array}{l} T(\ldots,C_n,\ldots) \\ R(\ldots,A_n,\ldots) \end{array}\right\} = \hat{\Pi}(n) \\ D(\ldots,E_m,\ldots) \quad = \hat{\Pi}(m) \end{array}\right\} = \hat{\Pi}(\mu). \qquad (4.1)$$

The set of operators $\{\hat{\Pi}(\mu)\}$ describing all the possible interactions contains 2N+M elements. It means that the number of operators is equal to the number of elements of the urban system with which a wave can independently interact. The wave i-path, on which k interactions are assumed, is described by the i-sequence of the operators $[\hat{\Pi}^{i}_{k}(\mu),\ldots,\hat{\Pi}^{i}_{1}(\mu)]$. It is an ordered combination of 2N+M operators, taken k at a time. In the i-sequence the same operator can appear more than once. In combinatorics, such i-sequence is called the k-tuple of the 2N+M elements of the set $\{\hat{\Pi}(\mu)\}$ with repetitions [180].

Now, the geometrical and diffraction part of the field (Eq.2.14) can be rewritten:

$$p^{g}(P) = \sum_{k=1}^{K} \sum_{i=1}^{I(N,k)} \prod_{k'=1}^{k} \hat{\Pi}^{i}_{k'}(n)\, Q(S), \qquad (4.2)$$

$$p^{d}(P) = \sum_{k=1}^{K} \sum_{i=1}^{I(N,M,k)} \prod_{k'=1}^{k} \hat{\Pi}^{i}_{k'}(\mu)\, Q(S). \qquad (4.3)$$

where the number of interactions is assumed to be taken up to the K-order.

The geometrical part of the field $p^g(P)$ is composed of the terms containing only transmissions and reflections. The diffraction part of the field $p^d(P)$ apart of transmissions and reflections contains the terms in which, at least, once appears diffraction. In extreme, the diffraction term can contain K diffractions operators, what means that on this path a wave is K-fold diffracted.

The different sequence of operators, acting on the source Q(S), gives different terms (waves) in Eqs.4.2, 4.3. The product of operators is non-commutative because the positions of transmission, and reflection points on panels, and the active points at wedges (edges) are determined by the position of the point where is the source of the incident wave for the process, and the position of the point at which the next interaction takes place [110].

4.1. Geometrical field

The geometrical part of the field (Eq.4.2) contains the sum of waves reaching the observation point by different paths, where the wave suffers subsequent transmissions and reflections. The i-path of wave, on which it suffers k interactions, is described by the i-sequence of operators $[\hat{\Pi}^i_k(n),\ldots,\hat{\Pi}^i_1(n)]$. It is one of the possible ordered combinations of 2N elements of the set of operators $\{\hat{\Pi}(n)\}$, taken k at a time.

The procedure of tree structure is useful in generation of the sequence of operators describing the i-path [110,180]. The only restriction applied in the procedure of tree structure is that the two neighbor operators in the sequence cannot concern the same n-panel. The number I(N,k) of terms in the geometrical field (Eq.4.2) is equal to the number of paths by which the wave can reach the observation point only by sequences of k

transmissions and reflections. For the set of operators $\{\hat{\Pi}(n)\}$ of 2N elements, the number of the i-paths at which k interaction appear is

$$I(N,k) = 2N\ (2N-2)^{k-1}, \qquad N > 1, \qquad (4.4.)$$

For interactions taken up to the K-order the total number of terms in the geometrical part of the field (Eq.4.2) is:

$$\sum_{k=1}^{K} I(N,k) = 2N\ \frac{(2N-2)^{K} - 1}{2N - 3}. \qquad (4.5)$$

In Eq.4.2 as one of the first order geometrical terms appears the term of k=1, which presents the direct wave (Eq.2.9). The other first order geometrical terms result from the single transmission through the panels and the single reflection from them.

The second order geometrical terms result from action of any combination of the pair of transmission, and reflection operators (T * T *), (R * R *), (T * R *), (R * T *).

The waves, twice reflected, first from the n-panel, next from the p-panel, give the acoustical pressure:

$$\begin{aligned} p^{g}(S,A_n,A_p,P) &= R(S,A_p,P)\left[R(S,A_n,P)\ Q(S)\right] = \\ &= \eta(A_n)\ \left[R(S,A_p,P)\ T(S^{(n)},P)\ Q(S)\right] \qquad (4.6) \\ &= \eta(A_n)\ \eta(A_p)\ T(S^{(n,p)},P)\ Q(S), \end{aligned}$$

where $S^{(n,p)}$ is the mirror image of the source at $S^{(n)}$ with respect to the p-panel, and the source $S^{(n)}$ is the mirror image of the real source at S with respect to the n-panel.

The total geometrical field (Eq.4.2) at the point P contains the product

$$\prod_{k'=1}^{k} \hat{\Pi}^{i}_{k'}(n) = \tag{4.7}$$

$$= \prod_{k'=1}^{k-1} \hat{\Pi}^{i}_{k'}(n) * \left\{ \begin{array}{l} T\left(S^{(\ldots,*,\ldots,P,\ldots)}, C(i)_n, P\right) \\ R\left(S^{(\ldots,*,\ldots,P,\ldots)}, A(i)_n, P\right) \end{array} \right\},$$

where, as the last interaction, can be transmission or reflection at the points $C(i)_n$, $A(i)_n$ of one of n-panels, respectively. The same is possible at others places of the product (Eq.4.7).

At the observation point, the acoustical pressure due to the wave which travels the i-path, represented by the i-sequence of operators $[\hat{\Pi}^{i}_{k}(n),\ldots,\hat{\Pi}^{i}_{1}(n)]$, is:

$$p^{g}[S(i),P] = p^{g}(S,\ldots,C(i)_s,\ldots,A(i)_p,\ldots,P) =$$

$$= T(\ldots,P) * \ldots * T[\ldots,C(i)_s,\ldots] * \ldots * \tag{4.8}$$

$$* R[\ldots,A(i)_p,\ldots] * \ldots * T(S,\ldots)\, Q(S).$$

In the i-sequence of k interactions some are transmissions other - reflections, thus

$$k = k_r + k_t. \tag{4.9}$$

where k_t is the number of transmissions, k_r - number of reflections. While the reflections on the i-path create the image source at S(i), the transmissions through the semi-transparent panels affect only the amplitude of the wave due to the source at S(i). After realization of k_r reflections on the i-path, one of the possible image sources of k_r-order results at the point:

$$S^{(\ldots,s,\ldots,p,\ldots,n)} = S(i). \qquad (4.10)$$

Thus, one of the possible sequences of k_r reflections, creating the image source of k_r- order at S(i), mixed with one of the possible sequences of k_t transmissions, establishes the i-path to the observation point.

The acoustical pressure due to the source at S(i) is equal to the acoustical pressure of the wave travelling the physical i-path, defined according to the Fermat principle in the geometrical acoustics. The physical i-path is described by the real source position S, the sequence of transmission points positions $C(i)_s$, reflection points positions $A(i)_p$, and the observation point position P.

The term of acoustical pressure (Eq.4.8) assumes the form:

$$p^q[S(i),P] = \prod_{p=1}^{k_r} \eta[A(i)_p] \prod_{s=1}^{k-k_r} \eta[C(i)_s] \frac{\exp(ikR_i)}{R_i}, \qquad (4.11)$$

which represents the acoustical pressure of the wave from the source at S(i), reaching the observation point P by the i-path, after transmissions at points $C(i)_s$ and reflections at points $A(i)_p$.

The total geometrical field at the point P is given by:

$$p^q(P) = \sum_{k=1}^{K} \sum_{i=0}^{I(N,k)} p^q[S(i),P]. \qquad (4.12)$$

The same is true when the concept of the image observation point is used. The introduction of the image source (Eq.4.10) is equivalent to the introduction of the image point:

$$p^{(n,\ldots,p,\ldots,s,\ldots)} = P(i). \qquad (4.13)$$

In the both concepts the physical i-path is the same as the same are reflection and transmission points $A(i)_p$, $C(i)_s$ and the path length is

$$R_i = [S(i),P] = [S,P(i)]. \qquad (4.14)$$

For each i-path all $A(i)_p$, $C(i)_s$ have to be found. As the panels have limited dimensions, some reflection coefficients appear to be equal to zero (Eqs.3.4, 3.5, 3.44), what means that some i-terms in Eq. 4.12 equals zero. Moreover, a building as a whole constitutes an opaque obstacle, what results in zero value of some transmission coefficient (Eqs.3.2, 3.3). Transmission can occur only through a semi-transparent acoustical screen for which transmission coefficient is given by Eq.3.60. This all diminishes the number of waves (terms in Eq.4.12) which have to be calculated and summed up.

Let us analyze the i-term (Eq.4.12) containing only reflections $k=k_r$. For each sequence of k_r reflections exists the subset of sources at $\{S(i)\}_k$, $k=k_r$. As the total number of reflections is assumed up to $K=K_r$, thus, the full set of sources at $\{\{S(i)\}_k\}_K$, $k=k_r=1,\ldots,K=K_r$, emitting wave reaching the observation point appears. The set of sources contains the real source at S(0) being the source of zero order and image sources (Eq.4.10) of order from the first up to K_r.

The total number of terms in the sum Eq.4.12, what means the number of the image sources, is the function of the number of panels N and the order of reflections K_r, and can be calculated:

$$I(N,K_r) = 1 + \sum_{k_r=1}^{K_r} I(N,k_r) = 1 + N\,\frac{(N-1)^{K_r} - 1}{N - 2}. \qquad (4.15)$$

For example, for five buildings on the ground, and only side walls taking part in reflections, the number of panels N=21. For reflections up to third order ($K_r=3$), the number of sources is:

$$I(N=21,K_r=3) = 8\ 842. \qquad (4.16)$$

Although, the number of active sources is smaller. For a building modeled by four side-panels and one as a roof, reflections between these five panels are impossible. When all obstacles are placed perpendicularly to the ground, there only exist the terms in which the reflection from the ground appears no more than once. As it follows, the terms which do not exist physically can be canceled straight from panels arrangement in the space. This allows saving of calculation time, yet at the stage of establishing the set of sources at $\{\{S(i)\}_k\}_K$.

When reflections between panels constructing a building are eliminated, what means that only one of side-walls of each building can participate in creation of the i-path, then the number of the active sources in the above example is:

$$I_a(N=21,K_r=3) = 842. \qquad (4.17)$$

The real number of terms in Eq.4.12 is smaller than this above due to the fact that panels are limited in dimensions and, depending on the the reflection point positions $A(i)_n$, some reflection coefficients are equal to zero.

In the description of the geometrical part of the field, the large-distance interaction is assumed. Thus, the reflections are presented as the action of image sources (Eq.2.11) or as the presence of image observation points (Eq.2.12). The amplitude of the reflected wave decreases with growth of travelling distance, and as the result of multiplication by the reflection coefficient which amplitude is equal or less than one.

The process of transmission through the semi-transparent panel results only in multiplication of the wave due to the appropriate source by the transmission coefficient (Eqs.2.9,2.10) whose amplitude is equal or less than one.

Therefore, as can be seen from the above, the sums in Eq.4.2 are arranged in such a way that the higher is the order of the term the smaller is its amplitude.

4.2. Diffraction field

4.2.1. Interaction chain with single diffraction

To build up the chain of interactions containing the diffraction process the general description of the process is needed. First, as an action of the secondary source at the active point E_m of the m-wedge, which appears due to the primary source of the wave undisturbed by diffraction (Eq.3.40). Secondly, in the explicit form with the appropriate diffraction coefficient:

$$
\begin{aligned}
p^d(S,E_m,P) &= D(S,E_m,P)\, Q(S) = \\
&= T(E_m,P)\, Q[E_m(S)] = \\
&= T(E_m,P)\, D\begin{bmatrix} S \\ E_m \\ P \end{bmatrix} T(S,E_m)\, Q(S) = \qquad (4.18) \\
&= \eta(S,E_m,P) \left[\frac{T(S,E_m)}{T(S,P)} \right] T(S,P)\, Q(S) = \\
&= \eta(S,E_m,P) \left[\frac{f(S,E_m)}{f(S,P)} \right] \frac{\exp(ikR)}{R}.
\end{aligned}
$$

Here, the case when the source of the undisturbed wave can be the directional one is included. The factor

$$\left[\frac{T(S,E_m)}{T(S,P)}\right] = \left[\frac{f(S,E_m)}{f(S,P)}\right], \tag{4.19}$$

is the source directional ratio where $f(S,E_m)$ is the source directional characteristics in direction to the point E_m, and $f(S,P)$ in direction to the point P, respectively.

In the terms of the diffraction field (Eq.4.3) containing single diffraction, the source of the undisturbed wave for the diffraction process can be the real source and its images of an appropriate order. As the real source is assumed to be an omnidirectional one, the source directional ratio (4.19) equals one. The first order diffraction terms result from diffraction of the direct wave:

$$p^d(S,E_m,P) = D(S,E_m,P)\ Q(S) =$$

$$= T(E_m,P)\ D\begin{bmatrix} S \\ E_m \\ P \end{bmatrix} T(S,E_m)\ Q(S) = \tag{4.20}$$

$$= \eta(S,E_m,P)\ T(S,P)\ Q(S).$$

When, before diffraction, the wave is transmitted through the panel or reflected from it, the second order terms (k=2) appear since they result from action of the two operators (D * T *) or (D * R *). Below is given the acoustical pressure of the wave which before reaching the m-wedge (edge) suffers transmission through the n-panel:

$$p^d(S,C_n,E_m,P) = D(S,E_m,P)\ T(S,C_n,E_m)\ Q(S) =$$

$$= T(E_m,P)\ D\begin{bmatrix} S \\ E_m \\ P \end{bmatrix} T(S,C_n,E_m)\ Q(S) = \qquad (4.21)$$

$$= \eta(C_n)\ T(E_m,P)\ D\begin{bmatrix} S \\ E_m \\ P \end{bmatrix} T(S,E_m)\ Q(S) =$$

$$= \eta(C_n)\ \eta(S,E_m,P)\ T(S,P)\ Q(S).$$

The next situation differs from the above in this that reflection from the p-panel takes place before diffraction:

$$p^d(S,A_p,E_m,P) = D(S,E_m,P)\ R(S,A_p,E_m)\ Q(S) =$$

$$= T(E_m,P)\ D\begin{bmatrix} S \\ E_m \\ P \end{bmatrix} R(S,A_p,E_m)\ Q(S) = \qquad (4.22)$$

$$= \eta(A_p)\ T(E_m,P)\ D\begin{bmatrix} S \\ E_m \\ P' \end{bmatrix} T(S^{(p)},E_m)\ Q(S) =$$

$$= \eta(A_p)\ \eta(S^{(p)},E_m,P)\ T(S^{(p)},P)\ Q(S).$$

The waves after diffraction at wedges (edges), before reaching the observation point, can be subjected to transmission or reflection. Then appear the second order terms (k=2) being product of operators (T * D *) or (R * D *). The acoustical pressure of the wave which straight, after leaving the source S, reaches the m-wedge (edge), next, suffers transmission through the n-panel, and finally reaches the point P is:

$$p^d(S,E_m,C_n,P) = T(E_m,C_n,P)\ D(S,E_m,P)\ Q(S) =$$

$$= T(E_m,C_n,P)\ D\begin{bmatrix} S \\ E_m \\ P \end{bmatrix} T(S,E_m)\ Q(S) = \qquad (4.23)$$

$$= \eta(C_n)\ T(E_m,P)\ D\begin{bmatrix} S \\ E_m \\ P \end{bmatrix} T(S,E_m)\ Q(S) =$$

$$= \eta(C_n)\ \eta(S,E_m,P)\ T(S,P)\ Q(S).$$

In the case when reflection from the r-panel takes place after diffraction, the pressure is:

$$p^d(S,E_m,A_r,P) = R(E_m,A_r,P)\ D(S,E_m,P)\ Q(S) =$$

$$= R(E_m,A_r,P)\ D\begin{bmatrix} S \\ E_m \\ P \end{bmatrix} T(S,E_m)\ Q(S) = \qquad (4.24)$$

$$= \eta(A_r)\ T(E_m,P^{(r)})\ D\begin{bmatrix} S \\ E_m \\ P \end{bmatrix} T(S,E_m)\ Q(S) =$$

$$= \eta(A_r)\ \eta(S,E_m,P^{(r)})\ T(S,P^{(r)})\ Q(S).$$

In the equivalent way the reflection from the r-panel after diffraction at the m-wedge (edge) can be related to the image secondary source $Q^{(r)}[E_m(S)]$ (Fig.4.1). The source $Q^{(r)}[E_m(S)]$ is the mirror image of the source $Q[E_m(S)]$ (Eq.3.40) with respect to the r-panel. In order to keep the proper φ_o-angle (Fig.4.1), the image point $E_m^{(r)}$ at the $m^{(r)}$-wedge (edge) and the image source $S^{(r)}$ have to be used:

$$p^d(S,E_m,A_r,P) = R(E_m,A_r,P)\ D(S,E_m,P)\ Q(S) =$$

$$= R(E_m,A_r,P)\ D\begin{bmatrix} S \\ E_m \\ P \end{bmatrix} T(S,E_m)\ Q(S) = \qquad (4.25)$$

$$= \eta(A_r)\ T(E_m^{(r)},P)\ D\begin{bmatrix} S \\ E_m^{(r)} \\ P \end{bmatrix} T(S^{(r)},E_m^{(r)})\ Q(S) =$$

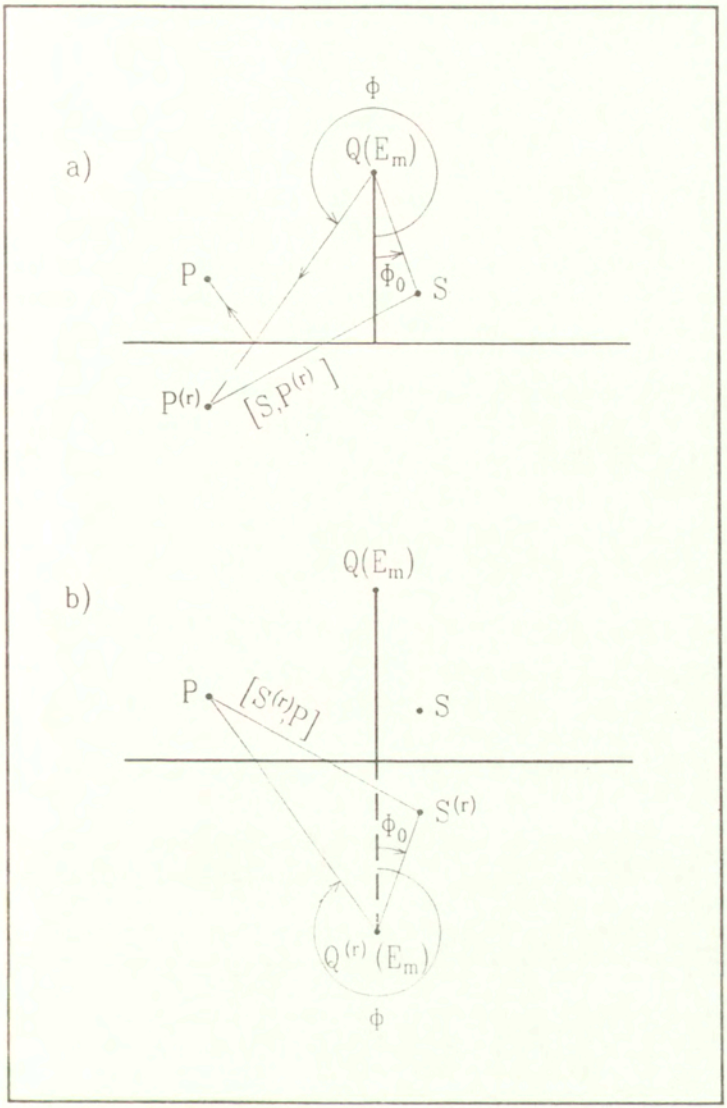

Fig.4.1. The reflection from the r-panel after diffraction at the m-wedge (edge): (a) the image observation point concept, (b) the image secondary source concept.

$$= \eta(A_r)\ \eta(S^{(r)},E_m^{(r)},P)\ T(S^{(r)},P)\ Q(S).$$

The two equivalent descriptions (Eqs.4.24,4.25) are applied in generation of an arbitrary chain of interactions (Chap.4.2.3).

The more complicated case is when the wave, before diffraction, suffers reflection from the p-panel, and after diffraction, is transmitted through the n-panel, then:

$$p^d(S,A_p,E_m,C_n,P) = T(E_m,C_n,P)\ D(S,E_m,P)\ R(S,A_p,E_m)\ Q(S) =$$

$$= T(E_m,C_n,P)\ D\begin{bmatrix}S\\E_m\\P\end{bmatrix} R(S,A_p,E_m)\ Q(S) =$$

$$= \eta(A_p)\ T(E_m,C_n,P)\ D\begin{bmatrix}S\\E_m\\P\end{bmatrix} T(S^{(p)},E_m)\ Q(S) = \qquad (4.26)$$

$$= \eta(A_p)\ \eta(C_n)\ T(E_m,P)\ D\begin{bmatrix}S\\E_m\\P\end{bmatrix} T(S^{(p)},E_m)\ Q(S) =$$

$$= \eta(A_i)\ \eta(C_n)\ \eta(S^{(p)},E_m,P)\ T(S^{(p)},P)\ Q(S).$$

Now, the example when the wave from the source S, before diffraction, is reflected from the i-panel, and after diffraction from the p-panel:

$$p^d(S,A_p,E_m,A_r,P) = R(E_m,A_r,P)\ D(S,E_m,P)\ R(S,A_p,E_m)\ Q(S) =$$

$$= R(E_m,A_r,P)\ D\begin{bmatrix}S\\E_m\\P\end{bmatrix} R(S,A_p,E_m)\ Q(S) =$$

$$= \eta(A_p)\ R(E_m,A_r,P)\ D\begin{bmatrix}S\\E_m\\P\end{bmatrix} T(S^{(p)},E_m)\ Q(S) = \qquad (4.27)$$

$$= \eta(A_p)\ \eta(A_r)\ T(E_m,P^{(r)})\ D\begin{bmatrix} S \\ E_m \\ P \end{bmatrix}\ T(S^{(p)},E_m)\ Q(S) =$$

$$= \eta(A_p)\ \eta(A_r)\ \eta(S^{(p)},E_m,P^{(r)})\ T(S^{(p)},P^{(r)})\ Q(S).$$

The more general case is, when on the wave path from the source at S to the observation point P, between sequences of transmissions and reflections, diffraction occurs. Then the wave path has to be divided into two parts: before diffraction and after diffraction and:

$$p^d[S(i),E_m,P(j)] = \qquad (4.28)$$

$$= p^d(S,\ldots,C(i)_s,\ldots,A(i)_p,\ldots,E_m,\ldots,C(j)_t,\ldots,A(j)_w,\ldots,P) =$$

$$= T(\ldots,P) *\ldots* T[\ldots,C(j)_t,\ldots] *\ldots* R[\ldots,A(j)_w,\ldots] *\ldots$$

$$*\ldots D[\ldots,E_m,\ldots] *\ldots$$

$$* T[\ldots,C(i)_s,\ldots] *\ldots* R[\ldots,A(i)_p,\ldots] *\ldots* T(S,\ldots)\ Q(S).$$

The points S, $C(i)_s$, $A(i)_p$, E_m describe the physical i-path, the points E_m, $C(j)_t$, $A(j)_w$, P - the physical j-path. As on the i-path and the j-path only reflections and transmissions appear, the i-path can be represented by an action of the source at S(i), the j-path by the point P(j), respectively. The wave, after travelling the i-path, creates the secondary source $Q[E_m[S(i)]]$ at the point E_m (Eq.3.40). The wave from this source, travelling the j-path, reaches the observation point P(j). Then the chain of interaction is represented by :

$$p^d[S(i),E_m,P(j)] = \qquad (4.29)$$

$$= \prod_{p=1}^{k_r(i)} \eta[A(i)_p] \prod_{s=1}^{k(i)-k_r(i)} \eta[C(i)_s] \prod_{t=1}^{k_r(j)} \eta[A(j)_t] \prod_{w=1}^{k(j)-k_r(j)} \eta[C(j)_w] *$$

$$* T[E_m,P(j)]\, Q[E_m[S(i)]].$$

As it comes from Eqs.4.18-25, calculation of the diffraction coefficient at the m-wedge needs representation of the path before diffraction in the form of the image source at S(i), while the path after diffraction - in the form of the image observation point P(j). Thus, the terms of the diffraction field (Eq.4.3) of k-order, $k=k(i)+k(j)+1$, which contains $k_r=k_r(i)+k_r(j)$ refections, $k_t=k_t(i)+k_t(j)$ transmissions and the single diffraction, have the form:

$$p^d[S(i),E_m,P(j)] = \tag{4.30}$$

$$= \prod_{p=1}^{k_r(i)} \eta[A(i)_p] \prod_{s=1}^{k(i)-k_r(i)} \eta[C(i)_s] \prod_{t=1}^{k_r(j)} \eta[A(j)_t] \prod_{w=1}^{k(j)-k_r(j)} \eta[C(j)_w] *$$

$$* T[E_m,P(j)]\, D\begin{bmatrix} S \\ E_m \\ P \end{bmatrix} T[S(i),E_m]\, Q(S) =$$

$$= \prod_{p=1}^{k_r(i)} \eta\,[A(i)_p] \prod_{s=1}^{k(i)-k_r(i)} \eta\,[C(i)_s] \prod_{t=1}^{k_r(j)} \eta\,[A(j)_t] \prod_{w=1}^{k(j)-k_r(j)} \eta\,[C(j)_w] *$$

$$* \eta\,[S(i),E_m,P(j)]\, \frac{\exp(ikR_{ij})}{R_{ij}},$$

where

$$R_{ij} = [S(i),P(j)] = [S(i,j),P] = [S,P(j,i)]. \sim \qquad (4.31)$$

Likewise as in the case of the geometrical field (4.12) the terms containing single diffraction between sequences of transmissions and reflections result in propagation of the undisturbed wave due to the source at S which reaches the point P(j,i) or due to the source at S(i,j) which reaches the point P. The interactions are represented by the products of the transmission and reflection coefficients, and by the diffraction coefficient at the m-wedge due to the wave from the source at S(i) which reaches the observation point P(j). Again, some terms of the form given by Eq.4.28 equal zero because obstacles are of limited dimensions and some are opaque ones.

4.2.2. Interaction chain with double diffraction

The double diffraction appears in such cases, for example, when two parallel acoustical screens along a highway are applied, and at building wedges. In the case of the two parallel, long screens, the double diffraction occurs at the upper edges i. e. between the two half-plane edges. In the case of the building on the ground, the three pairs of parallel, right angle wedges can be distinguished. The pair is comprised by the nearest wedges for which the amplitude of the double diffracted wave is expected to be the biggest one.

The double diffraction occurs when the wave due to the source at S creates the secondary source $Q[E_m(S)]$ at the m-wedge (edge). The wave from the source $Q[E_m(S)]$ is assumed to reach the E_{m+1} point of the (m+1)-wedge without any interaction. Thus, the next secondary source $Q\left[E_{m+1}[E_m(S)]\right]$ of higher order appears at the (m+1)-wedge (edge). After this, the wave travels to the observation point P. The process yields

$$p^d(S,E_m,E_{m+1},P) = T(E_{m+1},P)\ Q\left[E_{m+1}[E_m(S)]\right] =$$

$$= T(E_{m+1},P)\ D\begin{bmatrix} S \\ E_{m+1} \\ P \end{bmatrix} T(E_m,E_{m+1})\ Q[E_m(S)] =$$

$$= T(E_{m+1},P)\ D\begin{bmatrix} S \\ E_{m+1} \\ P \end{bmatrix} \left[\frac{T(E_m,E_{m+1})}{T(E_m,P)}\right] * \qquad (4.32)$$

$$* T(E_m,P)\ D\begin{bmatrix} S \\ E_m \\ P \end{bmatrix} T(S,E_m)\ Q(S) =$$

$$= \eta(E_m,E_{m+1},P) \left[\frac{T(E_m,E_{m+1})}{T[E_m,P]}\right] \eta(S,E_m,P)\ \frac{\exp(ikR)}{R},$$

where

$$\left[\frac{T(E_m,E_{m+1})}{T(E_m,P)}\right] = \eta(E_m,E_{m+1})\ \frac{P[\nu_m;\varphi_{om},\varphi_m(E_{m+1})]}{P[\nu_m;\varphi_{om},\varphi_m(P)]}, \qquad (4.33)$$

$$\eta(E_m,E_{m+1}) = \begin{cases} 1, & E_m,E_{m+1} \notin \text{n-panel}, \\ 1/2, & E_m,E_{m+1} \in \text{n-panel}, \end{cases} \qquad (4.34)$$

represents the source $Q[E_m(S)]$ directional ratio as it is defined in Eq.4.19. The step function $\eta(E_m,E_{m+1})$ (Eq.4.34) is introduced to differ the two situations when the m-wedge (edge) and (m+1)-wedge (edge) belong or not to the same n-panel. In the former case the source at the m-wedge (edge) acts as a source in a baffle. Therefore, the strength of the source $Q[E_m(S)]$, representing the source at the m-wedge (edge) in the free space,

has to be equal to the half of the strength of the source at the m-wedge (edge).

In Eq.4.32 the factor

$$T(E_m,P)\, D\begin{bmatrix} S \\ E_m \\ P \end{bmatrix} T(S,E_m)\, Q(S) = D(S,E_m,P)\, Q(S) =$$

$$= \eta(S,E_m,P)\, T(S,P)\, Q(S) = \qquad (4.35)$$

$$= T(E_m,P)\, Q[E_m(S)] = p^d(S,E_m,P),$$

represents the wave $p^d(S,E_m,P)$ due to the source $Q[E_m(S)]$ which would reach the observation point without the second diffraction at the (m+1)-wedge (edge). The diffraction coefficient $\eta([S,E_m,P)$ is given by Eqs.3.29-39 where the source position $S(\rho_{om},\varphi_{om},z_{om})$ and the observation position $P(\rho_m,\varphi_m,z_m)$ have to be given in the coordinates system with z-axis identical with the m-wedge (edge).

The m-wedge (edge) acts as a directional source radiating the wave of cylindrical type (Eq.3.40). It constitutes the source for the second diffraction process at the (m+1)-wedge (edge). When the second diffraction occurs, the wave from this source has to be multiplied by the diffraction coefficient at the (m+1)-wedge (edge) and by the source $Q[E_m(S)]$ directional ratio (Eq.4.33). The directional factors $P[\nu_m;\varphi_{om},\varphi_m(E_{m+1})]$, $P[\nu_m;\varphi_{om},\varphi_m(P)]$ are given by Eq.3.34 in the coordinates system connected with the m-wedge (edge), where $\varphi_m(E_{m+1})$, $\varphi_m(P)$ are the angular positions of the E_{m+1}-point and P-point, respectively.

As only vicinity of the wedge (edge) point E_m participates noticeably in radiation, the wedge is counted as an active one when the point E_m lies in the m-wedge (edge) limit (Eqs.3.29, 3.55). The positions of E_m-point and P-point are used to determine the shortest distance through the (m+1)-wedge (edge) and to define position of the active point E_{m+1}. From this it can

be judged whether the second diffraction can occur:

$$\eta(E_m, E_{m+1}, P) =$$

$$= \begin{cases} D\left(\nu; E_m(m+1), E_{m+1}, P(m+1)\right), & E_{m+1} \in (m+1)\text{-wedge}, \\ 0, & E_{m+1} \notin (m+1)\text{-wedge}, \end{cases} \tag{4.36}$$

The diffraction coefficient which describes the diffraction of the wave from the source $Q[E_m(S)]$ at the (m+1)-wedge (edge) is:

$$D\left(\nu; E_m(m+1), P(m+1)\right) = \tag{4.37}$$

$$= \eta(\varphi_{m+1} - \Omega)\ \eta(2\pi - \Omega - \varphi_{m+1})\ P(\nu; \varphi_{o(m+1)}, \varphi_{m+1})\ *$$

$$* D^c(R, \rho_{o(m+1)}, \rho_{m+1})\ V^c(R, R_{e(m+1)}, \rho_{m+1}).$$

The factors in Eq.4.37 are expressed for the source position $E_m[\rho_{o(m+1)}, \varphi_{o(m+1)}]$ and the observation point position $P(j)[\rho_{m+1}, \varphi_{m+1}]$ given in the coordinates system with z-axis identical with the (m+1)-wedge (edge). Their explicit forms are defined by Eqs.3.30-39, when the appropriate coordinates are put in. For example, when the two parallel wedges of a building (Fig.4.2) are considered then, in relation to the second wedge, the coordinates of the source for the second diffraction process and observation point are:

$$\rho_{o(m+1)} = d, \tag{4.38}$$

$$\varphi_{o(m+1)}(\nu=2) = \pi/2, \qquad \varphi_{o(m+1)}(\nu=3/2) = \pi/4, \tag{4.39}$$

$$\rho_{m+1} = \sqrt{\rho_m^2 + d^2 - 2\rho_m d \sin[(\pi/4) - \varphi_m]} \tag{4.40}$$

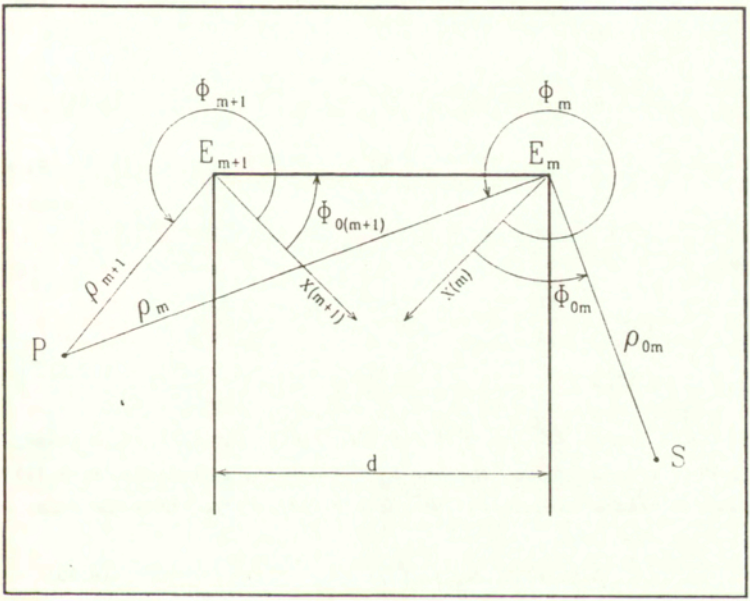

Fig.4.2. The double diffraction at wedges of a building.

$$\varphi_{m+1} = (\pi/4) - \arcsin\left[(\rho_m/\rho_{m+1})\,\sin[(\pi/4)-\varphi_m]\right], \tag{4.41}$$

$$R = \rho_m, \tag{4.42}$$

$$R_{e(m+1)} = d + \rho_{m+1}. \tag{4.43}$$

When before and after double diffraction a sequences of transmissions and reflections occur, the total wave path, as in the case of single diffraction, is divided into the parts: the i-path from S to E_m, the path from E_m to E_{m+1}, and the j-path from E_{m+1} to P. Then:

$$p^d[S(i),E_m,E_{m+1},P(j)] = \tag{4.44}$$

$$= p^d(S,\ldots,C(i)_s,\ldots,A(i)_p,\ldots,E_m,E_{m+1},\ldots,C(j)_w,\ldots A(j)_t,\ldots,P) =$$

$$= T(\ldots,P) *\ldots* T[\ldots,C(j)_t,\ldots] *\ldots* R[\ldots,A(j)_w,\ldots] *$$

$$*\ldots D[E_m,E_{m+1},\ldots]\; D[\ldots,E_m,\ldots] *\ldots$$

$$* T[\ldots,C(i)_s,\ldots] *\ldots* R[\ldots,A(i)_p,\ldots] *\ldots* T(S,\ldots)\; Q(S).$$

The terms of the diffraction field (Eq.4.3) of k-order, $k=k(i)+k(j)+2$, which contains $k_r=k_r(i)+k_r(j)$ refections, $k_t=k_t(i)+k_t(j)$ transmissions, and the double diffraction, have the form:

$$p^d[S(i),E_m,E_{m+1},P(j)] = \tag{4.45}$$

$$= \prod_{p=1}^{k_r(i)} \eta[A(i)_p] \prod_{s=1}^{k(i)-k_r(i)} \eta[C(i)_s] \prod_{t=1}^{k_r(j)} \eta[A(j)_t] \prod_{w=1}^{k(j)-k_r(j)} \eta[C(j)_w] *$$

$$* T[E_{m+1},P(j)]\ D\begin{bmatrix}S\\E_{m+1}\\P\end{bmatrix}\left[\frac{T(E_m,E_{m+1})}{T[E_m,P(j)]}\right] *$$

$$* T[E_m,P(j)]\ D\begin{bmatrix}S\\E_m\\P\end{bmatrix} T[S(i),E_m]\ Q[S(i)] =$$

$$= \prod_{p=1}^{k_r(i)} \eta[A(i)_p] \prod_{s=1}^{k(i)-k_r(i)} \eta[C(i)_s] \prod_{t=1}^{k_r(j)} \eta[A(j)_t] \prod_{w=1}^{k(j)-k_r(j)} \eta[C(j)_w] *$$

$$* \eta[E_m,E_{m+1},P(j)]\left[\frac{T(E_m,E_{m+1})}{T[E_m,P(j)]}\right] \eta[S(i),E_m,P(j)]\ \frac{\exp(ikR_{ij})}{R_{ij}},$$

where

$$R_{ij} = [S(i),P(j)] = [S(i,j),P] = [S,P(i,j)], \tag{4.46}$$

$$\left[\frac{T(E_m,E_{m+1})}{T[E_m,P(j)]}\right] = \eta(E_m,E_{m+1})\ \frac{P[\nu_m;\varphi_{om},\varphi_m(E_{m+1})]}{P[\nu_m;\varphi_{om},\varphi_m(P(j))]}, \tag{4.47}$$

and $\eta(E_m,E_{m+1})$ is given by Eq.4.34.

4.2.3. Arbitrary chain of interactions

The terms in Eq.4.3 are created as the result of an action of the i-sequence of operators $[\hat{\Pi}^i_k(\mu),\ldots,\hat{\Pi}^i_1(\mu)]$ which is one of the possible ordered combinations of 2N+M elements of the set of operators $\{\hat{\Pi}(\mu)\}$, taken k at a time.

In the sequence of k operators describing the wave i-path

$$k = k_t + k_r + k_d, \tag{4.48}$$

where k_t is the number of transmissions, k_r - number of reflections, k_d - number of diffractions.

The number I(N,M,k) of terms of the diffraction field (Eq.4.3) of k-order is equal to the number of paths at which anyone of k-elements combination is possible. By use of the procedure of tree structure, the only applied restriction is that the two neighbor operators in the sequence cannot concern the same n-panel. The restriction concerning transmissions and reflections in the i-sequence, related to panels forming a building and named in connection with the geometrical field, are also valid. The additional restriction concerns the diffraction operator $D(\ldots,E_m,\ldots)$ at the m-wedge (edge) formed by the n-panel and (n+1)-panel. This operator cannot neighbor any operator concerning the n-panel or (n+1)-panel. It is because all the four diffracted waves, connected with the source of a wave creating the secondary source at a wedge, are incorporated into the operator describing diffraction at a wedge (Chap.3.1).

Let us analyze an example of an infinite segment of a depressed road. It means that the propagation is from the source at S in a canyon of the p,t-walls and u-bottom (Fig.4.3). Let us take the wave due to the source at S, first reflected from the p-panel, next diffracted at the (1)-wedge. The further wave path contains reflection from the u-panel, diffraction at the (2)-wedge and, before reaching the observation point P, reflection from the t-panel. This results in:

$$p^d(S,A_p,E_1,A_u,E_2,A_t,P) = \tag{4.49}$$

$$= R(E_2,A_t,P)\, D(S,E_2,P)\, R(E_1,A_u,E_2)\, \left(D(S,E_1,P)\, R(S,A_p,E_1)\, Q(S)\right) =$$

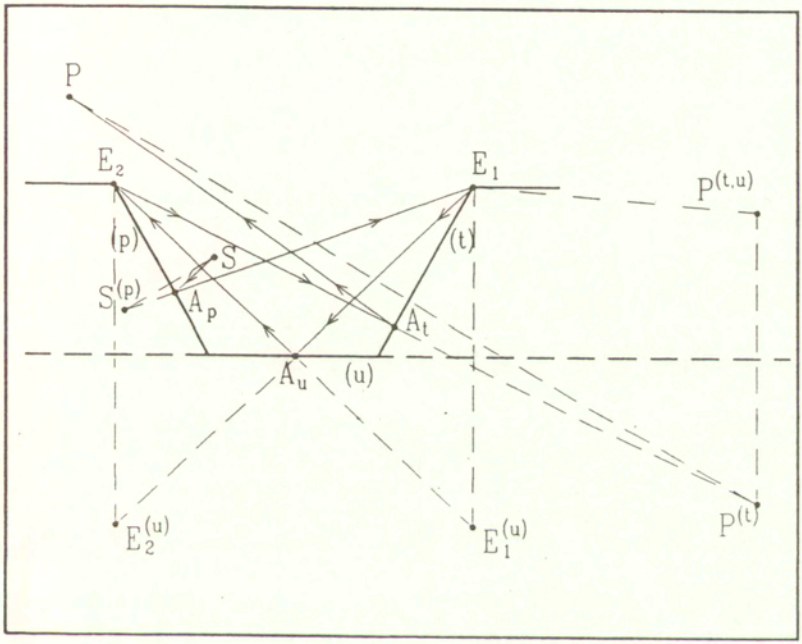

Fig.4.3. Propagation from the source S in a canyon.

$$= R(E_2,A_t,P)\ D\begin{bmatrix}S\\E_2\\P\end{bmatrix} R(E_1,A_u,E_2)\ *$$

$$* \left[\frac{T(E_1,E_2)}{T(E_1,P)}\right] T(E_1,P)\ D\begin{bmatrix}S\\E_1\\P\end{bmatrix} R(S,A_p,E_1)\ Q(S) =$$

$$= \eta(A_p)\ R(E_2,A_t,P)\ D\begin{bmatrix}S\\E_2\\P\end{bmatrix} R(E_1,A_u,E_2)\ *$$

$$* \left[\frac{T(E_1,E_2)}{T(E_1,P)}\right] T(E_1,P)\ D\begin{bmatrix}S\\E_1\\P\end{bmatrix} T(S^{(p)},E_1)\ Q(S) =$$

$$= \eta(A_p)\ \eta(A_u)\ R(E_2,A_t,P)\ D\begin{bmatrix}S\\E_2\\P\end{bmatrix} \left[\frac{T(E_1^{(u)},E_2)}{T(E_1,P^{(u)})}\right] *$$

$$* T(E_1,P^{(u)})\ D\begin{bmatrix}S\\E_1\\P\end{bmatrix} T(S^{(p)},E_1)\ Q(S) =$$

$$= \eta(A_t)\ \eta(A_u)\ \eta(A_p)\ T(E_2,P^{(t)})\ D\begin{bmatrix}S\\E_2\\P\end{bmatrix} \left[\frac{T(E_1^{(u)},E_2)}{T(E_1,P^{(t,u)})}\right] *$$

$$* T(E_1,P^{(t,u)})\ D\begin{bmatrix}S\\E_1\\P\end{bmatrix} T(S^{(p)},E_1)\ Q(S) =$$

$$= \eta(A_t)\ \eta(A_u)\ \eta(A_p)\ \eta(E_1^{(u)},E_2,P^{(t)}) \left[\frac{T(E_1^{(u)},E_2)}{T(E_1,P^{(t,u)})}\right] *$$

$$* \eta(S^{(p)},E_1,P^{(t,u)})\ T(S^{(p)},P^{(t,u)})\ Q(S).$$

Here, the directional ratio of the source at the (1)-wedge $Q[E_1(S)]$ appears

$$\left[\frac{T(E_1^{(u)},E_2)}{T(E_1,P^{(t,u)})}\right] = \left[\frac{T(E_1,E_2^{(u)})}{T(E_1,P^{(t,u)})}\right] = \qquad (4.50)$$

$$= \frac{P[\nu_m;\varphi_{om},\varphi_m(E_2^{(u)})]}{P[\nu_m;\varphi_{om},\varphi_m(P^{(t,u)})]}.$$

The directional factors $P[\nu_m;\varphi_{om},\varphi_m(E_2^{(u)})]$, $P[\nu_m;\varphi_{om},\varphi_m(P^{(t,u)})]$ are given by Eq.3.34 in the coordinates system connected with the (1)-wedge, where $\varphi_m(E_2^{(u)})$, $\varphi_m(P^{(t,u)})$ are the angular positions of the $E_2^{(u)}$-point and $P^{(t,u)}$-point, respectively.

In the terms of diffraction part of the field (4.3) with two diffraction processes at arbitrary place, the total wave path is divided into the parts: the i-path from S to E_m, the l-path from E_m to E_{m+1}, and the j-path from E_{m+1} to P. Then:

$$p^d[S(i),E_m,\ldots,E_m(l),E_{m+1},\ldots,P(j)] = \qquad (4.51)$$

$$= p^d(S,\ldots,C(i)_s,\ldots,A(i)_p,\ldots,E_m,\ldots,C(l)_r,\ldots,A(l)_u,\ldots,$$

$$E_{m+1},\ldots,C(j)_w,\ldots A(j)_t,\ldots,P) =$$

$$= T(\ldots,P) *\ldots* T[\ldots,C(j)_t,\ldots] *\ldots* R[\ldots,A(j)_w,\ldots] *\ldots*$$

$$\cdot * D[\ldots,E_{m+1},\ldots] *\ldots* T[\ldots,C(l)_r,\ldots] *\ldots* R[\ldots,A(l)_u,\ldots] *$$

$$* D[\ldots,E_m,\ldots] *\ldots* T[\ldots,C(i)_s,\ldots] *\ldots* R[\ldots,A(i)_p,\ldots] *$$

$$*\ldots* T(S,\ldots)\ Q(S).$$

When the term in Eq.4.51 is of k-order, then:

$$\begin{aligned} k &= k(i) + k(l) + k(j) + 2, \\ k(i) &= k_r(i) + k_t(i), \\ k(l) &= k_r(l) + k_t(l), \\ k(j) &= k_r(j) + k_t(j). \end{aligned} \tag{4.52}$$

The action proceeds in this way that after the sequence of transmissions and reflections on the i-path, the secondary source of diffraction waves $Q[E_m[S(i)]]$ is created at the m-wedge (edge). Next, the wave from this source suffers subsequent series of transmissions and reflections on the l-path. This results in an appearance of the image source $Q[E_m[S(i)]](l)$ which creates the next secondary source of diffraction waves $Q\left[E_{m+1}[E_m[S(i)]](l)\right]$ at the (m+1)-wedge (edge). The wave from this source reaches the observation point after suffering subsequent series of transmissions and reflections on the j-path. Then

$$p^d[S(i),E_m,\ldots,E_m(l),E_{m+1},\ldots,P(j)] = \tag{4.53}$$

$$= \prod_{p=1}^{k_r(i)} \eta[A(i)_p] \prod_{s=1}^{k(i)-k_r(i)} \eta[C(i)_s] \prod_{u=1}^{k_r(l)} \eta[A(l)_u] \prod_{q=1}^{k(l)-k_r(l)} \eta[C(l)_q] *$$

$$* \prod_{t=1}^{k_r(j)} \eta[A(j)_t] \prod_{w=1}^{k(j)-k_r(j)} \eta[C(j)_w] *$$

$$* T[E_{m+1}, P(j)]\ Q\left[E_{m+1}[E_m[S(i)]](l)\right] =$$

$$= \prod_{p=1}^{k_r(i)} \eta[A(i)_p] \prod_{s=1}^{k(i)-k_r(i)} \eta[C(i)_s] \prod_{u=1}^{k_r(l)} \eta[A(l)_u] \prod_{q=1}^{k(l)-k_r(l)} \eta[C(l)_q] *$$

$$* \prod_{t=1}^{k_r(j)} \eta[A(j)_t] \prod_{w=1}^{k(j)-k_r(j)} \eta[C(j)_w] *$$

$$* T[E_{m+1}, P(j)]\ D\begin{bmatrix} S \\ E_{m+1} \\ P \end{bmatrix} T[E_m(l), E_{m+1}]\ Q[E_m[S(i)]](l) =$$

$$= \prod_{p=1}^{k_r(i)} \eta[A(i)_p] \prod_{s=1}^{k(i)-k_r(i)} \eta[C(i)_s] \prod_{u=1}^{k_r(l)} \eta[A(l)_u] \prod_{q=1}^{k(l)-k_r(l)} \eta[C(l)_q] *$$

$$* \prod_{t=1}^{k_r(j)} \eta[A(j)_t] \prod_{w=1}^{k(j)-k_r(j)} \eta[C(j)_w] *$$

$$* T[E_{m+1}, P(j)]\ D\begin{bmatrix} S \\ E_{m+1} \\ P \end{bmatrix} \left[\frac{T[E_m(l), E_{m+1}]}{T[E_m, P(j,l)]}\right] *$$

$$* T[E_m,P(j,1)]\, D\begin{bmatrix} S \\ E_m \\ P \end{bmatrix} T[S(i),E_m]\, Q(S) =$$

$$= \prod_{p=1}^{k_r(i)} \eta[A(i)_p] \prod_{s=1}^{k(i)-k_r(i)} \eta[C(i)_s] \prod_{u=1}^{k_r(1)} \eta[A(1)_u] \prod_{q=1}^{k(1)-k_r(1)} \eta[C(1)_q]$$

$$* \prod_{t=1}^{k_r(j)} \eta[A(j)_t] \prod_{w=1}^{k(j)-k_r(j)} \eta[C(j)_w]\, \eta[E_m(1),E_{m+1},P(j)] *$$

$$* \left[\frac{T[E_m,E_{m+1}(1)]}{T[E_m,P(j,1)]}\right] \eta[S(i),E_m,P(j,1)]\, \frac{\exp\left(ikR_{i,1,j}\right)}{R_{i,1,j}},$$

where

$$\left[\frac{T[E_m(1),E_{m+1}]}{T[E_m,P(j,1)]}\right] = \left[\frac{T[E_m,E_{m+1}(1)]}{T[E_m,P(j,1)]}\right] = \qquad (4.54)$$

$$= \frac{P[\nu_m;\varphi_{Om},\varphi_m(E_{m+1}(1))]}{P[\nu_m;\varphi_{Om},\varphi_m(P(j,1))]},$$

$$R_{i,1,j} = [S(i),P(j,1)] = [S(i,1,j),P] = [S,P(j,1,i)]. \qquad (4.55)$$

The terms of the diffraction field (Eq.4.51), after realization of all the reflections $k_r=k_r(i)+k_r(1)+k_r(j)$ and transmissions $k_t=k_t(i)+k_t(1)+k_t(j)$, result in the undisturbed wave and the products of the appropriate reflection and transmission coefficients, and the two diffraction coefficients, which connect the appropriate source of their own directional ratio, and the

appropriate observation points.

In expressions Eq.4.51, 4.53 the wave path from the source at S to the place of the first process of diffraction at m-wedge (edge) is distinguished as the i-path. The last diffraction is assumed to occur at the (m+1)-wedge (edge) after that, by travelling the j-path, the observation point P is reached. What happens between diffraction at the m-wedge (edge) and the diffraction at the last wedge (edge) is ascribed to the l-path, containing sequence of transmissions and reflections. In the place of the l-path the segment containing sequences of transmissions and reflections with additional diffraction can be introduced. As the calculation procedure for the appropriate acoustical pressure is composed of the subsequent segments (Eqs.4.51-55) such enlargement does not cause any trouble. Thus:

$$p^d[S(i),E_m,\ldots,E_m(l),E_{m+1},\ldots,E_{m+1}(l+1),E_{m+2},\ldots,P(j)] =$$

$$= p^d(S,\ldots,C(i),\ldots,A(i),\ldots,E_m,\ldots,C(l),\ldots,A(l),\ldots,$$

$$E_{m+1},\ldots,C(l+1),\ldots,A(l+1),\ldots,E_{m+2},\ldots,C(j),\ldots A(j),\ldots,P) =$$

$$= \eta[A(i)] * \ldots * \eta[C(i)] * \ldots * \eta[A(l)] * \ldots * \eta[C(l)] *$$

$$* \ldots * \eta[A(l+1)] * \ldots * \eta[C(l+1)] * \ldots \qquad (4.56)$$

$$* \eta[A(j)] * \ldots * \eta[C(j)] *$$

$$* T[E_{m+2},P(j)]\, D\begin{bmatrix} S \\ E_{m+2} \\ P \end{bmatrix} \left[\frac{T[E_{m+1}(l+1),E_{m+2}]}{T[E_{m+1},P(j,l+1)]}\right] *$$

$$* T[E_{m+1},P(j,l+1)]\, D\begin{bmatrix} S \\ E_{m+1} \\ P \end{bmatrix} \left[\frac{T[E_m(l),E_{m+1}]}{T[E_m,P(j,l)]}\right] *$$

$$* T[E_m,P(j,l+1,l)]\, D\begin{bmatrix} S \\ E_m \\ P \end{bmatrix} T[S(i),E_m]\, Q(S) =$$

$$= \eta[A(i)] * \ldots * \eta[C(i)] * \ldots * \eta[A(l)] * \ldots * \eta[C(l)] *$$

$$* \ldots * \eta[A(l+1)] * \ldots * \eta[C(l+1)] * \ldots$$

$$* \eta[A(j)] * \ldots * \eta[C(j)] *$$

$$* \eta[E_{m+1}(l+1),E_{m+2},P(j)] \left[\frac{T[E_{m+1}(l+1),E_{m+2}]}{T[E_{m+1},P(j,l+1)]}\right] *$$

$$* \eta[E_m(l),E_{m+1},P(j,l+1)] \left[\frac{T[E_m(l),E_{m+1}]}{T[E_m,P(j,l)]}\right] *$$

$$* \eta[S(i),E_m,P(j,l+1,l)] \frac{\exp\left(ikR_{i,l,l+1,j}\right)}{R_{i,l,l+1,j}},$$

where

$$\left[\frac{T[E_m(l),E_{m+1}]}{T[E_m,P(j,l)]}\right] = \left[\frac{T[E_m,E_{m+1}(l)]}{T[E_m,P(j,l)]}\right] = \qquad (4.57)$$

$$= \frac{P[\nu_m;\varphi_{om},\varphi_m(E_{m+1}(l))]}{P[\nu_m;\varphi_{om},\varphi_m(P(j,l))]},$$

$$\left[\frac{T[E_{m+1}(l+1),E_{m+2}]}{T[E_{m+1},P(j,l+1)]}\right] = \left[\frac{T[E_{m+1},E_{m+2}(l+1)]}{T[E_{m+1},P(j,l+1)]}\right] = \qquad (4.58)$$

$$= \frac{P[\nu_{m+1};\varphi_{om+1},\varphi_{m+1}(E_{m+2}(l+1))]}{P[\nu_{m+1};\varphi_{om},\varphi_{m+1}(P(j,l+1))]},$$

$$R_{i,l,l+1,j} = [S(i),P(j,l+1,l)] = [S(i,l,l+1,j),P] = \qquad (4.59)$$

$$= [S,P(j,l+1,l,i)].$$

As can be seen from above, the higher order terms result when one of the operators T,R,D acts on the term of the lower order which provides the undisturbed wave - the direct wave - for the process. All the interactions are linear in relation to the direct wave being freely transmitted from the real source to the appropriate image observation point or from the appropriate image source to the real observation point (Eqs.4.53,4.56). Eventually, the product of transmission, reflection and diffraction coefficients with the appropriate source directional ratio, appears in front of the undisturbed wave.

The amplitudes of transmission and reflection coefficients are equal to or less than one. The diffraction coefficient has the maximum value, about one half, near the boundary of an existence of the direct (undisturbed) wave. The further from the boundary, the smaller is the diffraction coefficient amplitude. Thus, the higher is the order of the term the smaller is its

amplitude.

The total diffraction field (Eq.4.3) is the sum containing the terms with single diffraction (Eq.4.30), double diffraction (4.45), generally, an arbitrary number of diffractions at an arbitrary positions (4.56). Formally, it can be presented as below:

$$p^d(P) = \sum_{k=1}^{K} \sum_{i=1}^{I(N,M,k)} p^d[S(i),P], \qquad (4.60)$$

$$p^d[S(i),P] = \sum_{m} \sum_{l} \sum_{m'} \dots \sum_{l'} \sum_{m''} \dots \sum_{j} p^d[S(i), E_m, \dots, \qquad (4.61)$$

$$\dots, E_m(l), E_{m'}, \dots, E_{m'}(l'), E_{m''}, \dots, P(j)].$$

Depending on the positions of points C, A, E where the interaction occurs, some of the terms in Eq.4.61 can be zero. Likewise as the geometrical part of the field (Eq.4.12), the diffraction part (Eq.4.60) is the sum of the terms of decreasing amplitude.

4.3. Example of a plane screen in semi-space

Let us analyze the urban system where is one unlimited plane - the ground (n=1), and the plane screen of limited length. Its opposite sides can be different, and depending on that which side of the screen is reached by the direct wave, the reflection and transmission coefficients can be different. Therefore, the screen is treated as a double panel of surfaces n=2, n=3.

The geometrical part of the field is formed by the set of operators:

$$\{\hat{\Pi}(N=3)\} = \tag{4.62}$$

$$= \left\{ \begin{matrix} T(\ldots,C_1,\ldots),T(\ldots,C_2,\ldots),T(\ldots,C_3,\ldots), \\ R(\ldots,A_1,\ldots),R(\ldots,A_2,\ldots),R(\ldots,A_3,\ldots), \end{matrix} \right\}.$$

Assumption of interactions up to K=3 order results in number of terms of the geometrical field (Eq.4.5):

$$\sum_{k=1}^{K=3} I(N=3,k) = 126, \tag{4.63}$$

Assuming the source position at the (n=2)-side of the screen (Fig.4.4) it is apparent that the (n=3)-side of the screen does not participate in the interactions, thus

$$\{\hat{\Pi}(N=3)\} = \left\{ \begin{matrix} T(\ldots,C_1,\ldots),T(\ldots,C_2,\ldots), \\ R(\ldots,A_1,\ldots),R(\ldots,A_2,\ldots), \end{matrix} \right\}, \tag{4.64}$$

and

$$\sum_{k=1}^{K=3} I(N=2,k) = 28. \tag{4.65}$$

The next limitation concerns a fact that the ground is an opaque plane and $T(1)=0$. Other limitations come from the fact that the panels are perpendicular (Fig.4.4). Thus, the only possible terms appear for k=1,2:

$$p^{g}(S,C_2,P) = T(S,C_2,P)\ Q(S) = \eta(C_2)\ T(S,P)\ Q(S) \tag{4.66}$$

$$p^{g}(S,A_1,C_2,P) = T(S,C_2,P)\ R(S,A_1,P)\ Q(S) = \tag{4.67}$$

$$= \eta(A_1)\ \eta(C_2)\ T(S^{(1)},P)\ Q(S),$$

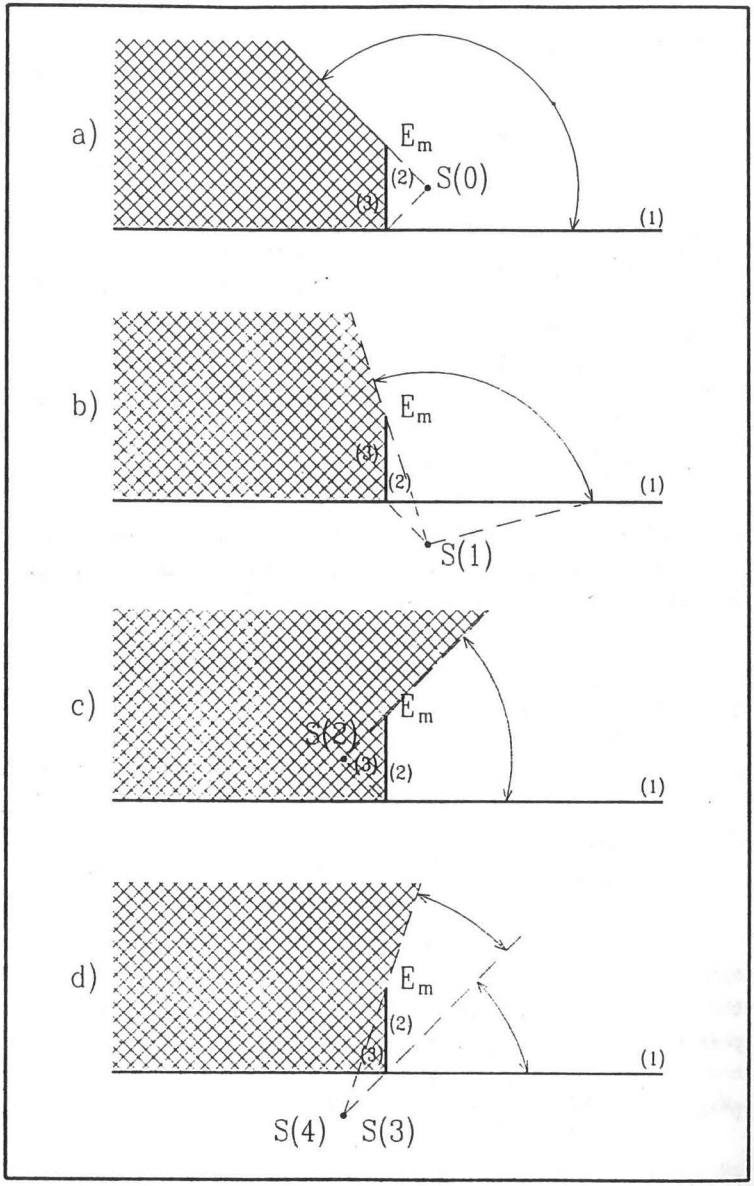

Fig.4.4. The image sources and the region of their existence for the plane screen on the ground.

$$p^{g}(S,A_2,P) = R(S,A_2,P)\ Q(S) = \eta(A_2)\ T(S^{(2)},P)\ Q(S), \qquad (4.68)$$

$$p^{g}(S,A_1,A_2,P) = R(S,A_1,P)\ R(S,A_2,,P)\ Q(S) = \qquad (4.69)$$

$$= \eta(A_1)\ \eta(A_2)\ T(S^{(1,2)},P)\ Q(S),$$

$$p^{g}(S,A_2,A_1,P) = R(S,A_2,P)\ R(S,A_1,P)\ Q(S) = \qquad (4.70)$$

$$= \eta(A_2)\ \eta(A_1)\ T(S^{(2,1)},P)\ Q(S).$$

The above can be proved by a creation of the set of image sources (Eq.4.10) for $K=K_r=3$, according to Eq.4.15 the image source number is:

$$I(N=2,K_r=3) = 7, \qquad (4.71)$$

they are at point:

$S = S(i=0)$,

$S^{(1)} = S(i=1)$, $S^{(2)} = S(i=2)$, for $k_r = 1$,

$S^{(1,2)} = S(i=3)$, $S^{(2,1)} = S(i=4)$, for $k_r = 2$, (4.72)

$S^{(1,2,1)} = S(i=5)$, $S^{(2,1,2)} = S(i=6)$, for $k_r = 3$.

The wave due to the source at S(i=0) is the direct wave from the real source S:

$$p^{g}(S(i=0),P) = p^{g}[S,C(i=0)_2,P] = \qquad (4.73)$$

$$= \eta[C(i=0)_2] \frac{\exp(ikR_0)}{R_0},$$

$$R_0 = [S(i=0),P], \tag{4.74}$$

which can be transmitted through the plane where the screen lies straight to the observation point or through the screen (n=2), at the point $C(i=0)_2$, to the points lying on the opposite screen side than the source at S=S(i=0) (Fig.4.4). Because of $\eta(C_2)$ definition (Eq.3.60) the term given by Eq.4.73 is equal to the term given by Eq.4.66.

The wave due to the source at S(i=1), being the mirror image of the source S(i=0) with respect to the ground (n=1), gives the acoustical pressure:

$$p^g[S(i=1),P] = p^g[S,A(i=1)_1,C(i=1)_2,P] =$$

$$= \eta[A(i=1)_1]\ \eta[C(i=1)_2] \frac{\exp(ikR_1)}{R_1}, \tag{4.75}$$

$$R_1 = [S(i=1),P]. \tag{4.76}$$

The physical path of the wave starts at the real source at S, next it is reflected from the ground (n=1) at the point $A(i=1)_1$, and finally can be transmitted through the plane, where the screen lies, straight to the observation point or through the screen (n=2) at the point $C(i=1)_2$, to the points lying behind the screen. This term is equivalent to the term given by Eq. 4.67.

The wave due to the source at S(i=2), being the mirror image of the source at S(i=0) with respect to the screen plane (n=2):

$$p^g[S(i=2),P] = p^g[S,A(i=2)_2,P] =$$

$$= \eta[A(i=2)_2] \frac{\exp(ikR_2)}{R_2}, \tag{4.77}$$

$$R_2 = [S(i=2),P]. \tag{4.78}$$

In this process the wave due to the source at S, before reaching the observation point P, is reflected from the screen plane (n=2) at the point $A(i=2)_2$. This term is equivalent to the term given by Eq. 4.68.

The sources at S(i=3), S(i=4) have the same position but radiate waves into the different regions (Fig.4.4). For the source at S(i=3):

$$p^g[S(i=3),P] = p^g[S,A(i=3)_1,A(i=3)_2,P] = \tag{4.79}$$

$$= \eta[A(i=3)_1]\ \eta[A(i=3)_2] \frac{\exp(ikR_3)}{R_3},$$

$$R_3 = [S(i=1),P], \tag{4.80}$$

the wave after leaving the source at S is reflected from the ground (n=1) at the point $A(i=3)_1$, next, from the screen (n=2) at the point $A(i=3)_2$, finally reaches the point P. This term is equivalent to the term given by Eq. 4.69.

In the case of the source at S(i=4):

$$p^g[S(i=4),P] = p^g[S,A(i=4)_2,A(i=4)_1,P] = \tag{4.81}$$

$$= \eta[A(i=4)\ ]_2\eta[A(i=4)_1] \frac{\exp(ikR_4)}{R_4},$$

$$R_4 = [S(i=4),P], \tag{4.82}$$

the wave is reflected from the screen at $A(i=4)_2$, next, from the ground at $A(i=4)_1$ to the point P. This term is equivalent to the term given by Eq. 4.70.

The sources at S(i=5), S(i=6) do not exist as (n=1) and (n=2) planes are perpendicular.

In the terms belonging to the geometrical field (Eqs.4.73, 4.75, 4.77, 4.79, 4.81) the current index "i" for the full set of sources (Eq.4.72) is applied. Thus, the total geometrical field (Eq.4.12) is the sum:

$$p^g[P;I(N=2,K_r=3)] = \sum_{i=0}^{4} p^g[S(i),P]. \qquad (4.83)$$

Since the geometrical field does not contain the terms of order higher than two, keeping with the assumed total number of interactions up to K=3, and assuming only the single diffraction at the three edges of the screen, the diffraction field (Eqs.4.60), can be summed up as a result of participation of the set of sources {S(i)} (Eq.4.72). The sources at S(2), S(3) containing as the last process reflection from the screen, are excluded because their actions are incorporated into the processes of diffraction at edges (Chap.3.2). The source S(4) can cause diffraction at the screen-ground junction what has been excluded by the assumption. Thus, the only active sources are the sources at S(0), S(1).

As the screen has three edges, the wave from each active source can be diffracted at the three edges. The diffraction waves have their sources $Q[E_m[S(i)]]$ at the edges. The waves on their j-paths to the observation point P can be reflected from the ground. This results in the image observation point P(j=1). The reflection takes place at the point $A(j=1)_1$.

According to Eqs. 4.30, 4.60 the total diffraction field is:

$$p^d(P;N=2,K=3,M=3) = \sum_{i=0}^{1} \sum_{m=1}^{3} \sum_{j=0}^{1} p^d[S(i),E_m,P(j)]. \qquad (4.84)$$

In the terms containing (Eq.4.84) the sources of zero and the real observation point, keeping up with the upper limit of interactions K=3, diffraction up to the third order would be possible but it is excluded by the assumption. In the terms containing the sources of the first order and the image observation point P(j=1), representing reflection from the ground, only single diffraction is possible. Thus, the terms in Eq.4.84 are:

$$p^d[S(0)] = \sum_{j=0}^{1} \sum_{m=1}^{3} p^d[S(0),E_m,P(j)] = \qquad (4.85)$$

$$= \sum_{m=1}^{3} \eta[S(0),E_m,P(0)] \frac{\exp(ikR_{00})}{R_{00}} +$$

$$+ \eta[A(j=1)_1] \eta[S(0),E_m,P(1)] \frac{\exp(ikR_{01})}{R_{01}},$$

$$R_{00} = [S(0),(0)], \qquad (4.86)$$

$$R_{01} = [S(0),P(1)], \qquad (4.87)$$

$$p^d[S(1)] = \sum_{j=0}^{1} \sum_{m=1}^{3} p^d[S(1),E_m,P(j)] = \qquad (4.88)$$

$$= \sum_{m=1}^{3} \eta[A(i=1)_1] \left[\eta[S(1),E_m,P(0)] \frac{\exp(ikR_{10})}{R_{10}} + \right.$$

$$\left. + \eta[A(j=1)_1] \eta[S(1),E_m,P(1)] \frac{\exp(ikR_{11})}{R_{11}} \right],$$

$$R_{10} = [S(1),P(0)], \tag{4.89}$$

$$R_{11} = [S(1),P(1)]. \tag{4.90}$$

As the result of the above analysis the explicit description of the geometrical (Eq.4.83) and diffraction parts (Eq.4.84) of the field are obtained, and the total field can be calculated.

5. APPLICATION

The sciences and techniques can provide the tools and measures for noise abatement but the scope of policy, making the process self-consistent and efficient, is decided by authorities. They issue the laws, being the legal tools of the standards execution, and can influence the process by forming the economic preferences [181].

The simulation models which can provide the alternative solutions are the best ground for decision making.

5.1. Source model

The prepared propagation model (Eq.2.7) has to be completed by the source model to obtain the noise environmental model (Eq.2.1).

The stationary sources present in urban area can be modeled by one or a few equivalent point sources of a given power spectra. The relative A-weighted power level spectrum of the equivalent source is

$$W_{rA}(f_m=\omega_m/2\pi)\ [dB(A)] =$$

$$= 10 \log [W(f_m)/W_o] - 10 \log [W(f=1kHz)/W_o] - \Delta L_A, \qquad (5.1)$$

$$W_o = 10^{-12} \text{ Watts}, \qquad (5.2)$$

where ΔL_A is the A-weighting correction. Now, the sound level, which for the stationary source is equal to the sound equivalent level, can be calculated:

$$L_{eq}[dB(A)] = SL[dB(A)] = \qquad (5.3)$$

$$= 10 \log \sum_{m=1}^{M} 10^{0,1 w_{rA}(f_m)} w(f_m,R) + SPL(R=1m,f=1kHz),$$

where SPL(R=1m,f=1kHz) is the sound pressure level in the 1kHz band, at distance of 1m from the equivalent point source. In calculation, the source power level spectrum $w_{rA}(f_m)$ of ten octaves is taken (M=10). The factor $w(f_m,R)$ represents the mean acoustical energy, at the distance R, due to the unit simple-harmonic point sources of frequency f_{ms}, emitting in the m-octave-band of the center frequency f_m

$$w(f_m,R) = \frac{1}{S_m} \sum_{s=1}^{S_m} |p(R,f_{ms})|^2, \tag{5.4}$$

$$f_{ms} \in \langle F_{m1}, F_{m2} \rangle. \tag{5.5}$$

The number S_m of the discrete frequencies f_{ms} in the $\langle F_{m1}, F_{m2} \rangle$ octave-band can be adjusted to the band width or kept constant for all bands.

The noise propagation model in an urban system has been prepared for the unit simple-harmonic point source, thus, Eqs. 2.7, 4.2, 4.3, 4.12, 4.60 give the system transfer function p(P) needed in calculation of the sound equivalent level (Eqs.5.3,5.4)

$$p(R,f_{ms}) = p(P). \tag{5.6}$$

A highway is a complex noise source, composed of individual vehicles, moving along its lanes. By adopting a concept of the sound exposure to a drive-by of a vehicle [5,6,9,10,14], the stationary model of a highway is assumed. The equivalent source representing vehicles emits noise of the average traffic noise

spectrum [10]. It is assumed to be the omnidirectional point source, at the height above the ground of 0.7 m [151], which radiates into a homogeneous, loss-free atmosphere at rest. Having empirical data, the differences between equivalent sources of light and heavy vehicles can be introduced by taking for them different spectra and heights above the ground.

For the freely flowing traffic on the highway segment of J lanes, parallel to x-axis (Fig.5.1), with the total average flow rate N [vehicles/h], and the average vehicles speed v [m/h], the sound equivalent level is obtained:

$$L_{eq}(T=1h)[dB(A)] = 10 \log \sum_{j=1}^{J} N_j E_{Aj}/p_o^2, \qquad (5.7)$$

where N_j is the vehicles flow rate on each j-lane

$$N_j = N/J. \qquad (5.8)$$

The sound exposure E_{Aj} is the A-weighted average sound energy, emitted during the drive-by of the j-lane segment by the single equivalent source representing a vehicle, and

$$N_j E_{Aj} = N_j \int_{-t/2}^{t/2} p_{Aj}^2(t)dt = \frac{1}{\Delta x} \int_{x_{j1}}^{x_{j2}} p_A^2(x_j)\, dx_j, \qquad (5.9)$$

where

$$\Delta x = v/N_j \ [m/vehicles] \qquad (5.10)$$

is the average spacing between successive vehicles on the j-lane segment of the length $(x_{j2}-x_{j1})$.

Although the sound exposure in the case of a vehicle drive-by is defined for $t \to \infty$, the finite boundaries are introduced (Eq.5.9). Taking as a limitation criterion the assumption that, at the observation point P, the sound level due to the source at

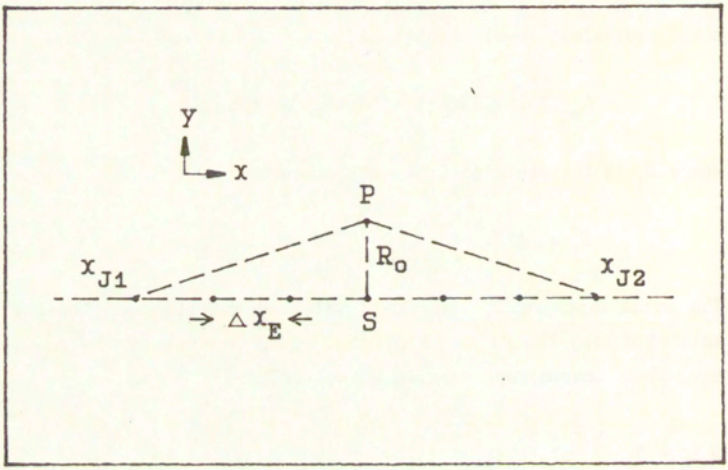

Fig.5.1. The point sources location on the highway segment.

the ends of the j-lane (x_{j2},x_{j1}) should be 10 dB lower than that due to the source at the nearest position, it is found

$$(x_{j2}-x_{j1}) = 6R_o, \tag{5.11}$$

where R_o (Fig.5.1) is the distance between the j-lane and the observation point.

The equivalent sound level of a highway can be obtained only when integration in Eq.5.9 is executed. In the simple way this can be done only for the free space when there are no buildings in the vicinity of the highway. In the other cases the integration can be replaced by discrete summation, then

$$N_j E_{Aj} = \frac{1}{\Delta x} \sum_{n_{Ej}=1}^{N_{Ej}} p_A^2(n_{Ej}\Delta x_E)\ \Delta x_E. \tag{5.12}$$

In this case the equivalent sound level is expressed by

$$L_{eq}(T=1h)[dB(A)] = 10\ \log \frac{\Delta x_E}{\Delta x} + SL_N, \tag{5.13}$$

where

$$SL_N = 10\ \log \sum_{j=1}^{J} \sum_{n_{Ej}=1}^{N_{Ej}} p_A^2(n_{Ej}\Delta x_E)/p_o^2 =$$

$$= 10\ \log \sum_{n=1}^{N} p_A^2(R_n)/p_o^2, \tag{5.14}$$

$$N_{Ej} = (x_{j2}-x_{j1})/\Delta x_E, \tag{5.15}$$

$$N = \sum_{j=1}^{J} N_{Ej}. \tag{5.16}$$

The quantity SL_N represents the sound level of the set of N stationary equivalent sources spread along the highway. The distance of the n-source from the observation point P(x,y,z) is:

$$R_n = \sqrt{\Delta x_n^2 + \Delta y_n^2 + \Delta z_n^2}, \tag{5.17}$$

$$\Delta x_n = x_{j1} + n_{Ej}\Delta x_E - x, \qquad j = 1,\ldots,J, \tag{5.18}$$

$$\Delta y_n = y_j - y, \qquad j = 1,\ldots,J, \tag{5.19}$$

$$\Delta z_n = 0.7m - z. \tag{5.20}$$

where y_j gives the j-lane position.

It is obvious that the value of L_{eq}, calculated according to Eq.5.13, depends on the chosen value of the summation step Δx_E. As the upper limit it can be taken

$$\Delta x_E = \Delta x, \tag{5.21}$$

where Δx is the average spacing between vehicles on the j-lane (Eq.5.10).

The relative A-weighted power spectrum of the equivalent source $w_{rA}(f_m)$ is, as before, given by Eq.5.1. Now, the sound level generated by the N equivalent sources representing the highway can be calculated:

$$SL_N[dB(A)] =$$

$$= 10 \log \sum_{m=1}^{10} 10^{0,1 w_{rA}(f_m)} w_N(f_m) + SPL(R=1m, f=1kHz). \tag{5.22}$$

The factor $w_N(f_m)$ represents the mean acoustical energy of the set of N unit simple-harmonic point sources, emitting in the m-octave-band of the center frequency f_m

$$w_N(f_m) = \frac{1}{S_m} \sum_{s=1}^{S_m} \sum_{n=1}^{N} |p(R_n, f_{ms})|^2. \qquad (5.23)$$

By substituting Eqs.5.22, 5.23 into Eq.5.13, the highway sound equivalent level is obtained.

5.2. Simulation model accuracy

The prepared environmental noise model (Eqs. 2.1, 2.7, 4.2, 4.3, 4.12, 4.60, 5.13-5.23) gives the ground for the simulation model which yields the sound equivalent level

$$L_{eq}[dB(A)] = \hat{\Pi}_o\left(10 \log; p_o^2; \int d\omega, \Delta L_A(\omega)\right) *$$

$$* \hat{\Pi}\left(N, \{\underline{R}(n)\}, \{R(n)\}, \{T(n)\}, K, \underline{R}(P)\right) Q_A(\ldots), \qquad (5.24)$$

The propagation model $\hat{\Pi}$ ( ) contains as the parameters:

N - number of panels,

$\{\underline{R}\}$ - set of vectors describing geometry of panels,

$\{R(n)\}$ - set of reflection coefficients of panels,

$\{T(n)\}$ - set of transmission coefficients of panels,

K - upper order of interaction,

$\underline{R}(P)$ - observation point position.

The two applied options of the source model Q_A( ) for a stationary source and a highway

$$Q_A(\ldots) = \begin{cases} Q\left(\underline{R}(S), w_{rA}(S, f_m)\right), SPL(1,1)\right), \\ Q\left(N, v, J, \{\underline{R}_j\}, \Delta x, \Delta x_E, w_{rA}(f_m), SPL(1,1)\right), \end{cases} \qquad (5.25)$$

contain as parameters:

N - total mean flow rate [vehicles/h],

v - average vehicles speed [m/h],

J - number of lanes,

$\{N_j\}$ - set of vehicles rate flow on lanes,

$\underline{R}(S)$ - position of source S,

Δx - average vehicle spacing,

$\{\underline{R}_j\}$ - set of vectors describing geometry of lanes,

Δx_E - summation step,

$w_{rA}(S,f_m)$ - relative, A-weighted power spectrum of S source,

$w_{rA}(f_m)$ - relative, A-weighted power spectrum of traffic noise,

SPL(1,1) - sound pressure level in 1kHz octave-band, at distance of 1m from the equivalent point source.

The simulation program PROP3 gives a quantitative answer how the sound equivalent level changes as a result of the change in the source parameters (Eq.5.25) and the urban system parameters (Eq.24) such as the mutual arrangement of buildings and their locations in relation to the source positions (Appendix, [113]). In an urban system, sometimes a change of the reflection coefficients of panels (walls, ground surface) is possible. The arrangement of buildings, their dimensions and a highway position could be any one, according to the designer architectural fantasy. The PROP3 can give answer what value of the sound equivalent level will be at the point of interest, especially on building facades (Appendix, [111]), for any imagined arrangement of buildings.

Analyzing the accuracy of the simulation model (Eq.5.24) the two kinds of causes affecting the accuracy have to be distinguished:

- the simulation model accuracy,
- adequacy of the simulation model to the real conditions.

As both, the source model and the propagation model, are worked out for far field conditions, taking into account the A-weighting and noise spectra met in urban area, it may be stated that for distances from a source to the place of the first interaction, and between interactions of order of few wavelengths, the simulation model is the proper one. Thus, the source model composed of point sources of a given power spectrum with directivity characteristic (when it is needed) is an adequate one, and its accuracy depends on the accuracy with which the parameters are measured.

In the propagation model, the description of elementary interactions includes transmission, reflection, diffraction and depends on the assumed upper order of interactions K which can be chosen in a step-by-step procedure. However, the geometry of an urban system is simplified and the real obstacles are replaced by the shoe-boxes or single panels. Also, all the effects connected with inhomogeneity of the propagation medium and changeable meteorological conditions are omitted. Because of these reasons the adequacy of this description is still an open question and some of its aspects have to be discussed.

The concept of the equivalent point source is valid for far field conditions, it means, for the distance from the source large enough in relation to the source dimensions. This concept is applied to stationary sources present in urban area as well to vehicles but in the last case special problems come out.

In the case of a vehicle, for emitted component of 62,5 Hz, the distance to the place of first interaction e. g. at an edge of screen applied along highway is of order of wavelength as is the length of passenger car. But in the case of buses and heavy trucks their lengths are of order of a few wavelengths. For such a case use of a few equivalent sources adequate to noise sources in a vehicle is more advisable. An additional problem appears for dense flow rate, when interactions between vehicles cases start. Fortunately, these left apart effects are not crucial as, because

of the A-weighting, the most important components of traffic noise are around 0.5 and 1 kHz.

In the case of a highway which is a noise source of statistical character, the two causes influence the accuracy. The traffic noise is related to the statistically established equivalent point source representing a vehicle. The accuracy of estimation of the equivalent source parameters determine the accuracy of the highway model but not alone. The equivalent sound level of a highway is calculated as the product of the mean flow rate of vehicle and the sound exposure caused by the equivalent point source drive-by (Eqs.5.13-5.23). The calculation error is brought in by calculation of the integral defining the sound exposure in a discrete way. This error can be diminished by increase of the number of steps in discretazation (Appendix, [113]) but it has to be compromised with the calculation time.

In the presented environmental noise model, the propagation model is determined as is the urban system for the atmospheric condition left apart. The statistical character of a highway model as a noise source can be explicitly introduced when some one is interested in noise fluctuations in a form of noise indexes L_1, L_{10}, L_{50}, L_{90}. Then the distribution function for vehicle parameters such as:

- vehicle position,
- number of vehicles,
- vehicle acoustical power,
- vehicle flow rate fluctuations.

has to be introduced into the source model which, combined with any determined propagation model, gives the awaited indices [60,61].

The propagation model accuracy depends on the description of elementary interactions (Eqs.2.9-2.13) and on the assumed upper order of interactions K (Eqs.4.2, 4.3). The free field propagation from the point source, reflection from a panel and

diffraction at its edges are described for the far field conditions, on the basis of the asymptotic forms of the canonical problems solutions. As transmission through a panel is not so important, it is described in the simplest way by the transmission coefficient. All these assumptions bring in the errors of the elementary interactions description which is simultaneously combined with the errors brought in by the experimentally established reflection and transmission coefficients.

By comparison with experimental data [182,183], it has been found that the adopted description of diffraction works up to a source (or observation point) distance from the wedge of the wavelength order. Also, comparing the description of double diffraction at the building wedges with the description applying the Keller theory of diffraction [105], an acceptable accordance has been found.

The importance of the accuracy in the diffraction description can be assessed when it is recalled that the acoustical pressure at the observation point is the sum of terms related to the image sources of the growing order. The diffraction wave causes redistribution of the energy in vicinity of the boundary of the geometrical wave with which it is connected, and which is emitted by one of the image sources. Thus, in the total field, the shadow regions, where the acoustical pressure of geometrical part of the field would equal zero, are canceled by diffraction. In these regions the acoustical pressure assumes a small value as the diffraction wave amplitude has the maximum value at the boundary, around one half of the geometrical wave amplitude, and fast decays with the distance from the boundary.

The most important components in the acoustical energy calculation are a few first reflections. It is possible that a smooth field can be obtained after a large number of reflections, but computation time increases. For example, when the image

theory is applied to a room with summation cut at sources of 60th order, the average increase in the total field of order of 5 % (1dB) is obtained by addition of the sources of one order higher [56].

In the example used here (Chap.4.2), for five buildings on the ground and reflections up to the third order (K_r=3), the number of the active sources in the geometrical part of the field is I_a(N=21,K_r=3)=842. The total geometrical field, created by reflection processes, contains the shadow regions where the acoustical pressure is zero and its level tends to minus infinity. When the field components resulting from K=3 interactions, including also diffraction, are added then the shadow regions disappear and, in the regions of the geometrical field maxima, the total field has a little higher value [Appendix, 110]. The calculation for one source and one observation point on PC 386/40 MHz has taken about 10 minutes.

As it come from the above, the accuracy of the propagation model can be judged in relation to the change in total field caused by the the first omitted image source of the (K+1)-order.

In the presented environmental noise model, the sound equivalent level of a highway is related to the sound exposure (acoustical energy) due to an individual vehicle drive-by. This energy is calculated not in the form of integral along the travelled path but as a sum of energies at the sequence of a vehicle discrete positions along the path. At each discrete position, the acoustical wave is emitted by the equivalent point source, thus, the acoustical pressure at the observation point is the sum over all the possible wave paths, with phases included. The assumption that the wave front is locally flat allows to calculate the energy of each discrete source position as proportional to the mean square pressure. Next, the energies of all the discrete positions are summed up to obtain the sound exposure.

It is obvious that for the given position of a source which can be treated as a point source, summation over diffident wave paths is coherent. The phases of waves traveling the different paths differ since for each wave the phase is defined by the length of the traveled distance and the jumps of phase during interactions with obstacles. This effect has been carefully observed during outdoor experiments of sound propagation over the impedance ground, especially, when an acoustic screen is placed there [84,92,168,184-187]. Also, during measurements of the sound level distribution along height of a building located parallel to a highway, when the maxima and minima have been observed in spite of monotonic decrease with the distance from sources [188,189].

It is possible that in outdoor events, after propagation in inhomogeneous atmosphere, the defined phase is destroyed. As it has been observed [166], it could happen after traveling the distance of order of 300 m. Since it is difficult to describe and control the propagation in real atmosphere, the opinions are divided and also the distance of 1 000 m has been given [184].

In an urban system of a few buildings and order of interactions up to K=3, the distances between buildings result in the path lengths that seem to be not large enough to destroy the defined phases. Other effects that can cause the phase indeterminacy are connected with the structure of a building facade (balcony, other small elements) that are omitted as the building is modeled in a form of the shoe-box. The two causes of phase destruction are related to the simulation model adequacy to the real urban situation but in the frame of presented simulation model coherent summation is justified.

There are attempts to control meteorological conditions in order to find the conditions which can be accepted as neutral ones [169]. The roughness of obstacle (building) surfaces can be incorporated into the propagation model by a concept of dividing the reflection coefficient into the part describing the specular

reflection and the scattering one [190,191]. Still, there will be the part of energy which will propagate according to the propagation model here presented, and the diffuse part related to the scattering part of reflection coefficient.

Despite of that the errors coming from all these simplifications are difficult to assess quantitatively, the adequacy of an urban system description and adequacy of a highway model can be assessed as comparable with the adequacy in the scale model investigations of relatively large urban segment, with scale factor of a range 1:100 [17,18].

Summing up, the simulation model accuracy depends on the modeling adequacy and the accuracy with which the parameters are measured. Some of these parameters are not easily obtained. However, the absolute value of the sound equivalent level L_{eq} is not always required. More often the change in the sound equivalent level L_{eq} caused by a change in the source and/or propagation parameters (Eqs.5.24,5.25) is searched for. The accuracy of the obtained relative change in L_{eq} is higher than this of its absolute value. Simultaneously, the absolute values of the sound equivalent level L_{eq} for the currently existing situation can be obtained by the field measurement.

While calculating the relative change in L_{eq}, the influence of some parameters may be canceled. For example, the source parameter SPL(1,1) (Eq.5.25) is removed when the change in L_{eq} caused by the acoustical screen application (the shielding efficiency) is investigated (Appendix, [122],[113]).

As another example when the relative change in the sound equivalent level is search for, it can be given the case of highway which is planned to be enlarged by addition of two extra lanes, and for which the flow rate the vehicles grows. Also, it could be obtained the change in L_{eq} caused by rearrangement of buildings in the segment of urban system tested at the stage of designing (Appendix, [113]).

Generally, when the assumption is made that the omitted phenomena and simplifications influence the different analyzed situation in the same way, the information provided by the simulation model can be regarded as reliable.

The level of mean acoustical energy is the aim of calculation as it is recommended by ISO for annoyance rating. Due to the statistical character of the highway as noise source and human ear sensitivity, the differences in the calculated sound equivalent level for various situations in an urban area of magnitude of ± 1 dB(A) can be subjectively noticeable, and can affect the judgment of the acoustical climate. For this purpose the sound exposure of an individual vehicle drive-by, vehicle flow rate and its average speed are sufficient.

5.3. Acoustical climate designing

In spite of the ISO recommendation to relate annoyance to the sound equivalent level L_{eq}, from noise physical characteristics (sound pressure) annoyance rating, apart of L_{eq}, can be enlarged by addition of such quantities as NCB curves, monaural and binaural loudness level, carrying the information about noise spectral structure, related to human perception [115,119,120]. The information about time structure of noise, especially in the case of traffic noise, is provided by statistical noise levels such as L_1, L_{10}, L_{50}, L_{90} [152-160].

Generally, the noise rating in the real environmental conditions depends on nonacoustical factors such as an accessibility to the public transportation, parking lots, schools, shopping centers, places of entertainment, and other conveniences associated with operation of noise sources. The rating is also influenced by aesthetic factors. Above that, the environmental sound brings with it information about what happens

around. This information is badly needed. In the extreme case of cutting the information stream, when someone is closed in an anechoic chamber, after a few minutes, the feeling of discomfort and anxiety occurs.

Therefore, the knowledge of the physical characteristics of environmental noise is not enough to reliably predict the community's subjective response to the noise.

Annoyance is an attitudinal response which integrates the emotional and behavioral effects of noise. It has been shown to be quite strongly correlated with measures of activity disturbance, especially speech interference and sleep disturbance. The self-response of annoyance may be treated as outcomes of decision-making process that is influenced by acoustical and nonacoustical factors. The net effect of nonacoustical factors on decision-making process may be regarded as a form of response bias.

It still remains unclear to what extent an annoyance-based approach is protective of human health and well being. Although, to keep up with the upper limit of sound equivalent level can be treated as a guide line in the acoustical climate designing but additional system of noise rating is needed.

As the consequence of all the above, and as the simple noise abatement is limited because of technical and economic reasons, the new tendency appears in the acoustical climate designing. It is called the soundscape designing [118,192,193].

The standardized scale of noise rating, containing acoustical and nonacoustical parameters, accompanied by the appropriate weighting functions has to be established by social surveys and psycho-acoustic tests [118,194-201]. It has to provide one global parameter rating the noise in the real environmental conditions. This scale has to be controlled and up-dated as new technologies and devices appear, social habits change, and awareness of environmental problems grow.

For having ability to control a validity and up-date the standardized scale of noise rating, the visualization of projects for cities in a form of movies, presenting, for example, the view from an apartment window, with the auralized sound of present sources, can be used [202].

The planning or engineering professionals can evaluate alternatives and make recommendations, but decisions are made by others. For decision-makers in authorities the visualization and auralization of alternative solutions have many advantages.

The auralization as a new technique is currently developed for assessment of concert halls, in parallel, it looks like advisable to apply it to soundscape designing.

The project of a computer system for soundscape designing was proposed in the application for grant to KBN (Committee for Scientific Researches). The system is thought out as an efficient designing tool and the aid for decision-makers. As such, it contains the environmental noise model and the standardized scale of noise rating with ability to present results in the visual and aural forms. In the computer system of soundscape designing, the environmental noise model in urban area with the propagation model presented here finds its application.

The system as the effective tool in the soundscape designing can find its application, among others, in designing an urban project with a new transportation network and other noisy devices, during reconstruction and reorganization of traffic inside an old urban structure.

For the user convenience, the system should provide a single package for all stages of acoustical climate designing, its assessment and correction. It has to be an open structure which can be enlarged in accord with state-of-the-art and by adding new functions. Depending on the user needs an import of data from external sources has to be possible.

The system should be easy in use, should provide rational

computation time, easy method of entering the data. The results presentation should be realized in the way very near to common experience. Fulfillments of all these requirements make the system cost-effective, thus, awaited by users.

Following the standard recommended by the joining meeting of National Contractor Association, Audio Engineering Society, Acoustical Society of America (SYN-AUD-CON Newsletter, Summer 1993), in the system has to be:

- ACQUISITION block,
- ALGORITHMS block,
- PRESENTATION block.

The ACQUISITION block should have communication ability with independent data base e. g. data base about noise sources [203]. For the architectural data, the combination of graphical and numerical entry should be assumed. The entry would allow the manual implementation of the architecture project by use of a mouse, light pencil and the like, or an import of data from the AUTOCAD files. A communication with other data banks should give the acoustical parameters of obstacles such as the complex values of reflection and transmission coefficients measured in situ [134,135,175-178].

The ALGORITHMS block contains the package of programs founded on the presented here the environmental noise model. The PROP31 program simulates noise propagation in the half-space containing plane acoustical screens and shoe-box obstacles. The obstacles surfaces are characterized by their reflection and transmission coefficients (in the case of screens). The point source of a given power spectrum is assumed. This gives an ability to construct any noise source by use of such point sources [14].

For a highway, the PROP32 program has the in-built highway model as a noise source where average noise spectrum, average flow rate of vehicles for each lane, percentage of heavy vehicles and sources position above the ground are the parameters.

Both programs in a form of PROP3 have been used in the calculation examples of noise penetration in a built-up area, and the shielding efficiency in such a complex structure (Appendix, [110-113]). In preparation is the special program for a canyon like structure where the expected number of interactions is greater than that for more open structures analyzed up to now. Here, a highway between two rows of buildings and a depressed road are included.

The calculation results in the form of narrow band spectrum of the acoustical pressure at the observation point are saved in the PRESENTATION block. The equivalent level L_{eq}[dB(A)] or other quantities characteristic for noise [114-120] can be calculated. The results can be presented as hardcopy documents, in the form of Reports or graphically, in the form of colorful 3D-maps. By use of the programmable noise source, the sound adequate to the applied solution could be auralized and given for subjective judgment [202].

In the PRESENTATION block the option realizing assessment of the standards fulfillments is assumed. The hot area would be presented. The additional data bank containing the set of possible solutions with technical and commercial data could be included e. g. the data of acoustical screen [204]. Depending on the user needs the data bank of windows insulation [134] could be included for presenting the sound level which penetrates into the rooms.

The proposed computer system of soundscape designing is an ideal example of the practical solution which combines the achievements of strict and humanistic sciences with modern technology.

6. CONCLUSIONS

The offered noise model consists of the source model which can be constructed by the unit simple-harmonic point source, and the propagation model. Generally, it can be used for all systems for which the high frequency approximation is an appropriate one, and where transmissions, reflections from panels and diffraction at wedges (edges) are predominant processes.

As both the source model and the propagation model are made for the far field conditions, taking into account the A-weighting and noise spectra met in urban area, it may be stated that for distances from a source and between interactions with obstacles about few wavelengths, the environmental noise model is the proper one.

The prepared for a built-up area noise environmental model contains the A-weighting allowing calculation of the sound equivalent level L_{eq}[dB(A)] recommended as annoyance rating. Apart from the noise equivalent level, the model can offer other noise indices which are thought out as quantities being related to the subjectively rating of annoyance.

The important achievement which allows to construct the noise propagation model is the way of diffraction description as one of interactions in a chain of multiple interactions. The high frequency approximations of the canonical solutions of a wave diffraction at a wedge are used as a starting point. The description of diffraction is written in the form containing an undisturbed direct wave multiplied by the diffraction coefficient. The description differs from the Keller geometrical theory of diffraction in that it is related to the undisturbed wave at the observation point while in the Keller theory it is related to the incident wave at the wedge. Generally, as the Keller diffraction theory is an extension of the ray tracing theory, the description presented here is an extension of the

image method.

This way of diffraction description is chosen since for high frequency approximation, the description of transmission and reflection have the same form, related to the undisturbed direct wave, with taking into account the fact that for reflection the direct wave is emitted by the image source. Thus, all the three kinds of interactions can be used as elements to build up a chain of interactions to which the wave subjected to on its path from the source to the observation point. The chain can contain an arbitrary number of interactions in an arbitrary sequence.

Likewise as the geometrical acoustics is more heuristic theory than the strict one, the presented diffraction description can be regarded as heuristic one. Thus, the two theories applied for description of the wave interaction with an obstacle: the geometrical acoustics for transmission and reflection, and the approximate description of diffraction are of the same nature. They are not strict mathematical theories but they are not in contradiction with the physical laws.

Having in mind the soundscape designing as an complex process, the computer system applicable as a design tool and offering an aid for decision-makers is planned to be prepared. The applied environmental noise model gives the narrow band spectrum of the acoustical pressure, from it, apart of the sound equivalent level, any noise index can be calculated if only its calculation procedure is introduced. The system can offer not only the noise parameters based on the acoustical pressure but can also be equipped with the standardized scale of noise rating related to the socio-psychological aspects of noise. The straight judgment would be possible by visualization and auralization of the projects for a town section.

ACKNOWLEDGEMENTS

This work has been realized in the framework of CPBP 02.21 Project and IPPT Project No 362. The part of work has been carried out during the author scholarship at Kansai University (Osaka, Japan). Personally, the author would like to thank Prof. Rufin Makarewicz (A. Mickiewicz University, Pozanań) and Prof. Yoshimasa Sakurai (Kansai University, Osaka) for many valuable criticism and comments during the course of these researches.

Special appreciations and gratefulness should be expressed to Dr Ryszard Janczur for the fruitful discussions on the environmental noise model construction and his cooperation in preparation of the computer realization of the model, and to all the colleagues for their inspired in valuable participation in discussion of the problems.

The author would like to thank MSc. Mieczysław Czechowicz for his help in English.

REFERENCES

[1] J. SADOWSKI, *Acoustics in town planing, architecture and construction,* (in Polish), Arkady, Warszawa 1971

[2] J. SADOWSKI, *Architectural acoustics,* (in Polish), Polish Scientific Publishers PWN, Warsaw 1976

[3] J. SADOWSKI, *Fundations of urban acoustics,* (in Polish), Arkady, Warszawa 1982

[4] A. LIPOWCZAN, *Noise and environment,* (in Polish) Ecological Foundation Silesia, Katowice 1995

[5] R. MAKAREWICZ, *Fundamentals of urban acoustics,* (in Polish), Polish Scientific Publishers PWN, Warsaw 1984

[6] R. MAKAREWICZ, Traffic noise in a built-up area, *Applied Acoustics* 34, 37-50, (1991)

[7] R. MAKAREWICZ, *Sound in environment,* (in Polish), Center of Scientific Publication, Pozań 1994

[8] Z. ENGEL, *Protection against vibrations and noise,* (in Polish), Polish Scientific Publishers PWN, Warsaw 1993

[9] R. MAKAREWICZ, Shielding of noise in a built-up area, *Journal of Sound and Vibration* 148 (3), 409-422, (1991)

[10] R. KUCHARSKI, Prediction of acoustical climate parameters in dwelling depending on terrain and noise sources characteristic, (PhD thesis, in Polish), *Institute of Environment Protection,* Warsaw 1990

[11] B. RUDNO-RUDZIŃSKA, Simulation model estimating sound level of freely flowing traffic, (PhD thesis, in Polish), *Wrocław Technical University Reports*, I-28, Pre-034, (1981)

[12] B. RUDNO-RUDZIŃSKA, Stationary environment model of traffic noise, *Proceedings of 38th Open Seminar on Acoustics*, 215-218, Poznań 1991

[13] B. RUDNO-RUDZIŃSKA, *Modeling sound emission and propagation for prediction of the acoustic climate in urban environment*, (in Polish) Scientific Papers of Institute of Telecommunication and Acoustics of Technical University of Wrocław No.75, Monography No.39, Wrocław 1994

[14] E. WALERIAN, R. JANCZUR, Model of highway as noise source, *Institute of Fundamental Technological Research Report* 32, (1991)

[15] K. W. YEOW, N. POPPLEWELL, J.F.W. MACKAY, Method of predicting L_{eq} created by urban traffic, *Journal of Sound and Vibration* 53 (1), 103-109, (1977)

[16] R. MAKAREWICZ, I. KRASNOWSKA, Traffic noise attenuation in an urban area in terms of A-weighted sound exposure level, *Applied Acoustics* 37, 65-74, (1991)

[17] M. E. DELANY, A. J. RENNIE, K. M. COLLINS, A scale model technique for investigating traffic noise propagation, *Journal of Sound and Vibration* 56 (3), 325-340, (1978)

[18] M. YAMASHITA, K. YAMAMOTO, Scale model experiments for the prediction of road traffic noise and the design of noise control facilities, *Applied Acoustics* 31, 185-196, (1990)

[19] R. JANCZUR, Theoretical and scale-model investigation of a point source acoustical field in the presence of reflecting surfaces and screen, (PhD thesis, in Polish) *Institute of Fundamental Technological Research Report* 8, (1990)

[20] Y. SAKURAI, E. WALERIAN, H. MORIMOTO, Noise barrier for building facade, *Journal of Acoustical Society of Japan* 11 (5), 257-265, (1990)

[21] M. STAWICKA-WAŁKOWSKA, Acoustical factor in town-planning, (in Polish) *Scientific Paper of the Building Research Institute*, XLIII, (1988)

[22] F. FRICKE, Sound propagation between buildings, *Proceedings of 2nd Western Pacific Regional Acoustic Conference*, 43-47, *Hong-Kong* 1985

[23] W. B. JOYCE, Sabine's reverberation time and ergodic auditoriums, *Journal of Acoustical Society of America* 58(3), 643-655, (1975)

[24] M. M. CARROLL, C. F. CHIEN, Decay of reverberation sound in spherical enclosure, *Journal of Acoustical Society of America* 62(6), 1442-1446, (1977)

[25] M. M. CARROLL, R. N. MILES, Steady-state sound in an enclosure with diffuse reflecting boundary *Journal of Acoustical Society of America* 64(5), 1424-1428, (1978)

[26] R. N. MILES, Sound field in a rectangular enclosure with diffuselly reflecting boundaries, *Journal of Sound and Vibration* 92(2), 203-226, (1984)

[27] W. B. JOYCE, Exact effect of surface roughness on the reverberation time of a uniformly absorbing spherical enclosure, *Journal of Acoustical Society of America* 64(5), 1429-1436, (1978)

[28] P. JANECEK, A model for the sound energy distribution in work spaces based on the combination of direct and diffuse field, *Acustica* 74(2), 149-156, (1991)

[29] K. FUJIWARA, Steady state sound field in an enclosure with diffusely and secularly reflected boundary, *Acustica* 54, 266-273, (1984)

[30] E. A. LINQVIST, Sound attenuation in large factory space *Acustica* 50(5), 313-328, (1982)

[31] E. A. LINQVIST, Noise attenuation in factory, *Applied Acoustics* 16, 183-214, (1983)

[32] E. KRUZINS, F. FRICKE, The prediction of sound field in non-diffuse spaces by 'random walk' approach, *Journal of Sound and Vibration* 81 (4), 549-564, (1982)

[33] E. KRUZINS, The prediction of sound fields inside non-diffuse space: transmission loss consideration, *Journal of Sound and Vibration* 91 (3), 439-445, (1983)

[34] H. KUTTRUFF, Sound decay in reverberation chamber with diffusing elements, *Journal of Acoustical Society of America* 69(6), 1716-17238, (1981)

[35] H. KURZE, Scattering of sound in industrial spaces, *Journal of Sound and Vibration* 98(3), 349-364, (1985)

[36] A. M. ONDET, J. L. BARRY, Sound propagation in fitted rooms - comparison of different models, *Journal of Sound and Vibration* 125(1), 137-149, (1988)

[37] A. M. ONDET, J. L. BARRY, Modeling of sound propagation in fitted workshops using ray tracing, *Journal of Acoustical Society of America* 85(2), 787-796, (1989)

[38] A. M. ONDET, J. L. BARRY, Note in connection with a comparison of different models for predicting sound level in fitted industrial rooms, *Journal of Sound and Vibration* 143(2), 343-350, (1990)

[39] M. HODGSON, On accuracy of models for predicting factory sound propagation in fitted rooms, *Journal of Acoustical Society of America* 88(2), 871-878, (1990)

[40] H. G. DAVIES, R. H. LYON, Noise propagation in cellular urban and industrial space, *Journal of Acoustical Society of America* 52(6), 1565-1570, (1973)

[41] R. BULLEN, Statistical evaluation of the accuracy of external sound level predictions arising from models, *Journal of Sound and Vibration* 65 (1), 11-28, (1979)

[42] R. BULLEN, Comments on "A mathematical model for noise propagation between buildings", *Journal of Sound and Vibration* 89 (2), 287-289, (1983)

[43] E. WALERIAN, R. JANCZUR, Statistical description of noise propagation in a built-up area, *Archives of Acoustics* 19(2), 201-225, (1994).

[44] H. KUTTRUFF, A mathematical model for noise propagation

between buildings, *Journal of Sound and Vibration* 85 (1), 115-128, (1982)

[45] K. W. YEOW, Room acoustical model of external reverberation, *Journal of Sound and Vibration* 67 (2), 219-229, (1979)

[46] R. BULLEN, F. FRICKE, Sound propagation through vegetation, *Journal of Sound and Vibration* 80 (1), 11-23, (1982)

[47] I. MALECKI, *Physical foundations of technical acoustics*, Pergamon Press, London 1969

[48] P. M. MORSE, *Vibration and sound*, McGraw-Hill, New York, 1948

[49] P. M. MORSE, K. U. INGARD, *Theoretical acoustics*, McGraw-Hill, New York, 1968

[50] Y. KAWAI, T. TERAI, The application of integral equation methods to the calculation of sound attenuation by barriers, *Applied Acoustics* 31, 101-117, (1990)

[51] T. TERAI, On calculation of sound fields around three dimensional objects by integral methods, *Journal of Sound and Vibration* 69, 71-100 (1980)

[52] D. C. HOTHERSALL, S. N. CHANDLER-WILD, M. N. HAJMIRZAE, Efficiency of single noise barriers, *Journal of Sound and Vibration* 142(2), 303-322, (1991)

[53] J. J. EMBRECHTS, Sound field distribution using randomly traced sound ray techniques, *Acustica* 51(6), 288-295, (1982)

[54] A. GIMENEZ, A. MARTIN, Model of energy calculation for acoustic analysis of closed rooms, *Applied Acoustics* 26(2), 99-111, (1989)

[55] A. KULOWSKI, The modification of the ray method of sound field modeling in room, (in Polish), Scientific Notebook of Gdańsk Technical University No.74, (1991)

[56] A. G. GALAITSIS, W. N. PATERSON, Prediction of noise distribution in various enclosures from free field measurements, *Journal of Acoustical Society of America* 60(4), 848-856, (1976)

[57] J. BORISH, Extension of the image model to arbitrary polyhedra, *Journal of Acoustical Society of America* 75(6), 1827-1836, (1984)

[58] G. LEMIRE, J. NICOLAS, Aerial propagation of spherical sound waves in bounded spaces, *Journal of Acoustical Society of America* 86(5), 1845-1853, (1989)

[59] R. MAKAREWICZ, Theoretical foundation of urban noise control, *Journal of Acoustical Society of America* 74 (2), 543-558, (1983)

[60] M. OHTA, Y. MITANI, A fundamental study for predicting the urban street noise by use of the image method approach, *Archives of Acoustics* 10(1), 59-74 (1985)

[61] K. W. YOEW, N. POPPLEWELL, J. F. W. MACKAY, Shielding of noise from statistically stationary traffic flow by simple obstacles, *Journal of Sound and Vibration* 57, 203-224, (1978)

[62] H. G. DAVIES, Multiple-reflection diffuse-scattering model for noise propagation in streets, *Journal of Acoustical Society of America* 64 (2), 517-521, (1978)

[63] K. P. LEE, H. G. DAVIES, Nomogram for estimating noise propagation in urban areas, *Journal of Acoustical Society of America* 57 (6), 1477-1480, (1975)

[64] R. H. LYON, Role of multiple reflections and reverberation in urban noise propagation, *Journal of Acoustical Society of America* 55 (3), 493-503, (1974)

[65] B. BULLEN, F. FRICKE, Sound propagation in a street, *Journal of Sound and Vibration* 46 (1), 33-42, (1976)

[66] ed J. J. BOWMAN, T. B. A. SENIOR, P. L. E. USLENGHI, *Electromagnetic and acoustical scattering by simple shapes*, North-Holland Company, 1970

[67] R. P. KENDING, S. I. HAYEK, Diffraction by a hard-soft barrier, *Journal of Acoustical Society of America* 70(4), 1156-1165, (1981)

[68] A. D. RAWLINS, The solution of mixed boundary value problem in the theory of diffraction by a semi-infinite plane, *Proceedings of Royal Society of London* A346, 469-484, (1975)

[69] H. KUDREWICZ, S. PRZEZDZIECKI, Plane wave diffraction by an impedance half-pane - solution analysis depending on the half-plane impedance, *Institute of Fundamental Technological Research Reports*, (1981)

[70] H. KUDREWICZ, Diffraction by an impedance half-pane - dependence on the impedance parameters, *Archives of Acoustics*

15(1-2), 151-183, (1990)

[71] Z. MAEKAWA, Noise reduction by screen, *Memoir of Faculty of Engineering, Kobe University* 11, 29-53, (1965)

[72] W. RUBINOWICZ, *Die Beuguengswelle in der Kirchhoffschen Theorie der Beugung*, PWN Publishing House, Warsaw, 1957

[73] M. YUZUWA, T. Sone, Noise reduction by various shape barrier, *Applied Acoustics* 14(1), 65-73, (1981)

[74] Z. MAEKAWA, Simple estimation method for noise reduction by variously shaped barriers, *Archives of Acoustics* 10(4), 369-382, (1985)

[75] A. L'ESPERANCE, The insertion loss of finite length barrier on the ground, *Journal of Acoustical Society of America* 86(1), 179-183, (1989)

[76] Y. W. LAM, S. C. ROBERTS, A simple method for accurate prediction of finite barrier insertion loss, *Journal of Acoustical Society of America* 93, 1445-1452, (1993)

[77] U. J. KURZE, Noise reduction by barriers, *Journal of Acoustical Society of America* 55(3), 504 -517, (1974)

[78] E. WALERIAN, R. JANCZUR, Theories of diffraction applied for description of acoustical field screen efficiency" (in Polish) *Institute of Fundamental Technological Research Reports* 25, (1985)

[79] A. D. RAWLINS, Plane-wave diffraction by rational wedge, *Proceedings of Royal Society of London* A411, 265-283, (1987)

[80] A. CIARKOWSKI, J. BOERSMA, R. MITRRA, Plane-wave diffraction by wedge - a spectral domain approach, *IEEE Transactions on Antennas and Propagation* AP-32, 20-29 (1984)

[81] J. CHANG-SUNG, R. JUNG, S. SANG-YUNG, Scattering by right angle dielectric wedge, *IEEE Transactions on Antennas and Propagation* AP-32, 61-69 (1984)

[82] A. D. PIERCE, W. J. HADDEN JR., Plane wave diffraction by a wedge with finite impedance, *Journal of Acoustical Society of America* 63(1), 17-27, (1978)

[83] K. FUJIWARA, Y. ANDO, Z. MAEKAWA, Noise control by barriers - Part I: Noise reduction by a thick barrier, *Applied Acoustics* 10, 147-159 (1977)

[84] H. G. JONASSON, Diffraction by wedge of finite acoustic impedance with applications to depressed roads, *Journal of Sound and Vibration* 25, 577-585 (1972)

[85] A. L'ESPERANCE, J. NICOLAS, G. A. DAIGLE, Insertion loss of absorbent barrier on ground, *Journal of Acoustical Society of America* 86(3), 1060-1064, (1989)

[86] S. J. HAYEK, Acoustic diffraction by wedge-shaped barriers, *Proceedings of INTERNOISE'84, Honolulu, USA*, 313-588, (1984)

[87] S. I. HAYEK, Mathematical modeling of absorbing highway noise barriers, *Applied Acoustics* 31, 77-100 (1990)

[88] G. L. JAMES, *Geometrical theory of diffraction for electromagnetic waves*, Peter Peregrinus Ltd., Englend 1976

[89] W. A. BOROVIKOV, B. E. Kinber, *Geometricgeskaya teorya difrakcyi*, Swyaz, Moskva 1978

[90] E. WALERIAN, M. CZECHOWICZ, R. JANCZUR, Barriers' efficiency dependence on types of environments, *Applied Acoustics* 44(4), 291-324, (1985)

[91] T. F. W. EMBLETON, Line integral theory of barriers attenuation in presence of the ground, *Journal of Acoustical Society of America* 67(1), 42-45, (1980)

[92] T. ISEI, T. F. W. EMBLETON, J. E. PIERCY, Noise reduction by barriers on finite impedance ground, *Journal of Acoustical Society of America* 67(1), 46-58, (1980)

[93] D. A. HUTCHINS, H. W. JONES, L. T. RUSSEL, Model studies of barrier performance in the presence of ground surface. Part I: Thin, perfectly reflecting barriers. Part II: Different shapes, *Journal of Acoustical Society of America* 75(6), 1807-1826, (1984)

[94] J. J. HAJEK, L. KAWAN, Effect of parallel highway noise barriers, *Proceedings of INTERNOISE'80, Miami, Florida, USA*, 595-598, (1980)

[95] S. J. HAYEK, Efficiency of double walls noise barriers, *Proceedings of INTERNOISE'80, Miami, Florida, USA*, 585-588, (1980)

[96] W. BOWLBY, L. F. COHN, R. A. HARRIS, A review of studies of Insertion Loss degradation for parallel highway noise barriers, *Noise Control Engineering Journal* 28(2), 40-53, (1987)

[97] S. CZARNECKI, E. KOTARBIŃSKA, Properties of acoustic barriers in a field of reflected waves, *Archives of Acoustics* 1(4), 269-298, (1976)

[98] S. CZARNECKI, Mirror image method of analyzing the combined effect of barriers and absorbing surfaces in industrial interior and apartments, *Noise Control Engineering Journal* 11(1), 18-30, (1978)

[99] Y. SAKURAI, K. ISHIDA, Multiple reflection between rigid plane panels, *Journal of Acoustical Society of Japan (E)* 3(3), 183-190, (1982)

[100] Y. SAKURAI, K. ISHIDA, Multiple reflection between rigid curved panels, *Journal of Acoustical Society of Japan (E)* 4(1), 27-33, (1983)

[101] Y. SAKURAI, K. ISHIDA, Multiple sound reflection between panels covered with reflection coefficients, *Journal of Acoustical Society of Japan (E)* 4(3), 121-126, (1983)

[102] Y. SAKURAI, The early reflection of the impulse response in an auditorium, *Journal of Acoustical Society of Japan (E)* 8(4), 127-138, (1987)

[103] A. D. CLAYDEN, R. W. D. CULLEY, P. S. MARSH, Modeling traffic noise, *Applied Acoustics* 8, 1-12 (1975)

[104] D. SOULAGE, C. SERVE, Les logiciels cartbruit et microbruit, *Proceedings of 17th AICB Congress*, (20-24), Prague 1992

[105] A. D. PIERCE, Diffraction of sound around corners and over wide barriers, *Journal of Acoustical Society of America*

55(5), 941-955, (1974)

[106] J. KIRSZENSTEIN, An image source computer model for acoustic analysis and electroacoustic simulation, *Applied Acoustics* 17, 275-290, (1984)

[107] J. B. ALLEN, D. A. BERKELEY, Image method for efficiently simulating small room acoustic, *Journal of Acoustical Society of America* 65, 943-950, (1975)

[108] M. GENSON, F. SANTON, Prediction of sound field in room of arbitrary shape: the validity of the image source method, *Journal of Sound and Vibration* 63, 97-108 (1979)

[109] W. STRASZEWICZ, *Geometrical analysis of acoustical field in bounded space,* (in Polish) Warsaw Technical University Publishing House, Warsaw 1974

[110] R. JANCZUR, E. WALERIAN, J. OGŁAZA, Acoustical field in space with obstacles. Part I: Description of geometrical field, *Acustica* 78, 154-162 (1993)

[111] E. WALERIAN, R. JANCZUR, Acoustical field in space with obstacles. Part II: Propagation between buildings, *Acustica* 78, 210-219 (1993)

[112] E. WALERIAN, Multiple diffraction at edges and right angle wedges, *Acustica* 78, 201-209 (1993)

[113] E. WALERIAN, R. JANCZUR, Noise shielding efficiency in an urban system, (submitted to *Journal of Sound and Vibration*)

[114] J. RENOWSKI, *Noise - indexes criteria,* Wrocław Technical University Publishing House, 1988

[115] L. L. BERANEK, Application of NCB noise criterion, *Noise Control Engineering Journal* 33(2), 45-56, (1989)

[116] H. TACHIBANA, H. YANO, Y. SONODA, Subjective assesment of indoor noise - basic experiment with artificial sound, *Applied Acoustics* 31, 173-184, (1990)

[117] M. TAYLOR, Determining acceptable levels of noise - the role of scientific research, *Journal of Acoustical Society of Japan (E)* 14 (3), 167-171, (1993)

[118] S. NAMBA, S. KUWANO, Global environmental problems and noise, *Journal of Acoustical Society of Japan (E)* 14 (3), 123-126, (1993)

[119] H. TACHIBANA, Y. SONODA, K. IWAMOTO, Validity of arithmetic average of sound pressure level in octave bands as a loudness index, *Journal of Acoustical Society of Japan (E)* 14 (3), 197-204, (1993)

[120] J. BLAUERT, K. GENUIT, Evaluating sound environments with binaural technology - some basic consideration, *Journal of Acoustical Society of Japan (E)* 14 (3), 139-145, (993)

[121] R. MAKAREWICZ, A. E. S. GREEN, Correlation between noise and air pollution, *Journal of Sound and Vibration* 12, 14-15, (1979)

[122] G. S. K. WONG, Approximation equations for some acoustical and thermodynamic properties of standard air, *Journal of Acoustical Society of Japan (E)* 11, 145-155 (1990)

[123] K. YAMAMOTO, M. YAMASHITA, Measurement and analysis of

sound propagation over lawn, *Journal of Acoustical Society of Japan (E)* 15, 1-12 (1994)

[124] Y. TAKUWARA, M. OHTA, M. NISHIMURA, H. MINAMIHARA, A simplified method using wind speed for the estimation of low-frequency acoustic signal under the contamination of wind noise, *Journal of Acoustical Society of Japan (E)* 15, 45-52 (1994)

[125] M. WEST, F. WALKDEN, R. A. SACK, The acoustic shadow produced by wind speed and temperature gradients close to the ground, *Applied Acoustics* 27, 239-260 (1989)

[126] B. HALLBERT, C. LARSSON, S. ISRAELSSON, Outdoor sound level variations due to fluctuating meteorological parameters, *Applied Acoustics* 26, 235-240 (1989)

[127] G. A. DAIGLE, J. E. PIERCY, T. F. W. EMBLETON, Effects of atmospheric turbulence on the interference of sound waves near a hard boundary, *Journal of Acoustical Society of America* 64, 622-630 (1978)

[128] A. R. KRIEBEL, Refraction and attenuation by wind and thermal profile over a ground plane, *Journal of Acoustical Society of America* 51, 19-23 (1972)

[129] U. INGARD, G. C. MALING JR., On the effect of atmospheric turbulence on sound propagated over ground, *Journal of Acoustical Society of America* 35, 1056-1058 (1956)

[130] B. HALLBERT, C. LARSSON, S. ISRAELSSON, Numerical ray tracing in the atmospheric surface layer, *Journal of Acoustical Society of America* 83, 2059-2068 (1988)

[131] D. K. WILSON, D. W. THOMSON, Natural temporal variability of atmospheric acoustic absorption coefficients, *Applied Acoustics* **34**, 11-121, (1991)

[132] R. MAKAREWICZ, Near-grazing propagation above a soft ground, *Journal of Acoustical Society of America* 82, 1706-1711, (1987)

[133] Z. WESOŁOWSKI, Acoustical properties of two parallel elastic panels, (in Polish), *Proceedings of 32th Open Seminar on Acoustics*, Kraków, 29-33, (1985)

[134] B. SZUDROWICZ ET AL, *Acoustical planning of partitions in buildings*, (in Polish), Building Research Institute Publishing House, Warszawa 1991

[135] S. KURA, N. TAMER, Rating criteria for facade insulation against transportation noise source, *Applied Acoustics* 40, 213-237, (1993)

[136] P. E. WATERS, Commercial road vehicle noise, *Journal of Sound and Vibration* 35(2), 155-222, (1974)

[137] D. Williams, W. Tempest, Noise in heavy goods vehicles, *Journal of Sound and Vibration* 43(1), 97-107, (1975)

[138] T. PRIEDE, The effect of operating parameters on sources of vehicles noise, *Journal of Sound and Vibration* 43(2), 239-252, (1975)

[139] R. HILLQUIST, W. N. SCOTT, Motor vehicle noise spectra: their characteristics and dependence upon operation parameters, *Journal of Acoustical Society of America* 58(1), 2-10, (1975)

[140] E. J. RATHE, F. CASULA, H. HARTWIG, H. MALLET, Survey of the exterior noise, *Journal of Sound and Vibration* 29(4), 483-499, (1973)

[141] W. KROPP, Structure-borne sound on smooth tyre, *Applied Acoustics* 26, 181-192, (1989)

[142] U. SANDBERG, J. A. EJSMONT, Development of three methods for measurement of tire/road noise emission: coast-by, trailer and laboratory drum, *Noise Control Engineering Journal* 27(3), 68-, (1986)

[143] J. J. V. HOUDT, TH. GOEMAN, TH. P. A. V. BREUGEL, M. SPRINGBORN, Influence of road surface noise: a comparison of mobile and stationary measuring technique, *Noise Control Engineering Journal* 41(3), 365-370, (1993)

[144] R. R. K. JONES, D. C. HOTHERSALL, Effect of operating parameters on noise emission from individual road vehicles, *Applied Acoustics* 13(2), 121-136, (1980)

[145] P. T. LEWIS, The noise generated by single vehicles in freely flowing traffic, *Journal of Sound and Vibration* 30(2), 191-206, (1973)

[146] B. M. FAVRE, Noise emission of road vehicles: evaluation of some simple models, *Journal of Sound and Vibration* 91(4), 571-582, (1983)

[147] J. JARZĘCKI, R. MAKAREWICZ, Propagation of noise generated by moving source in open area, *Archives of Acoustics* 7(2), 107-118, (1982)

[148] H. TACHIBANA, T. IWASE, K. ISHII, Sound power levels of road vehicles measured by a new method using a reverberent tunnel, *Journal of Acoustical Society of Japan (E)* 2(2), 117-125, (1981)

[149] M. G. S. RAO, P.R. ROA, K. S. DEV, K. V. RAO, A model for computing environmental noise level due to motor vehicle traffic in Visakhapatnam, *Applied Acoustics* 27, 129-136, (1989)

[150] L. NIJS, The increase and decrease of traffic noise levels at intersections measured with a moving microphone, *Journal of Sound and Vibration* 131(1), 127-141, (1989)

[151] S. A. L. GLEGG, J. R. YOON, Determination of noise source heights, Part II. Measurement of the equivalent source height of highway vehicles, *Journal of Sound and Vibration* 143(1), 39-50, (1990)

[152] U. J. KURZE, Statistic of road traffic noise, *Journal of Sound and Vibration* 18(2), 171-195, (1971)

[153] U. J. Kurze, Noise from complex road traffic, *Journal of Sound and Vibration* 19(2), 167-177, (1971)

[154] P. K. ANDERSEN, Regulatory of traffic noise signal, *Journal of Sound and Vibration* 80(2), 267-274, 1982

[155] S. YAMAGUCHI, A prediction method of non-stationary road traffic noise based on fluctuation patterns of an average number of flowing vehicles, *Applied Acoustics* 27, 103-118, (1989)

[156] Y. MITANI, M. OHTA, Y. XIAO, A new estimation method of

noise evaluation index, L_{eq}, by use of statistical information on the arbitrary type noise level fluctuation, *Journal of Acoustical Society of Japan (E)* 9(1), 47-51, (1988)

[157] M. OHTA, A. IKUTA, N. TAKAKI, A prediction method of road traffic noise from with non-Poisson type traffic flow based on the generalization of Stratonovich's theory for random point processes, *Acustica* 70, 273-283, (1990)

[158] Z. JIPING, A study on the highway noise prediction model applicable to different traffic flow, *Noise Control Engineering Journal* 41(3), 371-375, (1992)

[159] M. OHTA, Y. MITANI, A practical prediction method using an elementary response wave form for the road traffic noise at a T-type intersection, *Journal of Acoustical Society of Japan (E)* 9(4), 195- 200, (1988)

[160] M. OHTA, S. MIYATA, O. NAGANO, A comparison of different fluctuation probability expressions based on the dB scale measurement of the noise environment of road traffic, *Acustica* 73, 263-270, (1991)

[161] R. MAKAREWICZ, Moment of probability distribution of equivalent continuous A-weighted sound pressure level (L_{eqT}), *Journal of Acoustical Society of Japan (E)* 14, 25-28, (1993)

[162] E. WALERIAN, Half-plane edge and right angle wedge as elements causing diffraction in urban area, *Archives of Acoustics* 12, 157-189 (1988)

[163] J. L. VOLAKIS, A uniform geometrical theory o d diffraction for an imperfectly conduction half-plane, *IEEE Transactions*

on Antennas and Propagation AP-34 (2), 172-180 (1986)

[164] U. INGARD, On the reflection of a spherical sound wave from an infinite plane, *Journal of Acoustical Society of America* 23(3), 329-335, (1951)

[165] A. R. WENZEL, Propagation of wave along an impedance boundary, *Journal of Acoustical Society of America* 55(5), 956-963, (1974)

[166] T. F. W. EMBLETON, J. E. PIERCY, N. OLSON, Outdoor propagation over ground of finite impedance, *Journal of Acoustical Society of America* 59(2), 267-277, (1976)

[167] S. THOMASSON, Reflection of waves from a point source by an impedance boundary, *Journal of Acoustical Society of America* 59(4), 780-785, (1976)

[168] C. I. CHESSELL, Propagation of noise along a finite impedance boundary, *Journal of Acoustical Society of America* 62(4), 825-834, (1977)

[169] K. ATTENBOROUGH, Prediction ground effect for highway noise, *Journal of Sound and Vibration* 81(3), 431-424, (1982)

[170] M. A. NOBILE, S. I. HAYEK, Acoustical propagation over an impedance plane, *Journal of Acoustical Society of America* 78(4), 1325-1336, (1985)

[171] K. B. RASMUSSEN, Approximate formulae for short-distance outdoor sound propagation, *Applied Acoustics* 29, 313-324, (1990)

[172] J. PARMANEN, Rating of sound insulation proposed by the ISO

and CEN working groups, *Journal of Sound and Vibration* 169(5), 709-715, (1994)

[173] T. LEGOUIS, J. NICOLAS, Phase gradient method of measuring the acoustic impedance of material, *Journal of Acoustical Society of America* 81(1), 44-50, (1987)

[174] M. GARAI, Measurement of the sound-absorption coefficient in situ: The reflection method using periodic pseudo-random sequences of maximum length, *Applied Acoustics* 39, 119-139, (1993)

[175] H. G. JONASSON, Sound intensity reflection index, *Applied Acoustics* 40, 281-293, (1993)

[176] W. BARWICZ, A. PODGORSKI, A New Portable Sound & Vibration Analyzer, *IMEKO TC4 International Symposium On Intelligent Instrumentation for Remote and On-Site Measurement*, Brussels, Belgium, 315-319, (1993)

[177] W. BARWICZ, J. KAMIŃSKI, Determination of the acoustic reflection coefficient by measurement of the complex sound intensity, *Proceedings of INTERNOISE'90*, Gothenburg-Sweden, 127-130, (1990)

[178] W. BARWICZ, J. KAMIŃSKI, In situ measurement of reflection coefficient by measurement of complex sound intensity, *Proceedings of 3rd Workshop on Acoustic Itensometry*, Wrocław, 22-28, (1991)

[179] W. BARWICZ, Analysis of the stationary acoustic field. Part I: Fundamental vector relation, *Archives of Acoustics* (in press)

[180] C. BERGE, *Principles of combinatorics*, Academic Press, New York and London, 1971

[181] I. MALECKI, Z. ENGEL, A. LIPOWCZAN, J. SADOWSKI, Problems of noise control in Poland on the way to European integration, *Proceedings of NOISE CONTROL'95*, Warsaw, 1-39, (1995)

[182] P. AMBAUD, A. BERGASSOL, Le problem du diedre en acoustique, *Acustica* 27, 291-298, (1972)

[183] W .J. HADDEN JR, A. D. PIERCE, Sound diffraction around screens and wedges for arbitrary point source locations, *Journal of Acoustical Society of America* 69(5), 1266-1276, (1981)

[184] Y. W. LAM, On the modeling of the effect of ground terrain profile in environmental noise calculation, *Applied Acoustics* 42, 99-123, (1994)

[185] B. A. DE JONG, A. MOERKERKEN, J. D. VAN DER TOORN, Propagation of sound over grassland and over an earth barrier, *Journal of Sound and Vibration* 86(1), 23-46, (1983)

[186] L. K. LEANG, Y. YAMASHITA, M. MATSUI, Simplified calculation method for noise reduction by barriers on the ground, *Journal of Acoustical Society of Japan (E)* 11(4), 199-206, (1990)

[187] T. ISEI, Absorptive noise barrier on finite impedance ground, *Journal Acoustical Society of Japan (E)* 1(1), 3-10, (1980)

[188] C. H. CHEW, Prediction of traffic noise for expressways -

Part I: Building flanking one side of expressways, *Applied Acoustics* 28(3), 203-212, (1989)

[189] J. SADOWSKI, *Acousical climate shaping by urban means*, (in Polish) Building Research Institute, Warsaw 1982

[190] R. MAKAREWICZ, Surface reflection of noise generated by a moving point source, *Acustica* 80, 527-532,(1994)

[191] R. MAKAREWICZ, Surface reflection of noise generated by a moving line source, *Acustica* 80, 533-540,(1994)

[192] M. SASAKI, The preference of the various sound in environment and the discussion about the concept of the sound-scape design, *Journal of Acoustical Society of Japan (E)* 14, 189-195, (1993)

[193] K. HIRAMATSU, Some aspects of soundscape studies in Japan, *Journal of Acoustical Society of Japan (E)* 14, 133-138, (1993)

[194] J. IGARASHI, Comparison of community response to transportation noise: Japanese results and annoyance scale, *Journal of Acoustical Society of Japan (E)* 13, 301-309, (1990)

[195] J. IGARASHI, Development of community noise control in Japan, *Journal of Acoustical Society of Japan (E)* 14, 177-180, (1993)

[196] T. J. SCHULTZ, Synthesis of social surveys on noise annoyance, *Journal of Acoustical Society of America* 64, 377-405, (1978)

[197] K. D. KRYTER, Community annoyance from aircraft and ground vehicles noise, *Journal of Acoustical Society of America* 72, 1222-1242, (1982)

[198] D. M. GREEN, S. FIDELL, Variability in the criterion for reporting annoyance in community noise surveys, *Journal of Acoustical Society of America* 89, 234-243, (1991)

[199] G. JANSEN, G. NOTBOHN, S. SCHWARTZ, Appliance of physiological measurements for assessing sound amenity, *Journal of Acoustical Society of Japan (E)* 14, 155-158, (1993)

[200] K. KUNO ET AL, Comparison of noise environment of residences in Nagoya, Japan and Beijing, China, *Applied Acoustics* 40, 153-167, (1993)

[201] S. NAMBA ET AL, Verbal expression of emotional impression of sound: A cross-cultural study, *Journal of Acoustical Society of Japan (E)* 12, 19-29, (1991)

[202] D. T. DUBBINK, Presenting environmental noise data using recorded noise example, *Noise Control Engineering Journal* 41(3), 351-356, (1993)

[203] R. KUCHARSKI, The system of data collecting about environmental noise, (in Polish) *Institute of Environment Protection*, Warsaw 1993

[204] M. STAWICKA-WAŁKOWSKA, Catalogue acoustical screens, (in Polish) *Building Research Institute*, Warsaw 1990

APPENDIX

Example A.1. [110]

The example, for which the field of the single stationary source in an urban area can be observed, is presented. The point source with the power spectrum characteristic for traffic noise (Fig.A.1) is assumed.

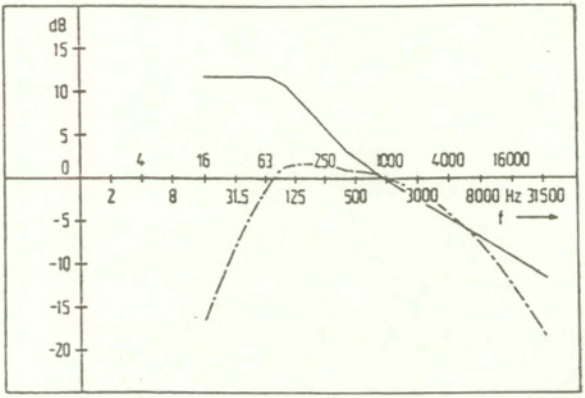

Fig.A.1. The typical traffic noise spectrum (solid line), and its A-weighted value (broken line) [2].

The results are presented in relation to the field due to the same source in the half-space limited by the ground surface. Thus, waves reaching the observation point are: the direct wave and the wave reflected from the ground.

The urban system is shown in Fig.A.2 where dimensions are given in meters. There are five buildings, the observation point

is moving along the line $P_1(-40;60;1,8)$, $P_2(160;60;1,8)$. The reflection coefficients are taken real and equal to 0.9, buildings are opaque obstacles.

When the reflections are taken up to the third order, there appear three regions of shadow where there is no geometrical field (Fig.A.3). In order to get the full description of the field, the diffraction part of the field has to be added. Then, the regions of the geometrical shadow disappear.

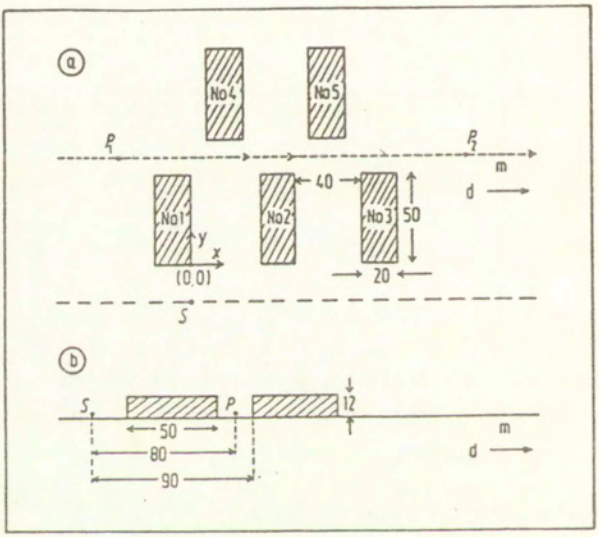

Fig.A.2. The urban system of five buildings in which the field was calculated.

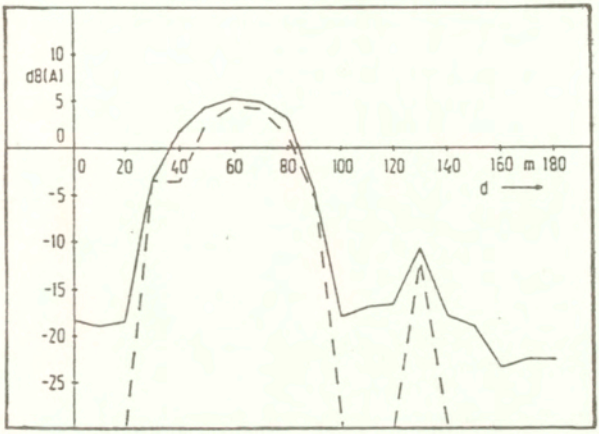

Fig.A.3. The sound level along line P_1,P_2 (Fig.A.2) of : broken line - geometrical field, solid line - total field.

Example A.2. [111]

The calculation has been performed for the urban system containing five buildings. Its geometry is shown in Fig.A.4, where dimensions are given in meters. The reflection coefficients of the ground and buildings walls are taken real and equal to 0.9.

The stationary model of highway noise is used. It is assumed that the highway has two lanes, and that the flow rate of vehicles is 1500 veh/h with average velocity of 60 km/h. For a vehicle, the equivalent point source with the power spectrum

typical for traffic noise (Fig.A.1) is used. This gives two lines of point sources distributed along lines with distance 80 m. It is assumed that sound pressure level at f=1kHz, at the distance of 3 m from point source, is 85 dB.

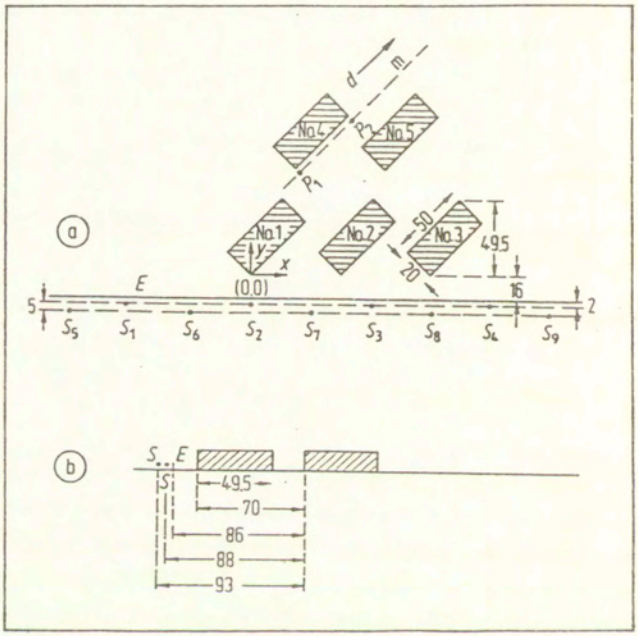

Fig.A.4. The urban system of five buildings in vicinity of highway: a) horizontal projection, b) vertical projection.

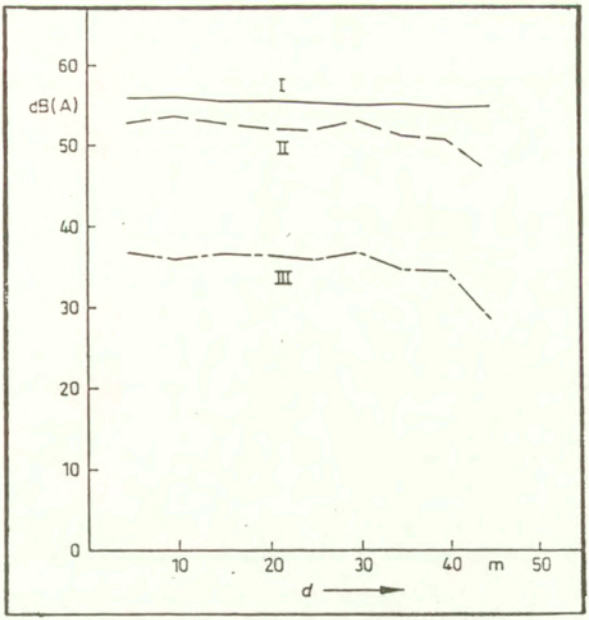

Fig.A.5. The sound level due to nine sources calculated along a line parallel to the facade of building No 4 (Fig.A.4): (I) - in the half-space with the ground, (II) - in the urban system of five buildings, (III) - in the urban system of five buildings with the applied screen.

The sound level has been calculated along the facade of the building No 4, at the height of 4,5 m (adequate to the height of the second floor). The sound levels were calculated for three cases: first, when there were only nine sources above the ground, next, for the case after erecting the five buildings, at last when the screen has been applied as the protector of buildings against the noise from highway. The screen (E) (Fig.A.4) parameters are: height of 3 m, reflection coefficient

of 0.9 and insulation of 20 dB. The results are presented in Fig. A.5. It can be observed how the sound level is changed, first, after putting the buildings into the system, next, after applying the screen as a protector.

Example A.3. [113]

The calculation of the shielding efficiency (difference between the actual sound level and the level in the half-space with the ground) has been performed for the urban system containing five buildings. The single building dimensions are (50 m x 20 m) x 12 m. The reflection coefficients of the ground and buildings walls are taken real and equal to 0.9. The three different arrangements of the buildings have been investigated (Fig.A.6):

- perpendicular to the highway,
- parallel to the highway,
- inclined to the highway at the angle $\alpha=45^{o}$.

The shielding efficiency is calculated for the stationary source at distance of 20 m from the right corner of the building No.1 (Table A.1, cases 10 - 12) and for the moving source (Table A.1, cases 13 - 20). The moving source is modeled by the sources distributed along the highway lane parallel to the building system in such a way that the stationary source investigated before is one of the sources on the lane. The source power spectrum is presented in Fig.A.7.

The observation points are at the line parallel to the highway, 10 m behind the first row of the buildings, at the height of 1.8 m. The ends of the highway lane are calculated in this way that the end sources participation in the total field is 10 dB less than the nearest one.

Table A.1. The system of five buildings investigation (Figs.A.6)

Case No.	Number of sources	(x_1, x_2) [m]	Δx_E [m]	α [deg]	(x_{p1}, x_{p2}) [m]	y_p [m]
10	1	(0,0)	-	90	(-60,160)	80
11	1	(0,0)	-	0	(-90,180)	50
12	1	(0,0)	-	45	(-60,200)	80
13	10	(-320,400)	80	90	(-60,160)	80
14	9	(-240,400)	80	0	(-90,180)	50
15	10	(-320,400)	80	45	(-60,200)	80
16	19	(-320,400)	40	90	(-60,160)	80
17	17	(-240,400)	40	0	(-90,180)	50
18	19	(-320,400)	40	45	(-60,200)	80
19	9	(-280,360)	80	0	(-90,180)	50
20	10	(-340,380)	80	45	(-60,200)	80

x_1, x_2 - ends of the highway lane

Δx_E - distance between sources position on lane

α - angle formed by the longer building side with x-axis, at the building corner nearest to the lane

x_{p1}, x_{p2} - ends of the line of the observation points

y_p - observation point coordinate

In Fig. A.8 the shielding efficiency in the three differently arranged urban systems are presented for the emission of stationary source at S(0,0) (Fig.A.6). In Fig.A.8.b. the axes are shifted to obtain for each curve l'= 0 at the center of the region where the direct wave from the source at S(0,0) arrives. In these regions, for all the three buildings arrangements the shielding efficiency is negative.

In Fig.A.9 the shielding efficiency in the three urban systems of different arrangements are presented for the moving source. The highest fluctuations are observed for the parallel arrangement, the smallest - for the inclined arrangement. For all the arrangements the most values lie in the strip (0,+5) dB(A).

In Fig. A.10 - A.12 the shielding efficiency in the given system is presented for the stationary point source and for the moving source with the two values of the summation step (distance between sources position on lane) Δx_E= 80 m, 40 m (Table A.1).

The examples show how the first row of buildings becomes transparent for noise when the highway model is introduced in the place of the single stationary source.

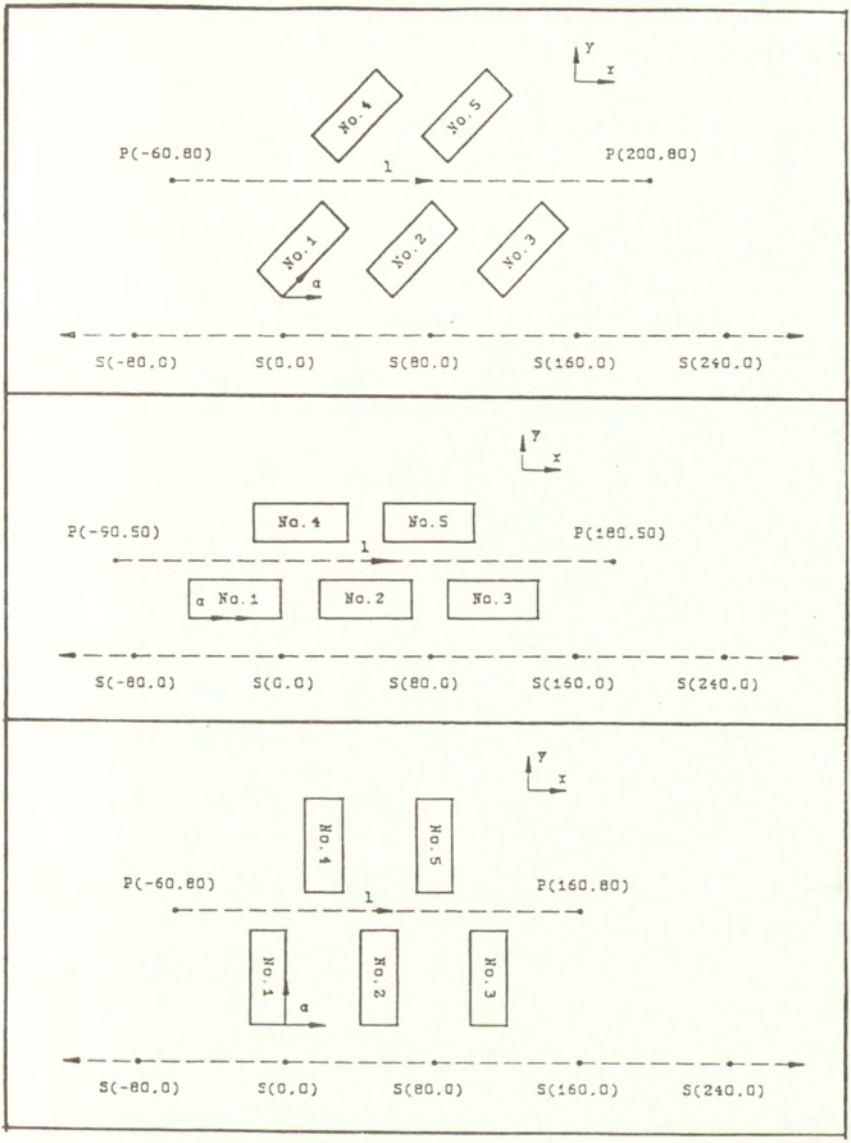

Fig.A.6. The urban system of five buildings located: a) perpendicularly, b) parallel, c) inclined to the highway lane (dimensions in meters).

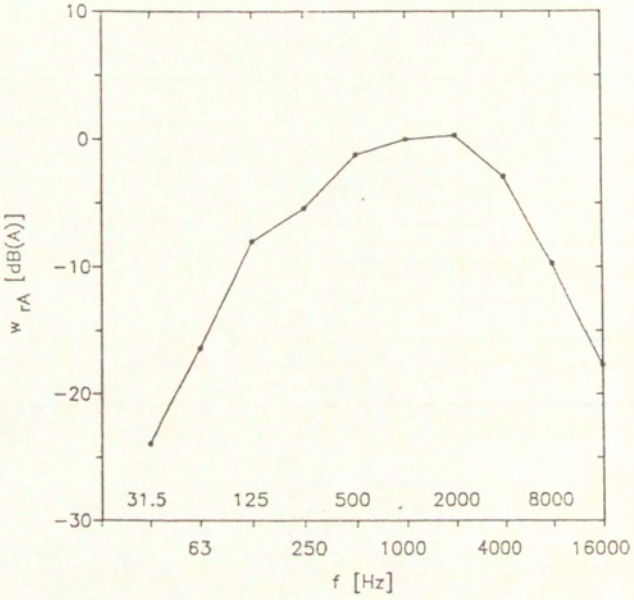

Fig.A.7. The average, A-weighted, relative power spectrum of traffic noise [10].

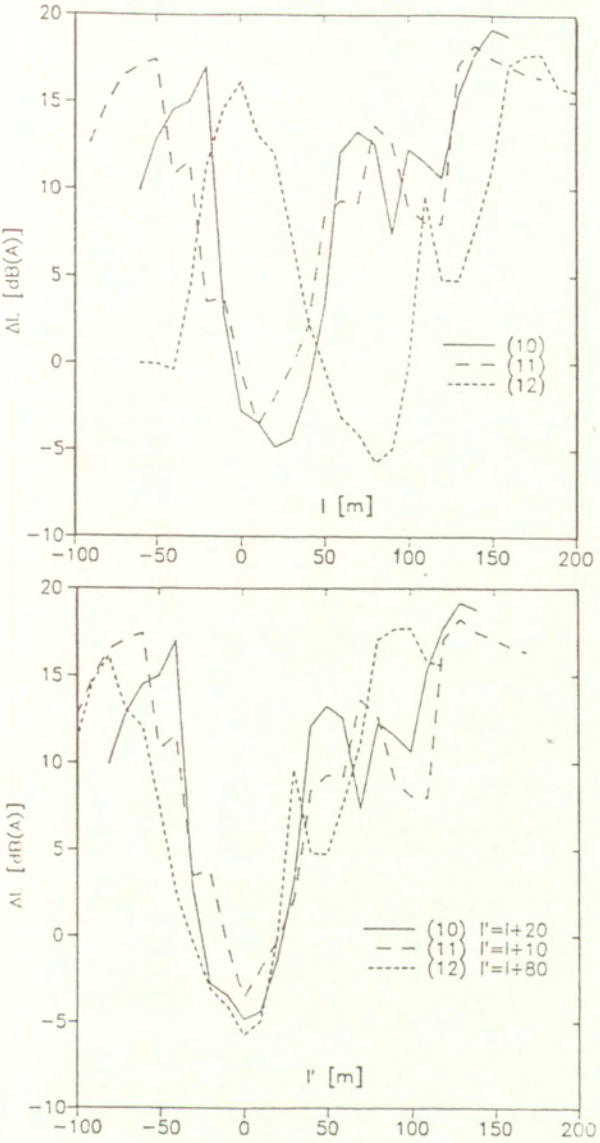

Fig.A.8. The shielding efficiency for the stationary source in the urban system of five buildings (Fig.A.6, Table.A.1) a): (10) - perpendicular, (11) - parallel, (12) - inclined, b) the same as a) but with the shifted l-axis.

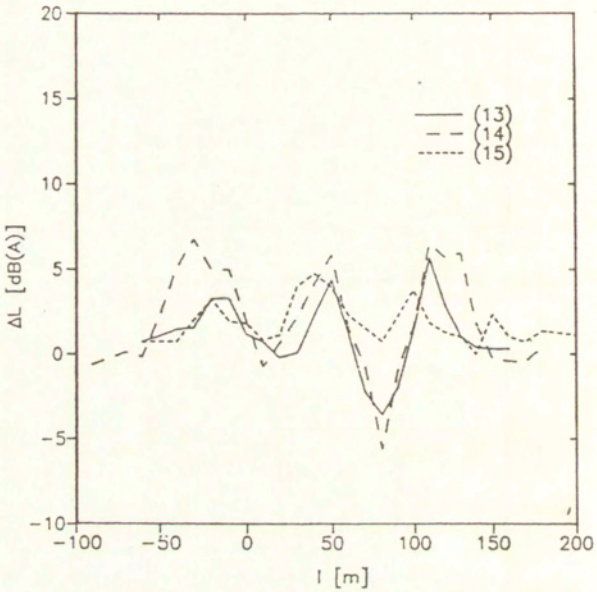

Fig.A.9. The shielding efficiency for the moving source in the urban system of five buildings (Fig.A.6, Table.A.1): (13) - perpendicular, (14) - parallel, (15) - inclined.

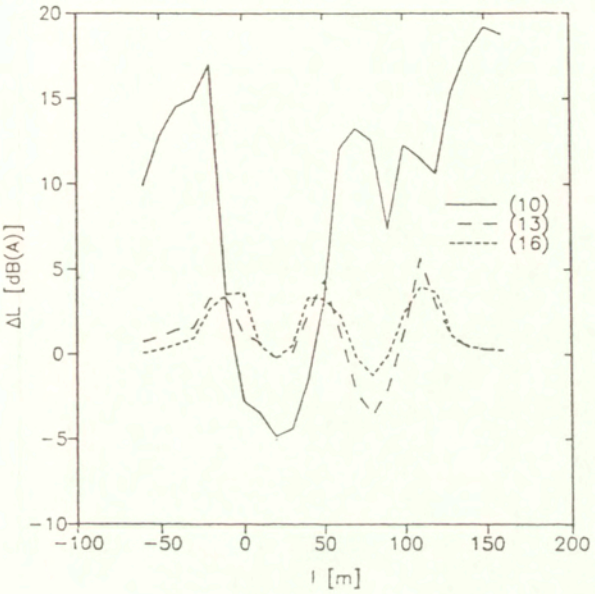

Fig.A.10. The shielding efficiency in the system of five buildings perpendicular to the highway lane (Fig.A.6, Table.A.1): (10) - for stationary source, (13) - for moving source with Δx_E= 80 m, (16) - for moving source with Δx_E= 40 m.

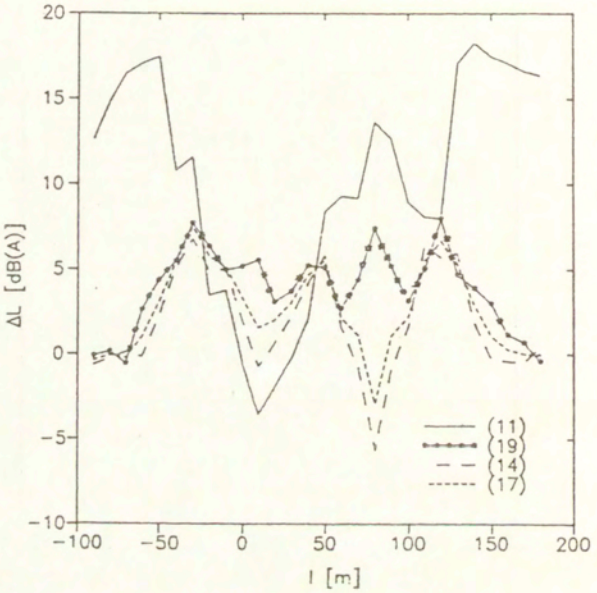

Fig.A.11. The shielding efficiency in the system of five buildings parallel to the highway lane (Fig.A.6, Table.A.1): (11) - for stationary source, (14) - for moving source Δx_E= 80 m, (17) - for moving source with Δx_E= 40 m, (19) - for moving source with Δx_E= 80 m and the source system moved by 40 m in relation to the case of the curve (14).

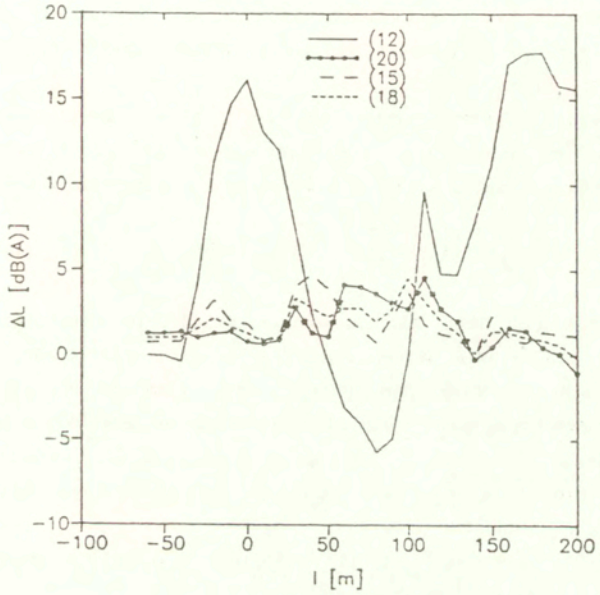

Fig.A.12. The shielding efficiency in the system of five buildings inclined to the highway lane (Fig.A.6, Table.A.1): (12) - for stationary source, (15) - for moving source Δx_E= 80 m, (18) - for moving source with Δx_E= 40 m, (20) - for moving source with Δx_E= 80 m and the source system moved by 20 m in relation to the case of the curve (15).

OPIS PROPAGACJI HAŁASU W TERENIE ZABUDOWANYM (skrót)

1. Model hałasu środowiskowego

Aby w racjonalny sposób kształtować klimat akustyczny potrzebne jest odpowiednie narzędzie - model hałasu środowiskowego - pozwalający w wariantowy sposób przewidywać parametry klimatu akustycznego.

Zgodnie z obowiązującymi normami, klimat akustyczny jest oceniany na podstawie poziomu równoważnego hałasu. W związku z tym formalnie model hałasu w środowisku można zapisać w postaci

$$L_{eq}[dB(A)] = \hat{\Pi}_o(\ldots)\ \hat{\Pi}(\ldots)\ Q(\ldots). \qquad (1)$$
$$(2.1)$$

Model (1) jest zdefiniowany w dziedzinie częstotliwości. $Q(\ldots)$ przedstawia model źródła w postaci zastępczgo źródła punktowego o określonym widmie mocy. Operator $\hat{\Pi}(\ldots)$ jest operatorem opisującym jakim oddziaływaniom podlega fala w trakcie propagacji. Operator $\hat{\Pi}_o\left(10\ \log;\ p_o^2;\ \int d\omega;\ \Delta L_A(\omega)\right)$ realizuje w dziedzinie częstotliwości operacje odpowiadające obliczeniu poziomu równoważnego dźwięku:

- sumowanie energii (kwadratów ciśnień) po wszystkich składowych widmowych,
- wprowadzenie korekcji krzywą A jako krzywej wrażliwości odbiornika jakim jest człowiek,
- obliczenie poziomu dźwięku w relacji do ciśnienia odniesienia p_o.

W przypadku propagacji hałasu od tras komunikacyjnych poziom równoważny dźwięku zdefiniowany jest w relacji do energii akustycznej docierającej do punktu obserwacji w wyniku przejazdu pojedynczego pojazdu. Źródłu reprezentującemu pojazd przypisane zostało widmo mocy typowe dla hałasów komunikacjnych. W ten sposób jednogodzinny poziom równoważny, pochodzący od trasy która

ma J pasów ruchu, obliczany jest na podstawie sumy energii akustycznej przejazdów N_j pojazdów na poszczególnych pasach

$$L_{eq}(T=1h)[dB(A)] = 10 \log \sum_{j=1}^{J} N_j E_{Aj}/p_o^2, \qquad (2)$$
(5.7)

N - średni strumień pojazdów [poj./h],

v - średnia prędkość pojazdów [m/h],

$$N_j = N/J, \qquad (3)$$
(5.8)

$$N_j E_{Aj} = N_j \int_{-t/2}^{t/2} p_{Aj}^2(t)dt = \frac{1}{\Delta x} \int_{x_{j1}}^{x_{j2}} p_A^2(x_j)\, dx_j, \qquad (4)$$
(5.9)

E_{Aj} - ekspozycja na hałas, tzn. ważona krzywą A średnia energia akustyczna emitowana w czasie przejazdu pojedynczego pojazdu po j-tym pasie,

$$\Delta x = v/N_j \ [m/poj.], \qquad (5)$$
(5.10)

Δx - odwrotność liniowej gęstości pojazdów na trasie, wynikająca z natężenia ruchu, średniej prędkości pojazdów, liczby pasów.

W związku z tym, że analityczne obliczenie zawartej w wyrażeniu (4) całki rzadko jest możliwe, została ona zastąpiona sumowaniem tak, że przejazd pojedyńczego pojazdu reprezentuje $N_{Ej} = (x_{j2}-x_{j1})/\Delta x_E$ źródeł zastępczych, rozmieszczonych wzdłuż toru ruchu. Odległości między nimi wynoszą Δx_E (Rys.1). Dyskretyzacja przejazdu pojazdu wzdłuż toru ruchu pozwala, dla każdego dyskretnego położenia pojazdu na trasie, sumować przyczynki do ciśnienia akustycznego fal dochodzących różnymi drogami do punktu obserwacji. Energia akustyczna E_{Aj} wyemitowana w czasie przejazdu pojedyńczego pojazdu po j-tym pasie jest sumą

przyczynków pochodzących od źródeł punktowych reprezentujących pojazd w kolejnych położeniach wzdłuż toru ruchu.

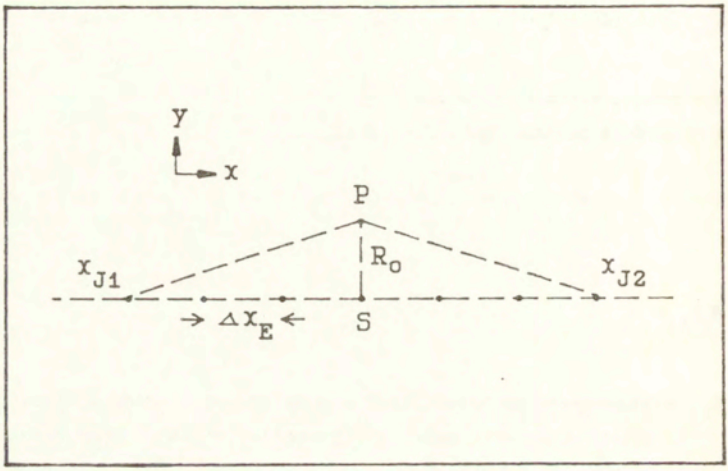

Rys.1

2. Konstrukcja modelu propagacji

W związku z tym że model źródła został przyjęty w postaci zastępczych źródeł punktowych o zadanym widmie mocy, szukany model propagacji w dziedzinie częstotliwości jest funkcją przejścia układu, która określa ciśnienie akustyczne w punkcie P, wywołane przez źródło punktowe Q(S) o jednostkowej amplitudzie, emitujące ton o częstotliwości $f=\omega/2\pi$, znajdujące się w punkcie S

$$p(P) = \hat{\Pi}\ (\ldots)\ Q(S) \qquad (6)$$
(2.7)

Operator $\hat{\Pi}\ (\ldots)$ opisuje sposób propagacji fali ze źródła Q(S) do punktu obserwacji.

Układ urbanistyczny został odwzorowany jako półprzestrzeń z przeszkodami umieszczonymi na podłożu. Zakłada się że ośrodek propagacji jest idealnym gazem w spoczynku. W związku z tym wszystkie zjawiska związane z niejednorodnściami ośrodka i zjawiskami atmosferycznymi zostały pominięte.

Przeszkody w układzie urbanistycznym zostały odwzorowane za pomocą prostokątnych paneli. Pięć takich paneli (ścian) tworzy na podłożu prostopadłościan reprezentujący budynek. Płaskie, wolno stojące przeszkody reprezentowane są przez pojedyncze panele (ściany). Panele łączone pod kątami różnymi od prostego mogą odwzorowywać spadziste dachy budynków oraz pochyłe ściany wykopu w którym przebiega trasa.

Dźwięk może docierać do punktu obserwacji różnymi drogami na których fala oddziałuje z przeszkodami (Rys.2). Jako elementarne zjawiska w procesie propagacji wyróżniono:

- transmisję w wolnej przestrzeni i przez półprzepuszczalne przeszkody,
- odbicia od podłoża i ścian przeszkód,
- ugięcia na krawędziach przeszkód.

Znane rozwiązania równania Helmholtza oddziaływania fali z prostymi elementami przeszkód, traktowane jako kanoniczne, zostały użyte do konstrukcji opisu ciągów wielokrotnych oddziaływań fali w układzie zawierającym wiele przeszkód o różnych kształtach.

Założeniem jest że wszystkie opisywane oddziaływania zachodzą w warunkach pola dalekiego. Dla tych warunków odbicie fali od nieograniczonej powierzchni można przedstawić jako działanie źródła pozornego, znajdującego się w punkcie będącym lustrzanym odbiciem źródła rzeczywistego. Amplituda tego źródła jest równa amplitudzie źródła rzeczywistego pomnożonej przez odpowiedni współczynnik odbicia, charakteryzujący własności akustyczne powierzchni. Jednocześnie, pozostając na tym samym poziomie przybliżenia, transmisję fali przez półprzepuszczalną przeszkodę przedstawiono jako przejście przez pewien układ tłumiący, czyli

jako mnożenie fali bezpośredniej przez odpowiedni współczynnik transmisji charakteryzujący izolacyjność przeszkody.

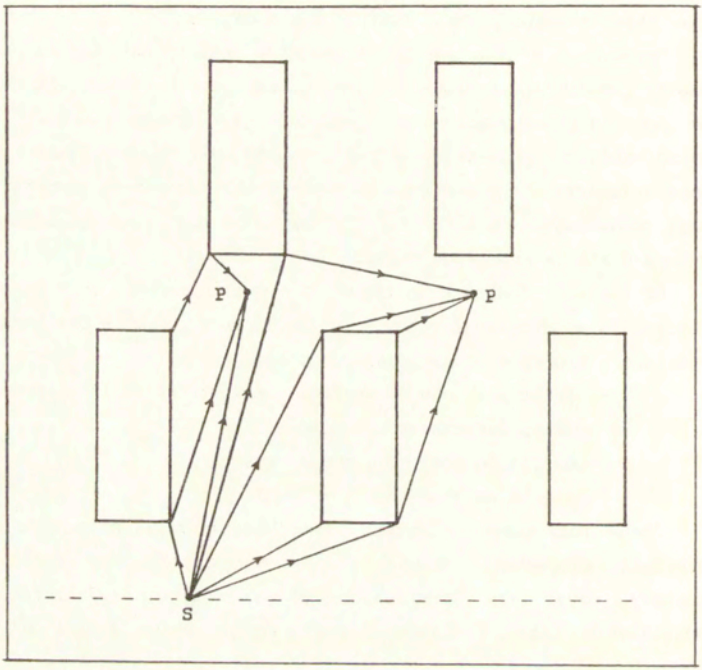

Rys.2

Na podstawie znanych rozwiązań kanonicznych, w warunkach pola dalekiego, oddziaływanie fali z przeszkodami można intepretować jako sumę składników opisujących odbicia od ścian przeszkody - reprezentowane przez źródła pozorne - i składników opisujących dyfrakcję na krawędziach przeszkód. W tych warunkach dyfrację można przedstawić jako mnożenie przez odpowiedni współczynnik dyfrakcji.

Podobny sposób rozumowania zastosował Keller tworząc geometryczną teorię dyfrakcji, która stanowi rozszerzenie geometrycznej teorii opisu pola polegającej na śledzeniu drogi promieni (ray tracing) o dyfrakcję na krawędziach.

W proponowanym opisie propagacji, dla części geometrycznej pola, zawierającej ciągi złożone z kolejnych transmisji i odbić, wykorzystano metodę źródeł pozornych. Dyfrakcję, występującą w części dyfrakcyjnej pola na przemian z transmisjami i odbiciami, można interpretować jako powstanie wtórnego źródła kierunkowego, emitującego falę typu cylindrycznego, związanego z punktem krawędzi przez który przechodzi najkrótsza droga ze źródła do punktu obserwacji. Wykorzystując ten fakt kolejne odbicie fal które powstały w wyniku dyfrakcji można przedstawić jako działanie źródła pozornego, będącego lustrzanym odbiciem punktu krawędzi stanowiącego źródło fal dyfrakcyjnych. W ten sposób, zaproponowany opis propagacji zawierający ciągi oddziaływań, w ramach których na przemian występują transmisje, odbicia i dyfrakcje, został przedstawiony w formie jednolitej pod względem strukturalnym i można go uważać za rozszerzenie metody źródeł pozornych o dyfrakcję na krawędziach przeszkód.

Współczynniki transmisji i odbicia przyjęto jako ustalane doświadczalnie parametry, charakteryzujące własności akustyczne przeszkód. Mogą one być wielkościami zespolonymi zależnymi od częstotliwości.

Współczynniki dyfrakcyjne są obliczane na postawie znanych rozwiązań kanonicznych dyfrakcji na krawędzi półpłaszczyzny i narożu o wewnętrznym kącie rozwarcia 2Ω, gdyż te właśnie dwa rodzaje krawędzi przyjęto w opisie geometrii układu urbanistycznego.

Wyróżnione oddziaływania elementarne, które zachodzą niezależnie na poszczególnych panelach (ścianach) i krawędziach można opisać przy pomocy odpowiednich operatorów działających na źródło Q(S). Transmisję w wolnej przestrzeni od źródła w punkcie S do punktu obserwacji P przedstawia operator transmisji T(S,P):

$$T(S,P)\ Q(S) = \frac{\exp[ikR(S,P)]}{R(S,P)}, \qquad (7)$$
(2.9)

transmisję przez półprzepuszczalny n-ty panel (ścianę) - operator $T(S,C_n,P)$:

$$T(S,C_n,P)\ Q(S) = T(C_n)\ T(S,P)\ Q(S), \qquad (8)$$
(2.10)

$T(C_n)$ - współczynnik transmisji,
C_n - punkt w którym zachodzi transmisja.

Odbicie od n-tego panelu (ściany) przedstawia operator odbicia $R(S,A_n,P)$:

$$R(S,A_n,P)\ Q(S) = R(A_n)\ T(S^{(n)},P)\ Q(S), \qquad (9)$$
(2.11)

$$R(S,A_n,P)\ Q(S) = R(A_n)\ T(S,P^{(n)})\ Q(S), \qquad (10)$$
(2.12)

$R(A_n)$ - współczynnik odbicia,
A_n - punkt w którym zachodzi odbicie.

Wyrażenia (9), (10) przedstawiają dwie możliwości opisu odbicia: albo jako transmisję od źródła pozornego, będącego lustrzanym odbiciem źródła rzeczywistego, do rzeczywistego punktu obserwacji, albo jako transmisję od rzeczywistego źródła do pozornego punktu obseracji będącego lustrzanym odbiciem rzeczywistego punktu obserwacji.

Dyfrakcję na m-tej krawędzi przedstawia operator dyfrakcji $D(S,E_m,P)$:

$$D(S,E_m,P)\ Q(S) = D\left(\nu;S(m),P(m)\right)\ T(S,P)\ Q(S), \qquad (11)$$
(2.13)

$D\left(\nu;S(m),P(m)\right)$ - współczynnik dyfrakcji,

E_m - punkt na krawędzi który jest źródłem fal dyfrakcyjnych.

Współczynnik dyfrakcji, jako zależny od położeń źródła S(m) i punktu obserawacji P(m) dla danego procesu, wyrażony jest w lokalnym układzie współrzędnych, w którym m-ta krawędź stanowi oś z.

W całkowitym polu wyróżniono część geometryczną i dyfrakcyjną:

$$p(P) = p^g(P) + p^d(P). \qquad (12)$$
(2.10)

Część geometryczna pola jest sumą składników pola po wszystkich możliwych drogach docierania fali, gdzie jako elementarne procesy występują tansmisje i odbicia, przy maksymalnym rzędzie oddziaływań równym K

$$p^g(P) = \sum_{k=1}^{K} \sum_{i=1}^{I(N,k)} \prod_{k'=1}^{k} \hat{\Pi}^i_{k'}(n)\, Q(S), \qquad (13)$$
(4.2)

$$\hat{\Pi}(n) = \begin{cases} T(\ldots,C_n,\ldots), \\ R(\ldots,A_n,\ldots). \end{cases} \qquad (14)$$
(4.1)

$\hat{\Pi}^i_k(n) * \ldots * \hat{\Pi}^i_1(n)$ jest uporządkowanym iloczynem, będącym k-elementową kombinacją z 2N-elemetowego zbioru operatorów $\{\hat{\Pi}(n)\}$, wyznaczającym i-tą drogę fali. Zbiór $\{\hat{\Pi}(n)\}$ tworzą operatory transmisji i odbicia dla kolejnych paneli (ścian), których w układzie jest N.

Część dyfrakcyjna pola jest sumą składników pola po wszystkich możliwych drogach docierania fali, gdzie jako elementarne procesy występują tansmisje, odbicia i dyfrakcje, przy maksymalnym rzędzie oddziaływań równym K

$$p^{d}(P) = \sum_{k=1}^{K} \sum_{i=1}^{I(N,M,k)} \prod_{k'=1}^{k} \hat{\Pi}_{k'}^{i}(\mu)\, Q(S), \qquad (15)$$
(4.3)

$$\hat{\Pi}(\mu) = \begin{cases} T(\ldots,C_n,\ldots), \\ R(\ldots,A_n,\ldots), \\ D(\ldots,E_m,\ldots). \end{cases} \qquad (16)$$
(4.1)

$\hat{\Pi}_k^i(\mu)$ * ... * $\hat{\Pi}_1^i(\mu)$ jest uporządkowany iloczynem, będącym k-elementową kombinacją z (2N+M)-elemtowego zbioru operatorów $\{\hat{\Pi}(\mu)\}$, wyznaczającym i-tą drogę fali. Zbiór $\{\hat{\Pi}(\mu)\}$ tworzą operatory transmisji i odbicia od kolejnych paneli (ścian), których w układzie jest N i operatory dyfrakcji na krawędziach których jest M.

Odpowiednie operatory, jako występujące w ciągach oddziaływań z obiektami o ograniczonych rozmiarach, mają postać zawierającą funkcję skoku jednostkowego $\eta(\ )$, która pozwala określić czy punkt w którym następuje oddziaływanie jest czy nie jest punktem danego obiektu:

$$T\left(S^{(p)},C_n,P^{(r)}\right) = \eta(C_n)T\left(S^{(p)},P^{(r)}\right), \qquad (17)$$
(2.15)

$$\eta(C_n) = \begin{cases} T(C_n), & C_n \in (n)\text{-panel}, \\ 1, & C_n \notin (n)\text{-panel}, \end{cases} \qquad (18)$$
(3.60)

$$R\left(S^{(p)},A_n,P^{(r)}\right) = \eta(A_n)T\left(S^{(p,n)},P^{(r)}\right) = \qquad (19)$$
(2.15)

$$= \eta(A_n)\, T\left(S^{(p)},P^{(n,r)}\right),$$

$$\eta(A_n) = \begin{cases} R(n), & A_n \in (n)\text{-panel}, \\ 0, & A_n \notin (n)\text{-panel}, \end{cases} \qquad (20)$$
(3.44)

$$D\left(S^{(p)},E_m,P^{(r)}\right) = \eta\left(S^{(p)},E_m,P^{(r)}\right)\ T\left(S^{(p)},P^{(r)}\right), \qquad (21)$$
(2.15)

$$\eta(S^{(p)},E_m,P^{(r)}) = \qquad (22)$$
(3.55)

$$= \begin{cases} D[\nu;S^{(p)}(m),P^{(r)}(m)], & E_m \in (m)\text{-krawędź}, \\ 0, & E_m \notin (m)\text{-krawędź}. \end{cases}$$

W zależnościach (17 - 22) źródło pozorne $S^{(p)}$ reprezentuje historię fali przed danym procesem a pozorny punkt obserwacji $P^{(r)}$- po danym procesie.

3. Pole geometryczne

Wyróżniona część geometryczna pola zawiera ciągi k-krotnych oddziaływań, gdzie

$$k = k_r + k_t \qquad (23)$$
(4.9)

k_r- liczba odbić,
k_t- liczba transmisji.

Pole geometryczne jest sumą składników o ogólnej postaci:

$$p^g[S(i),P] = p^g(S,\ldots,C(i)_s,\ldots,A(i)_p,\ldots,P) = \qquad (24)$$
(4.8)

$$= T(\ldots,P) *\ldots* T[\ldots,C(i)_s,\ldots]\ R[\ldots,A(i)_p,\ldots] *\ldots*$$

$$*\ldots* T(S,\ldots)\ Q(S),$$

$C(i)_s$- jeden z punktów transmisji na i-tej drodze fali,
$A(i)_p$- jeden z punktów odbicia na i-tej drodze fali.

Po podstawieniu jawnych postaci operatorów do zależności (24) otrzymuje się

$$p^g[S(i),P] = \prod_{p=1}^{k_r} \eta[A(i)_p] \prod_{s=1}^{k-k_r} \eta[C(i)_s] \frac{\exp(ikR_i)}{R_i}, \qquad (25)$$

(4.11)

$$R_i = [S(i),P] = [S,P(i)]. \qquad (26)$$

(4.14)

Ogólna postać składników pola geometrycznego zawiera ciągi iloczynów odpowiednich współczynników tranmsmisji i odbicia, przez które mnożona jest niezaburzona fala, docierająca z odpowiedniego źródła pozornego do rzeczywistego punktu obserwacji, lub z rzeczywistego źródła do odpowiedniego pozornego punktu obserwacji.

Dla źródeł pozornych powstających w wyniku kolejnych odbić, w miejsce wymieniania kolejnych paneli (ścian) od których następuje odbicie, wprowadzono ciągłą indeksację:

$$S^{(\ldots,s,\ldots,p,\ldots,n)} = S(i). \qquad (27)$$

(4.10)

Zbiór wszystkich źródeł, występujących dla danego rzędu odbić k_r, można ustalić przy użyciu procedury generacji struktury drzewa. Pole geometryczne przybiera wtedy postać sumy składników związanych z poszczególnymi źródłami:

$$p^g(P) = \sum_{i=0}^{I(N,K)} p^g[S(i),P]. \qquad (28)$$

(4.12)

Liczba występujących źródeł, która dla $K=K_r$ jest równa liczbie składników pola geometrycznego, może być obliczona:

$$I(N,K_r) = 1 + \sum_{k_r=1}^{K_r} I(N,k_r) = 1 + N\,\frac{(N-1)^{K_r} - 1}{N - 2}. \qquad (29)$$
(4.15)

Liczba źródeł dla układu pięciu budynków na podłożu, gdy źródło znajduje się w pobliżu podłoża a punkt obserwacji na wysokości mniejszej niż wysokość budynków (w oddziaływanie wchodzą tylko ściany boczne) wynosi:

$$I(N=21,K_r=3) = 8\ 842. \qquad (30)$$
(4.16)

Aby zmniejszyć liczbę analizowanych dróg można, już na etapie generacji źródeł, pominąć źródła nieistniejące (te które nie dają przyczynków do całkowitego pola). W związku z tym że budynek jako całość stanowi nieprzepuszczalną przeszkodę (brak odbić między ścianami tego samego budynku), o ścianach prostopadłych do podłoża (dla danej drogi propagacji możliwe jest tylko jedno odbicie od podłoża), liczba źródeł jest odpowiednio mniejsza:

$$I_a(N=21,K_r=3) = 842. \qquad (31)$$
(4.17)

4. Pole dyfrakcyjne

Fale dyfrakcyjne wraz ze związanymi z nimi, przez emisję ze wspólnego źródła, falami geometrycznymi tworzą pary. Fala geometryczna występuje w ograniczonym obszarze, fala dyfrakcyjna - w całej przestrzeni. Na granicy obszaru występowania fala geometryczna doznaje skoku, który "wygładza" fala dyfrakcyjna, przyjmując jednocześnie swoją maksymalną wartość. Pozwala to dla obu tych fal w procesie odbicia wprowadzić odpowiednie, różne od jedności, współczynniki odbicia.

W proponowanym opisie dyfrakcja na krawędzi została opisana jako niezależny proces, który występuje zawsze gdy fala dociera

do danej krawędzi. Proces jest opisany jako niezależny od oddziaływań geometrycznych (transmisji, odbić) fali z panelami (ścianami) tworzącymi daną krawędź. Zrobiono tak dlatego, że fale dyfrakcyjne mogą być składnikami dróg propagacji na których związane z nimi fale geometryczne nie występują.

Niezależny proces dyfrakcji na krawędzi opisany jest przez współczynnik dyfrakcji, w którym uwzględniono sytuację kiedy półpłaszczyzny tworzące klin są scharakteryzowane przez różne współczynniki odbicia. Dla półprzepuszczalnych paneli (płaskich ekranów) współczynnik dyfrakcji uwzględnia efekt dyfrakcji związany z falą transmitowaną przez panel.

Formalny opis dyfrakcji na krawędzi, przyjęty w postaci pozwalającej wyróżnić proces transmisji do krawędzi - opisany operatorem $T(S,E_m)$ i od krawędzi - opisany operatorem $T(E_m,P)$, ma istotne znaczenie gdy dyfrakcja jest jednym z procesów w ciągu oddziaływań:

$$p^d(S,E_m,P) = D(S,E_m,P)\,Q(S) = \tag{32}$$
(4.13)

$$= T(E_m,P)\,Q[E_m(S)] =$$

$$= T(E_m,P)\,D\begin{bmatrix} S \\ E_m \\ P \end{bmatrix} T(S,E_m)\,Q(S) =$$

$$= \eta(S,E_m,P)\left[\frac{T(S,E_m)}{T(S,P)}\right] T(S,P)\,Q(S) =$$

$$= \eta(S,E_m,P)\left[\frac{f(S,E_m)}{f(S,P)}\right] \frac{\exp(ikR)}{R}.$$

W wyrażeniu (32) stosunek

$$\left[\frac{T(S,E_m)}{T(S,P)}\right] = \left[\frac{f(S,E_m)}{f(S,P)}\right], \qquad (33)$$
(4.19)

przedstawia względną kierunkowość źródła, gdzie $f(S,E_m)$ i $f(S,E)$ są odpowiednio współczynnnikami kierunkowości źródła w kierunku punktu krawędzi E_m i w kierunku punktu obserwacji. Dla przyjętego jako źródło pierwotne wszechkierunkowego źródła punktowego względna kierunkowość (33) wynosi jeden. Natomiast przybiera różną od jedności wartość dla procesów dyfrakcyjnych wyższych rzędów, gdzie źródłem jest źródło kierunkowe, powstałe w procesie dyfrakcyjnym niższego rzędu.

Przykładowo, gdy przed dyfrakcją na m-tej krawędzi następuje odbicie od p-tego panelu (ściany) a po dyfrakcji od r-tego, aby obliczyć współczynnik dyfrakcji należy ustalić położenie źródła pozornego reprezentującego proces przed dyfrakcją i położenie pozornego punktu obserwacji reprezentującego proces zachodzący po dyfrakcji. Opis procesów przed dyfrakcją przy pomocy źródła pozornego a po dyfrakcji przy pomocy pozornego punktu obserwacji, gwarantuje ustalenie odpowiedniego kąta pod którym fala dociera do krawędzi i pod jakim jest odpromieniowywana po dyfrakcji. Wtedy

$$p^d(S,A_p,E_m,A_r,P) = \qquad (34)$$
(4.27)

$$= R(E_m,A_r,P)\, D(S,E_m,P)\, R(S,A_p,E_m)\, Q(S) =$$

$$= R(E_m,A_r,P)\, D\begin{bmatrix} S \\ E_m \\ P \end{bmatrix} R(S,A_p,E_m)\, Q(S) =$$

$$= \eta(A_p)\ R(E_m,A_r,P)\ D\begin{bmatrix} S \\ E_m \\ P \end{bmatrix}\ T(S^{(p)},E_m)\ Q(S) =$$

$$= \eta(A_p)\ \eta(A_r)\ T(E_m,P^{(r)})\ D\begin{bmatrix} S \\ E_m \\ P \end{bmatrix}\ T(S^{(p)},E_m)\ Q(S) =$$

$$= \eta(A_p)\ \eta(A_r)\ \eta(S^{(p)},E_m,P^{(r)})\ T(S^{(p)},P^{(r)})\ Q(S).$$

Podobnie jak w przypadku geometrycznych składników pola, otrzymuje się składnik pola dyfrakcyjnego mający postać zawierającą iloczyn odpowiednich współczynników odbicia i, w tym przypadku, współczynnika dyfrakcji oraz falę niezaburzoną, transmitowaną w wolnej przestrzeni.

Na Rys.3 przedstawiony jest bardziej złożony proces dla źródła znajdującego się w wykopie. Odpowiednie położenia pozornych źródeł i pozornych punktów obserwacji reprezentują fizyczną drogę propagacji, zaznaczoną na rysunku linią ciągłą. Składnik pola pochodzący od przedstawionej na Rys.3 drogi ma postać:

$$p^d(S,A_p,E_1,A_u,E_2,A_t,P) = \qquad (35)$$
(4.49)

$$= \eta(A_t)\ \eta(A_u)\ \eta(A_p)\ \eta(E_1^{(u)},E_2,P^{(t)})\left[\frac{T(E_1,E_2^{(u)})}{T(E_1,P^{(t,u)})}\right] *$$

$$* \eta(S^{(p)},E_1,P^{(t,u)})\ T(S^{(p)},P^{(t,u)})\ Q(S),$$

gdzie

$$\left[\frac{T(E_1,E_2^{(u)})}{T(E_1,P^{(t,u)})}\right] = \frac{P[\nu_m;\varphi_{om},\varphi_m(E_2^{(u)})]}{P[\nu_m;\varphi_{om},\varphi_m(P^{(t,u)})]}, \qquad (36)$$

(4.50)

jest względną kierunkowością wtórnego źródła fali dyfrakcyjnej $Q[E_1(S)]$ powstałego na pierwszej krawędzi, w punkcie E_1. Przedstawia ona stosunek współczynnika kierunkowości źródła $Q[E_1(S)]$ w kierunku punktu gdzie zachodzi następny proces dyfrakcji $E_2^{(u)}$, do współczynnika w kierunku docelowego punktu obserwacji $P^{(t,u)}$. Współczynnik kierunkowości źródła $Q[E_1(S)]$ wynika z jawnej postaci współczynnka dyfrakcji fali na pierwszej krawędzi.

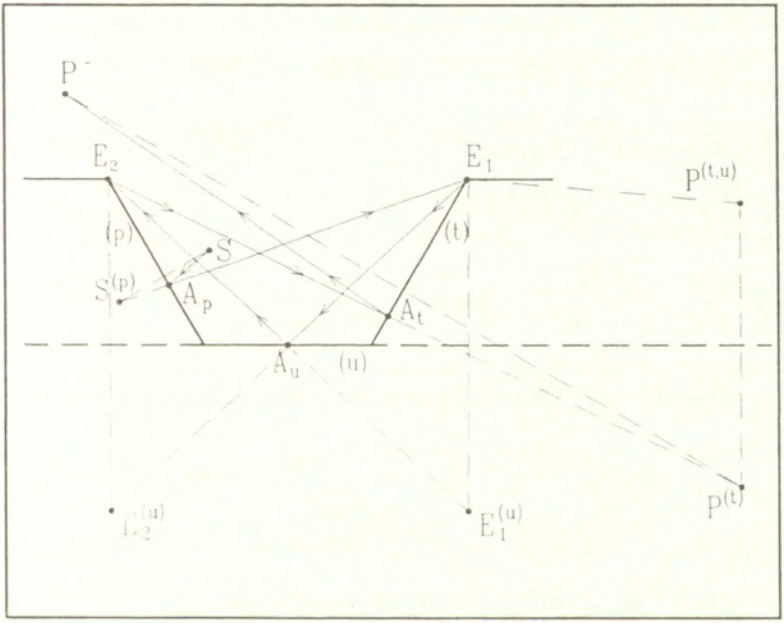

Rys.3

Część dyfrakcyjna pola całkowitego (15) zawiera ciągi k-krotnych oddziaływań

$$k = k_t + k_r + k_d, \tag{37}$$

(4.48)

k_t - liczba transmisji,
k_r - liczba odbić,
k_d - liczba dyfrakcji.

W składnikach pola dyfrakcyjnego (15) należy wyróżnić odcinki dróg przebywane między kolejnymi dyfrakcjami, na których występują tylko oddziaływania geometryczne (transmisje i odbicia). Poniżej przestawiono proces w którym fala przebywa i-tą drogę do miejsca pierwszej dyfrakcji na m-tej krawędzi, następnie l-tą drogę do dyfrakcji na (m+1)-szej krawędzi, po opuszczeniu której przebywa j-tą drogę aby osiągnąć punkt obserwacji P:

$$p^d[S(i),E_m,\ldots,E_m(l),E_{m+1},\ldots,P(j)] = \tag{38}$$

(4.51)

$$= p^d(S,\ldots,C(i)_s,\ldots,A(i)_p,\ldots,E_m,\ldots,C(l)_r,\ldots,A(l)_u,\ldots,$$

$$E_{m+1},\ldots,C(j)_w,\ldots A(j)_t,\ldots,P) =$$

$$= T(\ldots,P) *\ldots* T[\ldots,C(j)_t,\ldots] *\ldots* R[\ldots,A(j)_w,\ldots] *$$

$$* D[\ldots,E_{m+1},\ldots] T[\ldots,C(l)_r,\ldots] *\ldots* R[\ldots,A(l)_u,\ldots] *$$

$$* D[\ldots,E_m,\ldots] T[\ldots,C(i)_s,\ldots] *\ldots* R[\ldots,A(i)_p,\ldots] * \ldots.*$$

$$* \ldots.* T(S,\ldots) Q(S),$$

gdzie liczby odpowiednich oddziaływań są następujące

$$k = k(i) + k(l) + k(j) + k_d(=2), \tag{39}$$

(4.52)

$$k(i) = k_r(i) + k_t(i),$$

$$k(l) = k_r(l) + k_t(l),$$

$$k(j) = k_r(j) + k_t(j),$$

$$k_r = k_r(i) + k_r(l) + k_r(j), \qquad k_t = k_t(i) + k_t(l) + k_t(j).$$

W wyniku kolejnego działania operatorów otrzymuje się ostateczną postać omawianego składnika pola

$$p^d[S(i),E_m,\ldots,E_m(l),E_{m+1},\ldots,P(j)] = \qquad (40)$$
(4.53)

$$= \prod_{p=1}^{k_r(i)} \eta[A(i)_p] \prod_{s=1}^{k(i)-k_r(i)} \eta[C(i)_s] \prod_{u=1}^{k_r(l)} \eta[A(l)_u] \prod_{q=1}^{k(l)-k_r(l)} \eta[C(l)_q] *$$

$$* \prod_{t=1}^{k_r(j)} \eta[A(j)_t] \prod_{w=1}^{k(j)-k_r(j)} \eta[C(j)_w] \; \eta[E_m(l),E_{m+1},P(j)] *$$

$$* \left[\frac{T[E_m,E_{m+1}(l)]}{T[E_m,P(j,l)]}\right] \eta[S(i),E_m,P(l,j)] \; \frac{\exp\left(ikR_{i,l,j}\right)}{R_{i,l,j}},$$

$$R_{i,l,j} = [S(i),P(j,l)] = [S(i,l,j),P] = [S,P(j,l,i)], \qquad (41)$$
(4.55)

która zawiera iloczyny współczynników transmisji i odbicia na geometrycznych odcinkach dróg: i-tym, l-tym i j-tym oraz dwa współczynniki dyfrakcji przez które jest mnożona fala propagująca się w wolnej przestrzeni od odpowiedniego źródła do odpowiedniego

punktu obserwacji (41). Powstanie wtórnego, kierunkowego źródła fali dyfrakcyjnej na m-tej krawędzi w punkcie E_m, powoduje pojawienie się odpowiedniego czynnika opisującego jego kierunkowość

$$\left[\frac{T[E_m,E_{m+1}(1)]}{T[E_m,P(j,1)]}\right] = \frac{P[\nu_m;\varphi_{om},\varphi_m(E_{m+1}(1))]}{P[\nu_m;\varphi_{om},\varphi_m(P(j,1))]} \quad . \qquad (42)$$
(4.54)

W przypadku ogólnym, tak samo jak w przypadku dwukrotnej dyfrakcji (38,40), wyrażenie opisujące składnik pola dyfrakcyjnego również składa się z iloczynu odpowiednich współczynników transmisji, odbicia i dyfrakcji, wraz z odpowiednimi czynnikami opisującymi względne kierunkowości powstałych wtórnych źródeł fal dyfrakcyjnych.

Pierwszy proces dyfrakcji o współczynniku $\eta[S(i),E_m,P(j,1)]$ odbywa się dla fali ze źródła w punkcie S(i) (reprezentującego geometryczny odcinek drogi przed pierwszą dyfrakcją) i pozornego punktu obserwacji P(j,...,1) (reprezentującego wszystkie procesy odbić po pierwszej dyfrakcji do ostatniego na j-tym odcinku drogi włącznie).

Dla drugiego procesu dyfrakcji o współczynniku $\eta[E_m(1),E_{m+1},P(j,...)]$ źródłem jest punkt pierwszej krawędzi E_m gdzie powstała fala dyfrakcyjna. Po odbiciach na odcinku drogi do drugiej dyfrakcji, źródło to reprezentowane jest przez odpowiednie źródło pozorne w punkcie $E_m(1)$. Punkt obserwacji reprezentowany jest przez swój pozorny obraz P(j,...), odpowiadający wszystkim odbiciom po drugiej dyfrakcji. Tak aż do osiągnięcia ostatniej, M-tej krawędzi. W tym procesie o współczynniku dyfrakcji $\eta[E_{M-1}(L),E_M,P(j)]$ źródłem jest pozorny obraz źródła fal dyfrakcyjnych $E_{M-1}(L)$ na przedostatniej, (M-1)-szej krawędzi, gdzie uwzględniono procesy odbić na L-tej drodze od przedostatniej do ostatniej M-tej krawędzi. Punktem obserwacji jest pozorny punkt P(j) reprezentujący odbicia na drodze od

ostatniej dyfrakcji do rzeczywistego punktu obserwacji.

W przedstawionym modelu propagacji współczynnik odbicia został uwzględniony jako średnia wartość, wynikająca z pogłosowego współczynnika pochłaniania. Zrobiono tak w celu niekomplikowania nadmiernie przedstawianego opisu. Jednak, w związku z przyjęciem jako źródła pierwotnego źródła punktowego, współczynnik odbicia powinien mieć postać, właściwą dla fali kulistej, zależną od położenia źródła fali dla danego procesu i położenia punktu obserwacji dla danego procesu. Taka właśnie zależność występuje dla współczynnika dyfrakcji. W związku z tym podobieństwem, właściwą dla fali kulistej postać współczynnika odbicia można wprowadzić do ciągów wielokrotnych oddziaływań podobnie jak to zrobiono dla współczynnik dyfrakcji, dokonując w ten sposób uogólnienia modelu propagacji.

ZASTOSOWANIE

Zaprezentowany model hałasu środowiskowego może stanowić podstawę do tworzenia odpowiednich modeli symulacjynych powalających określać warunki klimatu akustycznego dla wybranych fragmentów zabudowy miejskiej. Rodzaje uwzględnionych przy konstrukcji modelu propagacji oddziaływań narzucają ograniczenia na odwzorowanie geometrii układu urbanistycznego. W ramach przedstawionej metody tworzenia modelu hałasu środowiskowego, uwzględniającej transmisję, odbicia i dyfrację na krawędziach naroży, można odwzorować ukształtowanie terenu (trasa w wykopie) i kształt przeszkód odpowiednio łącząc z sobą panele tak, aby tworzyły naroża o odpowiednim kącie wewnętrznym 2Ω. Jednocześnie założenie pola dalekiego wymaga aby wzajemne odległości między kolejnymi oddziaływaniami ze ścianami i krawędziami wynosiły kilka długości fali.

1. Opis modelu hałasu środowiskowego

W oparciu o model hałasu środowiskowego (1) można tworzyć odpowiednie modele symulacyjne, pozwalające przewidywać warunki klimatu akustycznego. Dokładność modelu symulacyjnego zależy od:

- dokładności odwzorowania warunków rzeczywistych przez model,
- dokładności z jaką zostały ustalone wprowadzone do modelu parametry.

Model symulacyjny zawiera opis "odbioru" hałasu przez człowieka, $\hat{\Pi}_o(\ )$ model propagacji $\hat{\Pi}(\ )$ i model źródła $Q(\ )$:

$$L_{eq}[dB(A)] = \hat{\Pi}_o\left(10\log;p_o^2;\int d\omega;\Delta L_A(\omega)\right) * \quad (43)$$

$$* \hat{\Pi}\left(N,\{\underline{R}\},\{R(n)\},\{T(n)\},K,\underline{R}(P)\right) Q(\ldots). \quad (5.25)$$

Zgodnie z obowiązującymi normami "odbiór" hałasu przez człowieka jest oceniany na podstawie poziomu równoważnego. W zależności od potrzeb, do modelu hałasu środowiskowego mogą być wprowadzone procedury obliczające inne potrzebne wskaźniki hałasu (np. poziom głośności).

Parametrami modelu propagacji są:

- N - liczba paneli odwzorowujących układ urbanistyczny,
- $\{\underline{R}\}$ - zbiór wektorów opisujących geometrię układu urbanistycznego,
- $\{R(n)\}$ - zbiór współczynników odbicia poszczególnych paneli,
- $\{T(n)\}$ - zbiór współczynników transmisji poszczególnych paneli,
- K - maksymalny rząd oddziaływań,
- $\underline{R}(P)$ - położenie punktu obsrwacji.

W modelu źródła wygodnie jest wyróżnić dwie opcje: źródło nieruchome i trasę komunikacyną:

$$Q(\ldots) = \begin{cases} Q\left(\underline{R}(S), W(S,f)\right), \\ Q\left(N, v, J, \{\underline{R}_j\}, \Delta x_E, W(f)\right), \end{cases} \qquad (44)$$
(5.26)

parametrami modelu źródła są:

N - średni strumień pojazdów [poj./h],

v - średnia prędkość pojazdów [m/h],

J - liczba pasów na trasie,

$\underline{R}(S)$ - położenie źródła S,

$\{\underline{R}_j\}$ - zbiór wektorów opisujących geometrię trasy,

Δx_E - krok przy sumowaniu energii przejazdu pojedynczego pojazdu,

W(S,f) - widmo mocy źródła S,

W(f) - średnie widmo hałasów komunikacyjnych.

Dokładność odwzorowania zależy od dokładności z jaką zostały opisane:

- geometria układu urbanistycznego,
- ośrodek propagacji,
- model źródła,
- zachodzące w trakcie propagacji procesy elementarne.

Prezentowany model hałasu środowiskowego jest strukturą o charakterze otwartym. Nie wychodząc poza jego ramy można, w zależności od potrzeb, odpowiednio zwiększać lub zmniejszać dokładność. Do opisu geometrii układu (odwzorowania ukształtowania terenu i brył budynków), oprócz naroży o wewnętrznym kącie rozwarcia 2Ω, można wprowadzić inne elementy np. walce o przekroju kołowym, eliptycznym lub hiperbolicznym dla których istnieją rozwiązania kononiczne mogące stanowić podstawę do określenia odpowiednich, jawnych postaci współczynników dyfrakcji. Tłumienie w rzeczywistym ośrodku można wprowadzić, jako uśredniony efekt, w postaci eksponencjalnego zaniku wraz z długością przebytej drogi. Rzeczywiste źródła można przedstawiać przy pomocy odpowiednio zwiększanej liczby zastępczych źródeł

punktowych o określonych charakterystykach kierunkowości.

Doświadczalne parametry modelu to współczynniki transmisji i odbicia, których ustalenia z odpowiednią dokładnością jako funkcji kąta padania i częstotliwości można oczekiwać wraz z rozwojem techniki pomiarowej natężenia dźwięku, przy użyciu programowanego źródła, co umożliwia pomiary in situ. Kolejnym doświadczalnym parametrem jest widmo mocy źródła, którego wprowadzenie w postaci wąskopasmowej odpowiednio zwiększa dokładność opisu. W przypadku pojazdów dochodzi jeszcze średnie natężenie ruchu i średnia prędkość pojazdów, które np. mogłyby być ustalane dla każdego pasa z osobna, z uwzględnieniem podziału pojazdów na klasy reprezentowane przez różne źródła zastępcze.

Parametrami modelu o charakterze operacyjnym są: maksymalny rząd oddziaływań K, który można odpowiednio zwiększać i długość kroku Δx_E przy sumowaniu energii emitowanej w czasie przejazdu pojedynczego pojazdu, który można zmniejszać.

Konstruując modele symulacyjne o odpowiednio dużej dokładności trzeba zawsze pamiętać o znalezieniu racjonalnego kompromisu między pożądaną dokładnością a czasem obliczeń.

W ramach prezentowanego modelu hałasu środowiskowego nie może być uwzględniony wpływ zjawisk atmosferycznych na propagację dźwięku inaczej niż w postaci uśrednionego efektu tłumienia w ośrodku, oraz takie zjawiska jak refrakcja. Dotyczy to również oddziaływań w polu bliskim jakie zachodzą w pobliżu fasady budynku, dla którego ma być oceniany klimat akustyczny, a których przyczyną jest właśnie bliskość tejże fasady. Oddziaływania z elementami struktury fasady takimi jak np. balkony, głównie wpływają na penetrację hałasu do wnętrza budynku, natomiast prezentowany model hałasu środowiskowego służy do oceny zewnętrznych warunków klimatu akustycznego.

2. Przykłady

Poniżej przedstawione są dwa przykłady wykorzystania modelu symulacjnego przygotowanego w oparciu o model hałasu środowiskowego.

Na Rys.4 przedstawiono względne widma:

(1) - krzywej korekcyjną A,

(2) - hałasów komunikacyjnych,

(3) - hałasów komunikacyjnych, skorygowane krzywą A, które przyjęto dla źródła zastępczego, reprezentującego pojazd.

W przykładach przyjęto maksymalny rząd oddziaływań K=3 i wszystkie współczynniki odbicia rzeczywiste, równe 0.9.

Dla układu urbanistycznego złożonego z pięciu budynków, przedstawionego na Rys.5, ze źródłem w punkcie S, obliczono poziom dźwięku w punktach leżących wzdłuż linii położonej za pierwszą linią zabudowy, na wysokości 1.5 m. Poziomem odniesienia jest poziom w półprzestrzeni bez budynków. Wyniki przedstawione są na Rys.6. Krzywa przerywana, na której widać obszary cienia gdzie poziom dźwięku ma wartość minus nieskończoność, przedstawia pole geometryczne. Krzywa ciągła przedstawia pole całkowite.

Dla układu urbanistycznego przedstawionego na Rys.7 źródłem jest trasa komunikacyjna o natężeniu ruchu N=1500 poj./h, przy średniej prędkości v=60 km/h i dwóch pasach ruchu ($\Delta x=\Delta x_E$=80 m). Bezwzględna wartość poziomu dźwięku w paśmie 1 kHz, w odległości 3 m od źródła zastępczego została przyjęta jako SPL(R=1m,f=1kHz)=85 dB. Na Rys.8 przedstawiono poziom dźwięku obliczony na lini leżącej wzdłuż fasady budynku No.4, na wysokości 4.5 m. Krzywa (I) przedstawia poziom dźwięku w półprzestrzeni bez budynków, krzywa (II) - z budynkami, krzywa (III) - po zastosowaniu ekranu E o wysokości 3 m i izolacyjności 20 dB.

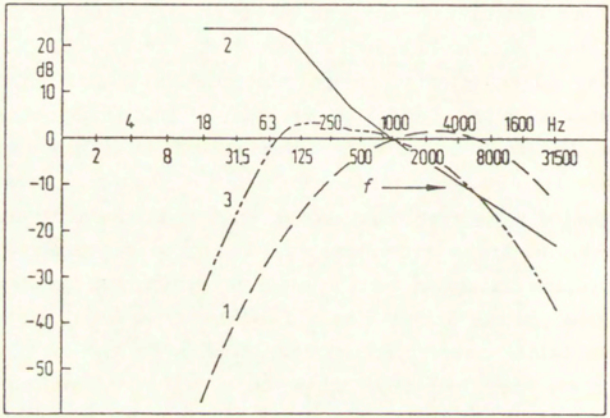

Rys.4

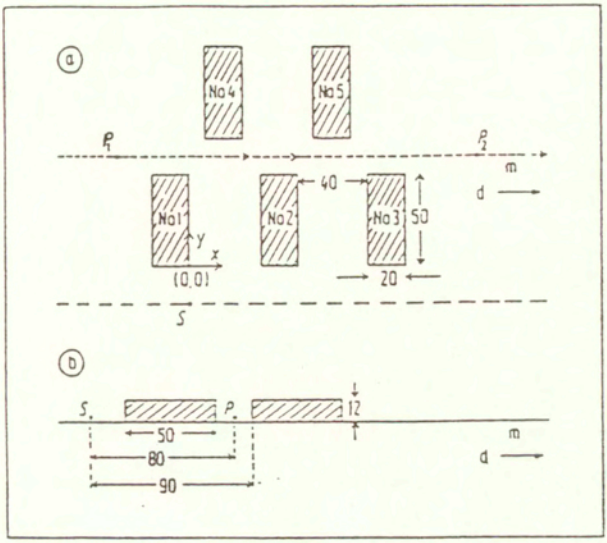

Rys.5

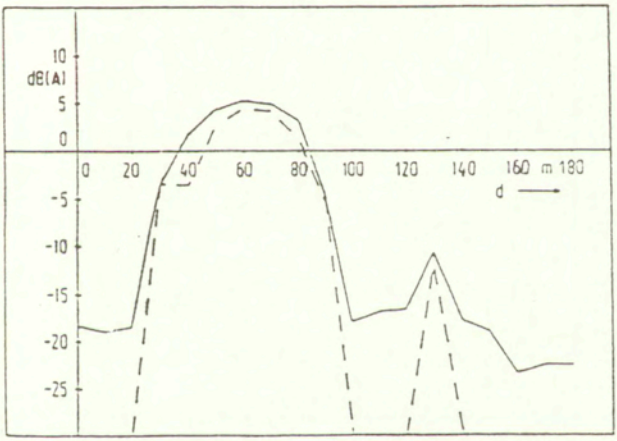

Rys.6

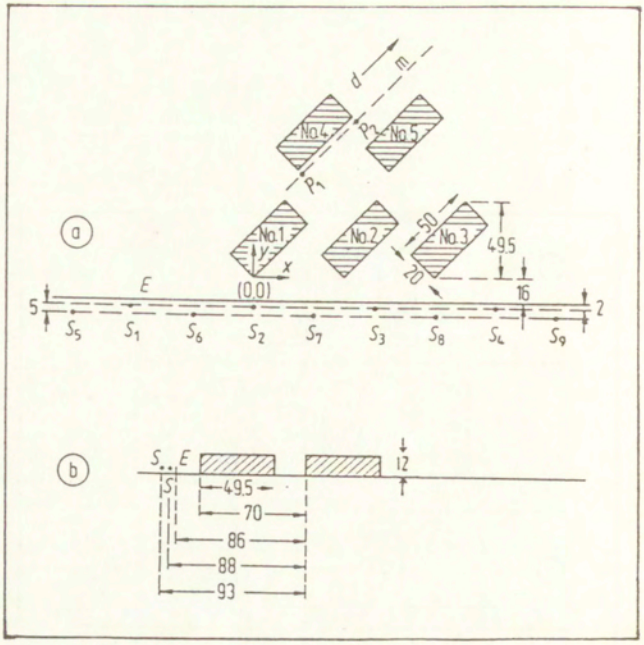

Rys.7

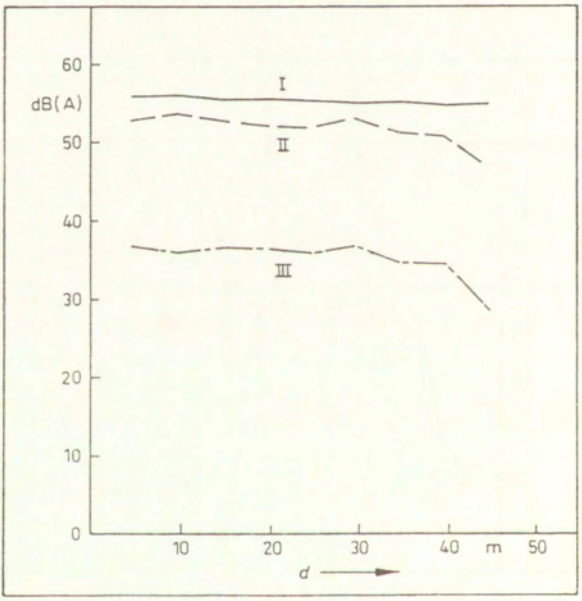

Rys.8